SIMPLIFIED METHODS TO SOLVE THE CONJUGATED HEAT TRANSFER PROBLEMS UNDER THE EFFECT OF PARABOLIC AND HYPERBOLIC HEAT CONDUCTION MODELS

By
Abdel-Muttaleb Khadrawi

Supervisor
Professor Mahmoud Hammad
University of Jordan

Co-Supervisor
Professor Mohammad Al-Nimr
Jordan University of Science and Technology

Submitted in Partial Fulfillment of the Requirements for the Degree of
Doctor of Philosophy in Mechanical Engineering

Faculty of Graduate Studies
University of Jordan

October 2000

This thesis was successfully defended and approved on: $16 - 10 - 2000$

Examination Committee   Signature

- Dr. Mahmoud Hammad, Supervisor
  Prof. of Mechanical Engineering,
  University of Jordan
                                                         $22/10/2000$

- Dr. Mohammad Al-Nimr, Co-Supervisor
  Associate Prof. of Mechanical Engineering,   Moh'd Al-Nimr
  Jordan University of Science and Technology $22/10/2000$

- Dr. Mohammad Al-Saad, Member
  Prof. of Mechanical Engineering   Mohamad Al-Saad
  University of Jordan

- Dr. Mohammad Hamdan, Member
  Prof. of Mechnical Engineering,
  University of Jordan

- Dr. Taha Aldoss, Member
  Prof. of Mechanical Engineering
  Jordan University of Science and Technology

ii

DEDICATION

To my mother,

To my dear wife and my daughters Darin and Ranim

ACKNOWLEDGMENT

It is my golden chance to acknowledge and greatly appreciate my supervisor, Dr. Mahmoud Hammad whose support, encouragement, and enthusiasm insisted me to do all best to complete this research. I can't find words to thank my co-supervisor Dr. Mohammad Al-Nimr for his valuable help during the research period.

I can't find words to describe the dept I owe to all of my professors and colleagues in the mechanical engineering department at Jordan University, for their help and support. I owe a special thank to Dr. Mohammad Hamdan, Dr. Mohammad Al-Saad and Dr.Taha Aldoss for their cooperation and being in the examination committee

Furthermore, to my family and all my friends, goes my eternal gratitude and dedication.

CONTENTS

LIST OF TABLES

LIST OF FIGURES

ix

x

LIST OF APPENDICES

NOMENCLATURE

a Width of the domain adjacent to the thin layer, m

c Specific heat capacity, $J/kg\,K$

f Specified surface temperature, K

Fo   Fourier number

g Heat source, W/m

G Dimensionless heat source, $g\,a^2/k_1\,\Delta T$

h Interfacial heat transfer coefficient, $W/m^2\,K$

h_i Interface heat transfer coefficient, $W/m^2\,K$

h_o Outer surface heat transfer coefficient, $W/m^2\,K$

k Thermal conductivity, $W/m\,K$

K_r Thermal conductivity ratio, k_2/k_1

L Length of the channel, m

P Normal stress, p_a

Pe   Pecklet number

q^c Convected heat flux, W/m^2

q^h Enthalpy flow, W/m^2

q^i Imposed heat flux, W/m^2

R Dimensionless thickness including the thin layer in cartesian coordinate, b/a

r_i Inner radius of the channel, m

r_1 Outer radius of the channel, m

S Laplacian domain

t Time, s

T_1	Temperature of the domain adjacent to the thin layer, K
T_2	Temperature of the thin layer, K
T_i	Initial temperature of the adjacent domain and the thin layer, K
T_o	Inlet temperature, K
T_∞	Ambient temperature, K
T_w	Wall temperature, K
u	Velocity component, m/s
V	Fluid flow velocity, m/s
W	Laplace transformation of the dimensionless temperature

Greek Symbols

α	Thermal diffusivity, $k/\rho c$
α_r	Thermal diffusivity ratio, α_2/α_1
Bi	Biot number, ha/k_1
Δy	Thickness of the thin layer in cartesian coordinate, m
Δ	Difference function
ε	Dimensionless small parameter
η	Dimensionless time, $\alpha_1 t/a^2$ or tV/r_1
θ	Dimensionless temperature defined in different forms
ξ	Dimensionless x-coordinate, x/a or z/r_1
μ	Viscosity, $kg/m\,s$
μ^*	Friction factor
ρ	Density, kg/m^3

$\tau^{\bullet}$ The half-period of oscillations, s

$\tilde{\tau}$ Thermal relaxation time, s

τ Dimensionless thermal relaxation time, $\tilde{\tau}\,\alpha_1/a^2$

Φ Dissipation function, $1/m\,s^2$

ω The wave frequency, $n\pi/\tau^{\bullet}$

Subscripts

1   Refers to the domain adjacent to the thin layer

2   Refers to the thin layer

f   Fluid

i   Initial

s   Solid

ABSTRACT

SIMPLIFIED METHODS TO SOLVE THE CONJUGATED HEAT TRANSFER PROBLEMS UNDER THE EFFECT OF PARABOLIC AND HYPERBOLIC HEAT CONDUCTION MODELS

By
Abdel-Muttaleb Khadrawi

Supervisor
Professor Mahmoud Hammad
University of Jordan

Co-Supervisor
Professor Mohammad Al-Nimr
Jordan University of Science and Technology

A generalized thermal boundary condition is derived for the parabolic and the hyperbolic models to include all thermal effects of a thin layer, whether solid-skin or fluid film, moving or stationary, in perfect or imperfect thermal contact with an adjacent domain. The thin layers thermal effects include, among others, thermal capacity of the layer, thermal diffusion, enthalpy flow, viscous dissipation within the layer and convective losses from the layer. Six different kinds of thermal boundary conditions can be obtained as special cases of the generalized boundary condition. The importance of the generalized boundary condition is demonstrated comprehensively in an example. The effects of different geometrical and thermophysical properties on the validity of the generalized thermal boundary condition are investigated. Also, the heat transfer mechanisms during rapid heating of two-layer composite thin slabs from a macroscopic point of view using the hyperbolic heat conduction model is studied. The composite slabs consist of two thin metal layers, which may be in perfect or imperfect thermal contact. The effects of different parameters, such as the two film thickness ratios, thermal conductivity ratio, heat capacity ratio, thermal relaxation time and interfacial heat transfer coefficient on the thermal behavior of the composite slabs are investigated.

It was found that the hyperbolic and the parabolic models give almost the same predictions as long as the values of $\tau_{q,1}$ and $\tau_{q,2}$ are relatively small. This implies that the hyperbolic concept has insignificant effect on the predictions of the parabolic heat conduction models when $\tau_{q,1}$ and $\tau_{q,2}$ are less than 0.01. The dual-phase-lag model aims to remove the precedence assumption made in the thermal wave model. It allows either the temperature gradient (cause) to precede the heat flux vector (effect) or the heat flux vector (cause) to precede the temperature gradient (effect). Also, It was found that the hyperbolic and the dual phase models give almost the same predictions as long as the values of $\tau_{T,1}$ and $\tau_{T,2}$ are relatively small. This implies that the phase-lag concept has insignificant effect on the predictions of the hyperbolic heat conduction models when $\tau_{T,1}$ and $\tau_{T,2}$ are less than 0.001.

A simple perturbation technique is used to reformulate the energy equations, which describe the transient thermal behavior of a radially lumped conjugated heat transfer problem in circular ducts of finite wall thickness. The simple perturbation technique used to eliminate the coupling between the fluid and solid-wall energy equations when the normalized temperature difference between the fluid and the solid wall is a small-perturbed quantity. The importance of this technique is demonstrated comprehensively in an example. It is found that there are three parameters H_1, H_3 and H_4 that control this technique.

1-INTRODUCTION

Energy transport during fast laser heating of solids has become a very active research area due to the tremendous applications of short-pulse lasers in the fabrication of microstructures, synthesis of advanced materials, measurement of thin-film properties, diagnostics of material's structure transformation, micromachining, laser patterning, laser processing of diamond films from carbon ion-implanted copper substrates, and laser surface hardening (Oui, 1992).

In the literature, there are basically four models that describe the mechanism of energy transport in very thin films or during short-pulse laser heating. The first model is the parabolic one-step model, which is based on the classical Fourier Conduction law. This model assumes that the solid lattice and electron gas is in local thermal equilibrium and the heat flux merges instantaneously when the temperature gradient exists. The expression electron gas is a terminology to describe the thermal behavior of the electrons. The second model used is the hyperbolic one-step model, Kim *et al.* (1990), Chen *et al.* (1994), Al-Nimr and Naji (1999) and Al-Nimr and Al-Huniti (2000), which was first postulated by (Maxwall, 1867). In this model, it is assumed that both lattice and electron gas are in local thermal equilibrium but the heat flux and the temperature gradient are non-local in time. This implies that the heat flux lags the temperature gradient by the relaxation time. The third and the fourth models are the parabolic and the hyperbolic two-step models, (Qui and Tien, 1992), (Tzuo, *et al.*, 1994), (Al-Nimr *et al.*, 1999) and (Al-Nimr and Kiwan, 2000). In these models it is assumed that solid lattice has different temperature than electron gas and the difference between these two temperatures depends on the coupling factor between both domains.

Conjugate heat transfer of laminar flow in duct has been widely analyzed in the past. Shah and London (1978) and Barozzi and Pagliarini (1985) presented an extensive review on this subject. Early attempts, Siegel (1959); Pellmutter and Siegel (1961); Chen *et al.* (1983) and Cotta *et al.* (1986) to solve unsteady conjugated heat transfer problems neglect the heat conduction in the solid wall and its heat capacity. The results of such investigations are valid for flows in the thin-walled ducts, but not for thick walled once. Sucec and Sawant (1984), and Cotta *et al.* (1987) analyzed the effect of wall heat capacity on unsteady heat transfer in laminar channel flows. Chung and Kassemi (1980), Krishan (1982), Lin and Kuo (1988), Yan *et al.* (1989), Al-Nimr and Hader (1994) and El-Shaarawi *et al.* (1995) examined the heat conduction in the solid. In the preceding works, the methods of solution where either approximate, Chung and (Kassemi, 1980); (Krishan, 1982) or numerical, (Lin and Kuo, 1988) and (Yan *et al.* 1989). Sparrow and Farias (1986) seem to make the first attempt to evaluate the eigenvalues of equation associated with conjugated transient forced convection of slug flow in parallel plate channels. Using quasi-steady approach, Sucec (1981), treated the conjugated forced convection slug flow problem in a parallel plate duct with transient initiated by step change in the inlet fluid temperature. Neglected the axial variation of temperature and using Laplace transformation, Krishan (1982), obtained series solution which are valid for small time period after the occurrence of a step change in wall heat flux temperature. Sucec and Sawant (1984) used quasi-steady approach with the actual parabolic fully developed velocity profile to study the unsteady conjugated heat transfer problems in a parallel plate channel with periodic variations in inlet fluid temperature with time. Travelho and santos (1991) presented analytical solution for transient conjugated forced convection in the entrance region of a duct with periodically varying inlet temperature. Olek et. al. (1991) presented analytical solution for a similar problem

2

in laminar pipe flow, where the flow is both hydrodynamically and thermally fully developed. Issa and Al-Nimr (1989) analyzed the transient behavior of hot water storage tanks where the wall effects are not taken into account. Sucec (1984) and Kakac *et al.* (1990) proposed a model, which solves the energy equation within the fluid domain only using a general so-called fifth kind boundary condition. This kind of boundary conditions, which assumes that the wall is lumped radially, takes the effects of the wall into account by combining the external convection losses from the wall, the radial conducted heat into the wall and the thermal capacity of the wall. Sakakibara *et al.* (1987) analytically investigated the steady conjugate heat transfer problem in an annular with a heated core and an insolated outside tube when the laminar flow is hydrodynamically fully developed. Al-Nimr and El-Shaarawi (1992) present analytical exact solutions for the problem of conjugated heat transfer in parallel plate and circular ducts. Al-Nimr (1993) modified the fifth kind boundary condition to include axial conduction in the wall and imposed heat flux on the outer surface of the wall. El-Shaarawi and Al-Nimr (1995) presented a finite-difference scheme to solve the transient conjugated heat transfer problem in a concentric annulus with simultaneously developing hydrodynamic and thermal boundary layers. Also, Al-Nimr (1998) used a simple perturbation technique to reformulate the energy equations which describe the transient thermal behavior of radially lumped conjugated heat transfer problem in circular and parallel plate ducts of finite wall thickness.

Cattaneo (1958) and Vernotte (1961) were the earliest investigators to formulate, independently, the hyperbolic wave energy equation. Peshkov (1944) was the earliest investigator to detect experimentally the existence of thermal waves using super fluid liquid helium near absolute zero. Since then, various analytical and numerical methods have been proposed to solve the hyperbolic heat conduction problems under different

applications and in different configurations. Vick and Ozisik (1983) investigated the wave nature of heat propagation in a semi-infinite medium containing volumetric energy sources by solving analytically the hyperbolic heat conduction equation. Gembarovic and Majernik (1988) investigated analytically non-Fourier effects in a finite slab using the hyperbolic heat conduction model. Ozisik and Tzou (1994) studied the engineering applications of the thermal wave theory, special features in thermal wave propagation, and the thermal wave model in relation to the microscopic two-step model. Kumar and Raju (1991) described numerical simulations for hyperbolic heat conduction problems involving non-Fourier effects via explicit self-starting Lax-Wendorff-based finite element formulations. Chen and Lin (1994) developed various analytical and numerical schemes for hyperbolic heat conduction problems with constant thermal properties.

This work will concentrate on finding simplified methods to solve the conjugated heat transfer problems under the effect of parabolic and hyperbolic one-step heat conduction models.

1.1 Lagging behavior

The lagging response, in general, describes the heat flux vector and the temperature gradient occurring at different instants of time in the heat transfer process. If the heat flux precedes the temperature gradient in the time history, the heat flux is the cause and the temperature gradient is the effect of heat flow. If the temperature gradient precedes the heat flux, on the other hand, the temperature gradient becomes the cause and the heat flux becomes the effect. This concept of precedence does not exist in the classical theory of diffusion because the heat flux vector and the temperature gradient are assumed to occur simultaneously.

4

This part establishes the theoretical foundation for the lagging response in conductive heat transfer. It results in a new type of energy equation, capturing the classical theories of diffusion (macroscopic in both space and time) and thermal waves (macroscopic in space but microscopic in time). The resulting model employing the two phase lags in describing the transient process is called the dual-phase-lag model.

In the classical theory of diffusion, the heat flux vector (q) and the temperature gradient (∇T) across a material volume are assumed to occur at the same instant of time. Mathematically this is represented by Fourier's law:

$$q(x,t) = -k\nabla T(x,t), \qquad (1.1)$$

where x denoting the position vector of the material volume t is the physical time. It results in an infinite speed of heat propagation, implying that the thermal distribution applied at a certain location in a solid medium can be sensed immediately anywhere else in the medium. Because the heat flux vector and the temperature gradient are simultaneous, there is no difference between the cause and the effect of heat flow. In the wave theory of heat conduction, on the other hand, the heat flux vector and the temperature gradient across a material volume are assumed to occur at different instant of time. To account for the phenomena involving the finite propagation velocity of the thermal wave, the classical Fourier heat flux should be modified. Cattaneo (1958) and Vernotte (1961) suggested independently a modified heat flux model in the form

$$q(x,t+\tilde{\tau}) = -k\frac{\partial T(x,t)}{\partial x} \qquad 533439 \qquad (1.2)$$

where $\tilde{\tau}$ is the time delay, called the "relaxation time". The constitution law of Eq. (1.2) assumes that the heat flux vector (the effect) and the temperature gradient (the cause) across a material volume occur at different instant of time and the time delay between the heat flux and the temperature gradient is the relaxation time $\tilde{\tau}$. The first order

5

expansion of q in Eq. (1.2) with respect to t bridges all the physical quantities at the same time. It results in the expansion:

$$\tilde{\tau}\frac{\partial q(x,t)}{\partial t} + q(x,t+\tilde{\tau}) = -k\frac{\partial T(x,t)}{\partial x} \qquad (1.3)$$

In Eq. (1.3) it is assumed that $\tilde{\tau}$ is small enough so that the first-order Taylor expansion of $q(x,t+\tilde{\tau})$ is an accurate representation for the convection heat flux. The equation of energy conservation for such problems is given as:

$$\rho c\frac{\partial T}{\partial t} = -\frac{\partial q}{\partial x} \qquad (1.4)$$

where ρ is the density and c is the specific heat. Elimination of q between Eqs. (1.3) and (1.4) leads to the hyperbolic heat conduction equation:

$$\rho c\tilde{\tau}\frac{\partial^2 T}{\partial t^2} + \rho c\frac{\partial T}{\partial t} = k\frac{\partial^2 T}{\partial x^2} \qquad (1.5)$$

The wave model represented in Eq. (1.5) removes the paradox of infinite speed of heat propagation assumed in Fourier's law. Tzou (1997), relates the relaxation time to the thermal wave speed as:

$$\tilde{\tau} = \frac{\alpha}{C^2} \qquad (1.6)$$

where α is the thermal diffusivity and C denotes the thermal wave speed. In the case of C approaching infinity, the relaxation time decreases to zero $(\tilde{\tau}=0)$ and the wave model reduces to Fourier law.

The Cattaneo and Vernotte *(CV)* wave model assumes an instantaneous heat flow. The temperature gradient is always the cause for the heat transfer, while the heat flux vector is always the effect. The dual-phase-lag model aims to remove the precedence assumption made in the thermal wave model. It allows either the temperature gradient

6

(cause) to precede the heat flux vector (effect) or the heat flux vector (cause) to precede the temperature gradient (effect). Mathematically this is represented by (Tzou, 1995a-c).

$$q\left(x, t+\tilde{\tau}_q\right) = -k\nabla T\left(x, t+\tilde{\tau}_T\right)$$ (1.7)

where $\tilde{\tau}_T$ is the phase lag of the temperature gradient and $\tilde{\tau}_q$ is the phase lag of the heat flux vector. For the case $\tilde{\tau}_T > \tilde{\tau}_q$, the temperature gradient established across a material volume is a result of the heat flow, implying that the heat flux vector is the cause and the temperature gradient is the effect. For $\tilde{\tau}_T < \tilde{\tau}_q$, on the other hand, heat flow is induced by the temperature gradient established at an earlier time, implying that the temperature gradient is the cause, while the heat flux vector is the effect.

1.2 Method of Laplace transform

The method of Laplace transform has been widely used in the solution of time-dependent heat conduction problems. The Laplace transform technique is convenient for the solution of composite medium problems involving regions of semi-infinite or infinite in extent. In this approach, the partial derivatives with respect to time is removed by the application of the Laplace transform, the resulting system of ordinary differential equations is solved and the transforms of temperatures are inverted; but the principal difficulty lies in the inversion of the resulting transform. The Laplace transform and the inversion formula of a function $F(t)$ are defined by:

Laplace transform $L\{F(t)\} \equiv \bar{F}(S) = \int_0^\infty e^{-St} F(t)\,dt$ (1.8)

Inversion formula: $F(t) = \dfrac{1}{2\pi i} \int_{\gamma - i\infty}^{\gamma + i\infty} e^{St} \bar{F}(S)\,dS$ (1.9)

where S is the Laplace transform variable, $i = \sqrt{-1}$, γ is a positive number, and the bar denotes the transform. Thus, the Laplace transform of a function $F(t)$ consists of

multiplying the function $F(t)$ by e^{-St} and integrating it over t from 0 to ∞. The inversion formula consists of the complex integration as defined by Eq. (1.9).

Some remarks on the existence of the Laplace transform of a function $F(t)$ as defined by Eq. (1.8) might be in order to illustrate the significance of this matter. For example, the integral (1.8) may not exist because, (1) $F(t)$ may have infinite discontinuities for some values of t, or (2) $F(t)$ may have singularity as $t \to 0$, or (3) $F(t)$ may diverge exponentially for large t. The conditions for the existence of the Laplace transform defined by Eq. (1.8) may be summarized as follows:

1. Function $F(t)$ is continuous or continuous in any interval $t_1 \le t \le t_2$, for $t_1 > 0$

2. $t^n |F(t)|$ is bounded as $t \to 0^+$ for some number n when $n < 1$.

3. Function $F(t)$ is of exponential order, namely, $e^{-rt}|F(t)|$ is bounded for some

   positive number γ as $t \to \infty$.

1.3 Properties of Laplace transform

Here we present some of the properties of Laplace transform that are useful in the solution of heat conduction problems, used in the present work, with Laplace transformation.

1.3.1 Laplace transform of derivatives

The Laplace transform of the first derivative $dF(t)/dt$ of a function $F(t)$ is readily obtained by utilizing the definition of the Laplace transform and integrating it by parts:

$$L\{F'(t)\} = \int_0^\infty F'(t)e^{-St}dt = \left[F(t)e^{-St}\right]_0^\infty + S\int_0^\infty F(t)e^{-St}dt$$

$$L\{F'(t)\} = S\bar{F}(S) - F(0) \tag{1.10}$$

where the prime denotes differentiation with respect to t and $F(0)$ indicates the value of $F(t)$ at $t = 0^+$, namely, as we approach zero the positive side. Thus, the Laplace

8

transform of the first derivative of a function is equal to multiplying the transform of the function by S and subtracting from it the value of this function at $t = 0^+$. This result is now utilized to determine the Laplace transform of the second derivative of a function $F(t)$ as:

$$L\{F^{\cdot\cdot}(t)\} = SL\{F^{\cdot}(t)\} - F^{\cdot}(0) = S\left[\bar{F}(S) - F(0)\right] - F^{\cdot}(0)$$

$$= S^2 \bar{F}(S) - SF(0) - F^{\cdot}(0)$$

(1.11)

1.3.2 Numerical inversion of the Laplace transform

A special technique employing the Riemann-sum approximation is developed for the Laplace inversion, (Tzou *et al.*, 1994) and (Chiffelle, 1994). The required Laplace inversion is given by:

$$\theta(\xi,\eta) = \frac{1}{2\pi i} \int_{\gamma-i\infty}^{\gamma+i\infty} W(\xi,S) e^{S\eta} ds$$

(1.12)

where $W(\xi,S)$ is the Laplace transform solution, η is the dimensionless time and ξ is the dimensionless distance. Introducing a variable transformation from S (complex) to ω (real),

$$S = \gamma + i\omega,$$

with γ being the real constant specifying the vertical segment in the Bromwich contour, Tzou (1997). Eq. (1.12) is reduced to a Fourier transform:

$$\theta(\xi,\eta) = \frac{e^{\gamma\eta}}{2\pi} \int_{-\infty}^{\infty} W(\xi,S = \gamma + i\omega) e^{i\omega\eta} d\omega$$

(1.13)

The Fourier integral thus obtained can be approximated by its Riemann-sum. Denoting ω as the wave frequency and τ^* the half-period of its oscillations, i.e, $\omega = n\pi/\tau^*$ for the nth wave mode and $\Delta\omega_n = \pi/\tau^*$ for all modes,

$$\theta(\xi,\eta) = \frac{e^{\gamma\eta}}{2\tau^*} \sum_{n=-\infty}^{\infty} W\left(\xi,S = \gamma + \frac{in\pi}{\tau^*}\right) e^{i(n\eta\pi/\tau^*)}$$

(1.14)

9

Noticing further that the wave modes with positive and negative n values appear in pairs and

$$W\left(\xi,\gamma+\frac{in\pi}{\tau^*}\right)e^{i\left(n\eta\pi/\tau^*\right)}+W\left(\xi,\gamma-\frac{in\pi}{\tau^*}\right)e^{-i\left(n\eta\pi/\tau^*\right)}=2\,\mathrm{Re}\left[W\left(\xi,\gamma+\frac{in\pi}{\tau^*}\right)e^{i\left(n\eta\pi/\tau^*\right)}\right] \quad (1.15)$$

Equation (1.14) can be expressed as:

$$\theta(\xi,\eta)=\frac{e^{\gamma\eta}}{\tau^*}\left[\frac{1}{2}W(\xi,\gamma)+\mathrm{Re}\sum_{n=1}^{\infty}W\left(\xi,\gamma+\frac{in\pi}{\tau^*}\right)e^{i\left(n\eta\pi/\tau^*\right)}\right] \quad (1.16)$$

where Re represents the real part of the summation. Since the function $e^{i\left(n\beta\pi/\tau^*\right)}$ has a fundamental period of 2π, the physical domain of η in Eq. (1.16) is $0\leq\eta\leq 2\tau^*$. At $\eta=\tau^*$, more precisely, Eq. (1.16) yields:

$$\theta(\xi,\eta)\cong\frac{e^{\gamma\eta}}{\eta}\left[\frac{1}{2}W(\xi,\gamma)+\mathrm{Re}\sum_{n=1}^{N}W\left(\xi,\gamma+\frac{in\pi}{\eta}\right)(-1)^{n}\right] \quad (1.17)$$

which is the inverse solution for $W(\xi,S)$. The Riemann-sum approximation for the Laplace inversion, Eq. (1.17), involves a single summation for numerical process. Its accuracy depends on the value of γ and the truncation error dictated by N. The value of γ must be selected so that the Bromwich contour encloses all the branch points, (Tzou, 1997). For faster convergence, however, numerous numerical experiments have shown that value satisfying the relation, (Tzou et al., 1994) and (Tzou, 1995a-c).

$$\gamma\eta\cong 4.7 \quad (1.18)$$

gives the most satisfactory results. The appropriate value of γ for faster convergence, in other words, depends on the instant of time (η) at which the lagging phenomenon is studied. The criterion shown by Eq. (1.18) is independent of the dimension of η. Should the energy equation be solved with dimensions, be solved by the method of Laplace transform, η in Eq. (1.18) is replaced by the real time t while the constant 4.7 remains. The quantity γ in this case, of course, has a dimension of 1/s. Selection for the

10

number of terms used in the Riemann-sum, N, is straightforward. At given values of γ, ξ, and η, the summation in Eq. (1.17) should continue until a prescribed threshold for the accumulated partial sum is satisfied.

The Riemann-sum approximation represented by Eq. (1.17) for the Laplace inversion has been rigorously examined, including the fundamental trigonometric, exponential, and hyperbolic functions, Chiffelle (1994) whose Laplace inversions are known. With Eq. (1.18), which guides the "optimal" values of γ at various times η, satisfactory convergence is usually achieved within several tens of terms in the Riemann-sum. The same numerical inversion technique has also been examined by the solution of the Love's wave equation in elasticity and some complicated solutions of thermo-mechanical coupling in the fast-transient process.

1.4 Objectives

- Formulate the basic concepts of the two approaches for both the parabolic and the hyperbolic heat conduction models.

- Select different case studies in conjugated heat transfer problems under the effect of parabolic, hyperbolic and dual phase heat conduction models and solve these case studies exactly with the proper boundary conditions.

- Resolve the parabolic and hyperbolic problems using the proposed simplified methods.

- Investigate the validity of the proposed methods as compared to the exact solution, which was conducted in this work.

- Resolve the case studies in conjugated heat transfer problems under the effect of parabolic, hyperbolic and dual-phase heat conduction models for imperfect contact.

- Using a perturbation technique to simplify the conjugated heat transfer problem.

11

1.5 Thesis layout

The thesis is divided into eight chapters, the first chapter is the introduction, it contains introduction to literature survey, lagging behavior, Laplace transform technique, and the objectives of the thesis. Chapters two and three present the generalized thermal boundary condition for parabolic and hyperbolic heat conduction models, respectively. First, mathematical formulation of the generalized boundary conditions. Second, an illustrative example as a case study. Third, the exact and approximate solutions using the Laplace transformation techniques are achieved. Chapter four shows the exact solution under the case study using Laplace transformation technique for conjugated heat conduction under the effect of dual phase model. Also, the lagging behavior is obtained. The conjugated heat conduction problems under the parabolic, hyperbolic and dual phase models are resolved exactly for imperfect contact in Chapter five. Chapter six, a perturbation technique is applied to solve the conjugated heat transfer problem under the case study using Laplace transformation technique. Chapter seven, results and discussions where the results of the case study models are shown graphically. Chapter eight contains the conclusions. Then, references are shown. Finally, the appendices present where the Laplace inverse programs that are used in the present work.

2- A GENERALIZED THERMAL BOUNDARY CONDITION FOR THE PARABOLIC HEAT CONDUCTION MODEL

2.1 Introduction

Situations in which a thin layer is in contact with an adjacent domain have numerous applications in engineering. The thin layer may be a thin solid-skin or thin fluid-film; both may be stationary or moving. The thermal behavior of such systems is usually described by two energy equations coupled at the interface between the thin layer and its adjacent domain. However, there are applications in which temperature variation in the transverse direction of the thin layer may be neglected. For these applications, a simplified thermal model can be introduced in which the boundary conditions, which describe the thermal interaction between the adjacent domain and its surroundings, are modified to include different thermal effects of the thin layer.

In the literature, there are two modified thermal boundary conditions that include the thermal effects of the thin layer and its interaction with both the adjacent domain and the surrounding conditions. The first modified boundary condition is the fourth kind (or Carslaw) boundary condition, (Beck *et al.*, 1992); (Carslaw and Jaeger, 1980). This boundary condition takes into account the thermal capacity of the thin layer and its capability to store thermal energy. The second modified boundary condition is of the fifth kind (or Jaeger) boundary condition, (Beck *et al.* 1992); (Carslaw and Jaeger, 1980). The fifth kind boundary takes into account the thermal capacity of the thin layer and permits heat losses by convection from the thin layer to the ambient.

It is worth mentioning that the above referenced modified boundary conditions assume a perfect thermal contact between the thin layer and its adjacent domain.

In reality, thin layers in contact with adjacent domains may have other effects on the thermal behavior of their adjacent domains. These effects are:

1. The enthalpy flow within the thin layer. This effect appears when the thin layer is in the form of a moving solid-skin or a moving fluid-film.

2. Multi-dimensional thermal diffusion effects. These effects appear when the thin layer has a very high thermal conductivity or when the temperature variation in directions other than the transverse must be taken into account.

3. Other thermal effects such as the viscous dissipation due to the fluid flow within the thin film, heat generated due to friction at the interface between the moving solid-skin and its adjacent domain, and heat transfer due to evaporation or melting of the thin layer. Viscous dissipation may be very important in applications involve thin fluid layer moving at very high velocity. In these applications, high velocity gradients enhance the generated energy by viscous dissipation.

4. Situations in which the thermal contact between the thin layer and its adjacent domain is imperfect.

The aim of this part of the present work is to derive a generalized thermal boundary condition, which takes into account all thermal effects of the thin layer. These effects are the thermal capacity, enthalpy flow, thermal diffusion, viscous dissipation and other aspects of thermal interaction between the thin layer and both its surroundings and adjacent domain. An example is given to demonstrate the importance of the introduced generalized thermal boundary condition. The effects of different geometrical and thermophysical properties on the validity of the generalized thermal boundary condition are investigated.

2.2 Analysis

Consider a thin layer that is in perfect thermal contact with an adjacent domain as shown in Fig. 2.1. The thin layer may be a stationary or a moving solid-skin or a fluid-film. The thin layer has high thermal conductivity and as a result, the temperature distribution in the transverse direction of the layer is assumed to be lumped. Applying the balance of thermal energy on a differential element of the thin layer yields:

$$q_y{}^k dx - \frac{dq_x{}^k}{dx} dx \Delta y - \frac{dq_x{}^h}{dx} dx \Delta y - q^c dx + q^i dx = \rho_2 c_2 \frac{\partial T_2}{\partial t} dx \Delta y \tag{2.1}$$

where q^k, q^c and q^h refer to heat transfer by conduction, convection and enthalpy flow, respectively, and q^i refers to different forms of heat fluxes imposed on the outer surface of the thin layer. The enthalpy flow term accounts for the energy carried due to the thin layer movement. Substituting for $q_y{}^k$, $q_x{}^k$, $q_x{}^h$ and q^c by their constitutive laws yields:

$$-k_1 \frac{\partial T_1(t,x,y_i)}{\partial y} + \Delta y \frac{\partial}{\partial x}\left(k_2 \frac{\partial T_2(t,x,y_i)}{\partial x}\right) - h_o(T_2(t,x,y_i) - f(t,x)) + q^i(t,x)$$

$$- \rho_2 c_2 \Delta y u_x \frac{\partial T_2(t,x,y_i)}{\partial x} - \rho_2 c_2 \Delta y \frac{\partial T_2(t,x,y_i)}{\partial t} = 0 \tag{2.2}$$

where subscripts 1 and 2 refer to the properties of the adjacent (thick) domain and the thin layer, respectively, and u_x refers to the velocity (in the x-direction) of the moving solid–skin or to the average velocity (in the x-direction) of the fluid flow within the thin film since the velocity distribution is assumed to be lumped in the transverse direction of the film. Also, $\Delta y = (y_o - y_i)$ is the thickness of the thin layer, $f(x,t)$ is a space-and time-dependent surface temperature and h_o is the heat transfer coefficient at the outer surface of the thin layer.

15

$$y_i \quad \Delta y \quad y_o \qquad \qquad y$$

$$q_x^{\,k} \quad q_x^{\,h}$$

$$q_y^{\,k} \longrightarrow \qquad \longleftarrow q^i \qquad dx$$

$$\longrightarrow q^c$$

$$q_x^{\,k} + \frac{\partial q_x^{\,k}}{\partial x} dx \qquad q_x^{\,h} + \frac{\partial q_x^{\,h}}{\partial x} dx$$

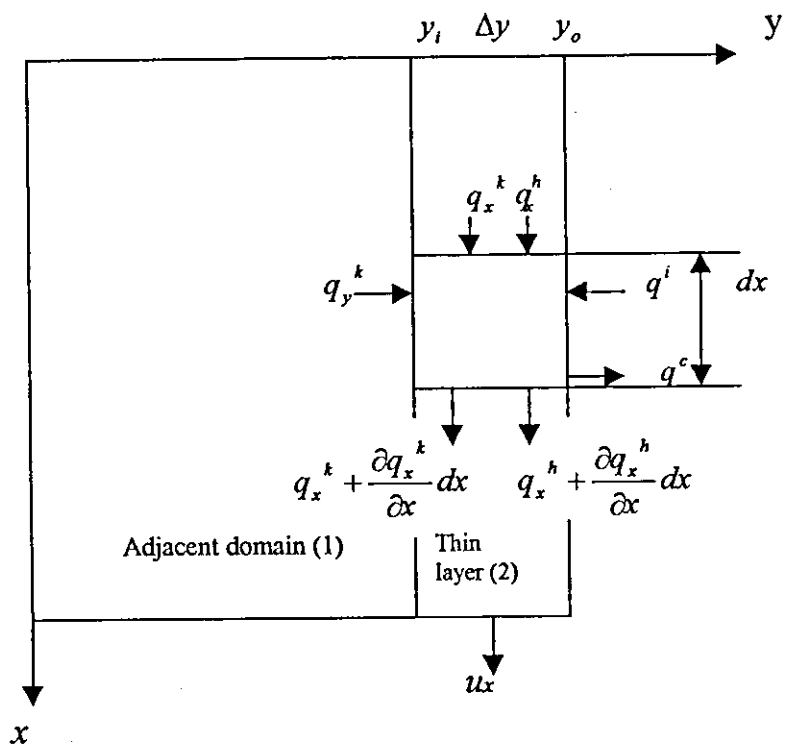Adjacent domain (1)   Thin layer (2)

$$u_x$$

$$x$$

Fig.2.1. Schematic diagram of the thin layer and its adjacent domain

16

For thin layers having high thermal conductivity and in perfect thermal contact with their adjacent domains, the temperature of the thin layer is assumed to be lumped transversally and equal to the boundary temperature of the adjacent domain, and as a result, $T_1(t,x,y_i) = T_2(t,x,y_i)$. This reduces Eq. (2.2) to:

$$-k_1 \frac{\partial T_1(t,x,y_i)}{\partial y} + \Delta y \frac{\partial}{\partial x}\left(k_2 \frac{\partial T_1(t,x,y_i)}{\partial x}\right) - h_o(T_1(t,x,y_i) - f(t,x)) + q'(t,x)$$
$$-\rho_2 c_2 \Delta y u_x \frac{\partial T_1(t,x,y_i)}{\partial x} - \rho_2 c_2 \Delta y \frac{\partial T_1(t,x,y_i)}{\partial t} = 0 \qquad (2.3)$$

Equation (2.3) is generalized to three-dimensional cases as:

$$\mp k_1 \frac{\partial T_1(t,x,y_i,z)}{\partial y} + \Delta y\left[\frac{\partial}{\partial x}\left(k_2 \frac{\partial T_1(t,x,y_i,z)}{\partial x}\right) + \frac{\partial}{\partial z}\left(k_2 \frac{\partial T_1(t,x,y_i,z)}{\partial z}\right)\right] - h_o(T_1(t,x,y_i,z)$$
$$- f(t,x,z)) + q'(t,x,z) + \Delta y \mu_2 \Phi - \rho_2 c_2 \Delta y\left[u_x \frac{\partial T_1(t,x,y_i,z)}{\partial x} + u_z \frac{\partial T_1(t,x,y_i,z)}{\partial z}\right]$$
$$- \rho_2 c_2 \Delta y \frac{\partial T_1(t,x,y_i,z)}{\partial t} = 0 \qquad (2.4)$$

The first term in Eq. (2.4) has a negative sign when the outward drawn normal to the thin layers has the same direction as the positive y-direction, otherwise it has a positive sign. The term Φ represents the thermal energy generated within the flowing of a thin fluid film as a result of dissipation which is given as follows:

$$\Phi = 2\left[\left(\frac{\partial u_x}{\partial x}\right)^2 + \left(\frac{\partial u_z}{\partial z}\right)^2\right] + \left(\frac{\partial u_x}{\partial y}\right)^2 + \left(\frac{\partial u_z}{\partial y}\right)^2 + \left(\frac{\partial u_z}{\partial x} + \frac{\partial u_x}{\partial z}\right)^2 \qquad (2.5)$$

Where it is assumed that $u_y=0$ within the thin flowing film. Terms such as $\partial u_x/\partial y$ and $\partial u_z/\partial y$ may be given by their average values within the transverse direction of the flowing film. When the thin layer is a moving solid skin, then $\Phi=0$, and q' will contain a term that represents the thermal energy generated as a result of friction between the surface of the moving solid skin and that of the adjacent domain, as follows:

17

$$q^i = \mu^* P \left[\sqrt{u_x^{\,2} + u_z^{\,2}} \right] \tag{2.6}$$

where μ^* is the friction coefficient and P is the normal stress acting on the thin skin to maintain its contact with the adjacent domain. Equation (2.4) is considered as the generalized thermal boundary condition at the interface between the thin layer and its adjacent domain and it can be used to solve the energy equation in the adjacent (thick) domain. The derived boundary condition takes into account all possible effects of the thin layer and its interaction with both the ambient conditions and the adjacent domain. These effects are the thermal capacity of the thin layer, thermal diffusion in different directions of the layer, enthalpy flow within the layer, friction and viscous dissipated energy, convective losses from the skin, and other forms of incident energy fluxes.

Six boundary conditions may be considered as special cases of Eq. (2.4). To obtain these cases, rewrite Eq. (2.4) in the following form:

$$\mp F_1 k_1 \frac{\partial T_1(t,x,y_i,z)}{\partial y} + F_2 \Delta y \left[\frac{\partial}{\partial x} \left(k_2 \frac{\partial T_1(t,x,y_i,z)}{\partial x} \right) + \frac{\partial}{\partial z} \left(k_2 \frac{\partial T_1(t,x,y_i,z)}{\partial z} \right) \right] -$$

$$F_3 h_o (T_1(t,x,y_i,z) - f(t,x,z)) + F_4 q^i(t,x,z) + F_5 \Delta y \mu_2 \Phi - F_6 \rho_2 c_2 \Delta y$$

$$* \left[u_x \frac{\partial T_1(t,x,y_i,z)}{\partial x} + u_z \frac{\partial T_1(t,x,y_i,z)}{\partial z} \right] - F_7 \rho_2 c_2 \Delta y \frac{\partial T_1(t,x,y_i,z)}{\partial t} = 0 \tag{2.7}$$

where F_i, with i=1,2,3,.........7, and may have a value of 0 or 1 depending on the particular case. The six special cases of Eq. (2.7) are given as follows:

1. **The first kind or Dirichlet boundary condition.**

For this kind: $F_1 = F_2 = F_4 = F_5 = F_6 = F_7 = 0$, and $F_3 = 1$, and as a result:

$$T_1(t,x,y_i,z) = f(t,x,z) \tag{2.8}$$

In this kind of boundary condition, the boundary is maintained at a prescribed temperature $f(t,x,z)$.

18

2. The second kind or Neumann boundary condition

For this kind: $F_2 = F_3 = F_5 = F_6 = F_7 = 0$, and $F_1 = F_4 = 1$, and as a result:

$$\pm k_1 \frac{\partial T_1(t,x,y_i,z)}{\partial y} = q^i(t,x,z) \tag{2.9}$$

This boundary condition represents a prescribed heat flux q^i imposed on the boundary.

3. The third kind or Robin boundary condition:

For this kind: $F_2 = F_4 = F_5 = F_6 = F_7 = 0$, and $F_1 = F_3 = 1$, and as a result:

$$\mp k_1 \frac{\partial T_1(t,x,y_i,z)}{\partial y} = h_o(T_1(t,x,y_i,z) - f(t,x,z)) \tag{2.10}$$

This kind represents a convective heat transfer from the outer surface of the thin layer to a prescribed ambient temperature $f(t, x, z)$

4. The fourth kind or Carslaw boundary condition:

For this kind: $F_2 = F_3 = F_5 = F_6 = 0$, and $F_1 = F_4 = F_7 = 1$, and as a result:

$$\mp k_1 \frac{\partial T_1(t,x,y_i,z)}{\partial y} = q^i(t,x,z) - \rho_2 c_2 \Delta y \frac{\partial T_1(t,x,y_i,z)}{\partial t} \tag{2.11}$$

In this kind of boundary condition, the heat capacity effect of the thin layer is taken into consideration. A physical example of this kind is heat transfer into a large ceramic object with a thin metal coating on the surface. The temperature distribution in the metal coating may be neglected across the small thickness Δy because the thermal conductivity of the metal is far greater than that of ceramic, but storage of thermal energy in the metal coating may not be neglected. This boundary condition can also describe a surface film composed of a well-stirred fluid with heat capacity $\Delta y \rho_2 c_2$.

5. The fifth kind or Jaeger boundary condition:

For this kind: $F_2 = F_4 = F_5 = F_6 = 0$, and $F_1 = F_3 = F_7 = 1$, and as a result:

$$\mp k_1 \frac{\partial T_1(t,x,y_i,z)}{\partial y} = h_o(T_1(t,x,y_i,z) - f(t,x,z)) + \rho_2 c_2 \Delta y \frac{\partial T_1(t,x,y_i,z)}{\partial t} \tag{2.12}$$

19

This kind of boundary condition takes into consideration heat losses from the film and it is physically identical to the fourth kind except that, instead of a specified heat flux on the outer surface of the thin layer, there is a specified heat transfer coefficient h_o.

6. The sixth kind boundary condition:

For this kind: $F_1 = F_2 = F_3 = F_4 = F_5 = F_6 = F_7 = 1$.

In addition to the above mentioned six kinds of boundary conditions, there is the zeroth kind boundary condition which can not be derived from the generalized kind given by Eq.(2.4). The reason for this is that the zeroth kind boundary condition has no physical content.

2.3 Case study

Consider a two-layer slab consists of the first layer (thick) in $0 \leq x \leq a$ and the second layer (thin) in $a \leq x \leq b$, which are in perfect thermal contact as illustrated in Fig. 2(a). Let k_1 and k_2 be the thermal conductivities, and α_1 and α_2 the thermal diffusivities for the first and second layers, respectively. Initially, the first and the second region are at temperature T_i. For $t>0$ the boundary surface at x=0 is kept at T_w and the boundary surface at $x=b$ is kept insulated. The thickness of the two layers is assumed to be very small relative to the height of the slab, so it is reasonable to assume that the conducted heat is transferred in the x-direction only.
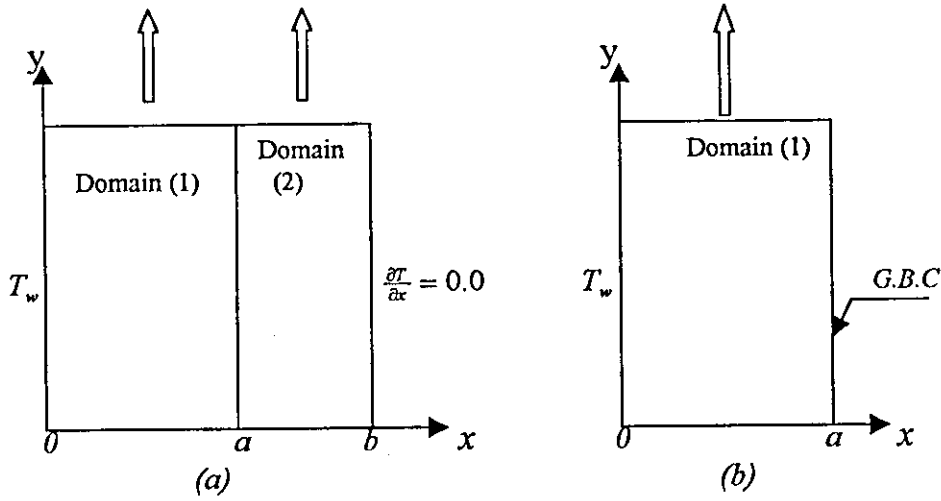
Fig. 2.2: Schematic diagram of the thin layer and its adjacent domain.

2.3.1 Exact model

In this case, two energy equations coupled at the interface have to be solved. These equations are written as:

$$\alpha_1 \frac{\partial^2 T_1}{\partial x^2} = \frac{\partial T_1}{\partial t} \qquad \text{in } 0 \le x \le a \qquad (2.13)$$

$$\alpha_2 \frac{\partial^2 T_2}{\partial x^2} = \frac{\partial T_2}{\partial t} \qquad \text{in } a \le x \le b \qquad (2.14)$$

which assume the following initial and boundary conditions

$$T_1(x,0) = T_2(x,0) = T_i$$

$$T_1(0,t) = T_w$$

$$T_1(a,t) = T_2(a,t) \qquad (2.15)$$

$$k_1 \frac{\partial T_1(a,t)}{\partial x} = k_2 \frac{\partial T_2(a,t)}{\partial x}$$

$$\frac{\partial T_2(b,t)}{\partial x} = 0.0$$

Using the following dimensionless parameters

$$\theta = \frac{T - T_w}{T_i - T_w}, \qquad \xi = \frac{x}{a}, \qquad \eta = \frac{\alpha_1 t}{a^2}$$

21

Equations (2.13) and (2.14) and their initial and boundary conditions become:

$$\frac{\partial^2 \theta_1}{\partial \xi^2} = \frac{\partial \theta_1}{\partial \eta} \qquad \text{in} \quad 0 \le \xi \le 1.0 \qquad\qquad (2.16)$$

$$\frac{\partial^2 \theta_2}{\partial \xi^2} = \frac{1}{\alpha_r}\frac{\partial \theta_2}{\partial \eta} \qquad \text{in} \quad 1.0 \le \xi \le R \qquad\qquad (2.17)$$

$$\theta_1(\xi,0) = \theta_2(\xi,0) = 1.0 \qquad\qquad (2.18)$$

$$\theta_1(0,\eta) = 0.0$$

$$\theta_1(1,\eta) = \theta_2(1,\eta) \qquad\qquad (2.19)$$

$$\frac{\partial \theta_1(1,\eta)}{\partial \xi} = K_r \frac{\partial \theta_2(1,\eta)}{\partial \xi}$$

$$\frac{\partial \theta_2(R,\eta)}{\partial \xi} = 0.0$$

where $K_r = k_2/k_1$ is the thermal conductivity ratio, $\alpha_r = \alpha_2/\alpha_1$ is the thermal diffusivity ratio and $R=b/a$. From the definition of R, it is clear that (R-1) represents the dimensionless thin layer thickness $(=\frac{b-a}{a})$. Now, with the notation that $L\{\theta(\xi,\eta)\} = W(\xi,S)$, Laplace transformation of Eqs. (2.16) and (2.17), yields:

$$\frac{d^2 W_1}{d\xi^2} - SW_1 = -1 \qquad\qquad (2.20)$$

$$\frac{d^2 W_2}{d\xi^2} - \frac{S}{\alpha_r}W_2 = -\frac{1}{\alpha_r} \qquad\qquad (2.21)$$

These two equations assume the following solutions:

$$W_1(\xi,S) = C_1 e^{\xi\sqrt{S}} + C_2 e^{-\xi\sqrt{S}} + \frac{1}{S} \qquad\qquad (2.22)$$

$$W_2(\xi,S) = C_3 e^{\xi\sqrt{S/\alpha_r}} + C_4 e^{-\xi\sqrt{S/\alpha_r}} + \frac{1}{S} \qquad\qquad (2.23)$$

Also, the Laplace transformation Eq. (2.19) yields:

22

$$W_1(0,S) = 0.0$$

$$W_1(1,S) = W_2(1,S)$$

<div style="text-align:right">(2.24)</div>

$$\frac{dW_1(1,S)}{\partial \xi} = K_r \frac{dW_2(1,S)}{\partial \xi}$$

$$\frac{dW_2(R,S)}{\partial \xi} = 0.0$$

Insert Eqs. (2.22) and (2.23) into (2.24) and solve for C_1, C_2, C_3, C_4 to yield:

$$C_1 = \frac{\left(-\dfrac{1}{S}\right)\left\{\dfrac{e^{-2\sqrt{S}}\left\{\left(1+\dfrac{K_r}{\sqrt{\alpha_r}}\right)+\left(e^{(2R-2)\sqrt{S/\alpha_r}}\right)\left(1-\dfrac{K_r}{\sqrt{\alpha_r}}\right)\right\}}{\left\{\left(1-\dfrac{K_r}{\sqrt{\alpha_r}}\right)+\left(e^{(2R-2)\sqrt{S/\alpha_r}}\right)\left(1+\dfrac{K_r}{\sqrt{\alpha_r}}\right)\right\}}\right\}}{\left\{1+\dfrac{e^{-2\sqrt{S}}\left\{\left(1+\dfrac{K_r}{\sqrt{\alpha_r}}\right)+\left(e^{(2R-2)\sqrt{S/\alpha_r}}\right)\left(1-\dfrac{K_r}{\sqrt{\alpha_r}}\right)\right\}}{\left\{\left(1-\dfrac{K_r}{\sqrt{\alpha_r}}\right)+\left(e^{(2R-2)\sqrt{S/\alpha_r}}\right)\left(1+\dfrac{K_r}{\sqrt{\alpha_r}}\right)\right\}}\right\}} ,$$

$$C_2 = \frac{-\dfrac{1}{S}}{\left[1+\dfrac{e^{-2\sqrt{S}}\left\{\left(1+\dfrac{K_r}{\sqrt{\alpha_r}}\right)+\left(e^{(2R-2)\sqrt{S/\alpha_r}}\right)\left(1-\dfrac{K_r}{\sqrt{\alpha_r}}\right)\right\}}{\left\{\left(1-\dfrac{K_r}{\sqrt{\alpha_r}}\right)+\left(e^{(2R-2)\sqrt{S/\alpha_r}}\right)\left(1+\dfrac{K_r}{\sqrt{\alpha_r}}\right)\right\}}\right]} ,$$

$$C_3 = \frac{C_1 e^{\sqrt{S}} + C_2 e^{-\sqrt{S}}}{e^{\sqrt{S/\alpha_r}}\left(1+e^{\sqrt{S/\alpha_r}(2R-2)}\right)} \quad \text{and} \quad C_4 = \left\{\frac{C_1 e^{\sqrt{S}} + C_2 e^{-\sqrt{S}}}{e^{\sqrt{S/\alpha_r}}\left(1+e^{\sqrt{S/\alpha_r}(2R-2)}\right)}\right\} e^{2RM_1}$$

Equations (2.22) and (2.23) are inverted numerically using a computer program based on Riemann-sum approximation as:

$$\theta_k(\xi,\eta) \cong \frac{e^{\gamma\eta}}{\eta}\left[\frac{1}{2}W_k(\xi,\gamma) + \text{Re}\sum_{n=1}^{N} W_k\left(\xi,\gamma+\frac{in\pi}{\eta}\right)(-1)^n\right]$$

<div style="text-align:right">(2.25)</div>

23

where k=1 for the thick domain and k=2 for the thin domain. In Eq. (2.25), Re represents the real part of the summation, $i = \sqrt{-1}$ and $\gamma\eta = 4.7$ gives the most satisfactory results, (Tzou, 1997). Equation (2.25) yields the exact temperature distribution in both domains for the perfect contact parabolic heat conduction model case. The computer model results with changing thickness ratios, thermal diffusivity ratios and thermal conductivity ratios were exhibited in the figures which will be analyzed later.

2.3.2 Approximate model

In this case, we intend to solve one energy equation in the thick domain (domain 1), ignore the existence of the thin layer and replace its thermal effect by using the generalized thermal boundary condition at the thick domain interfacial boundary with the thin domain. It will be assumed that the two layers are in perfect thermal contact and the thin layer is thin enough so that it has the same lumped temperature distribution in its transverse direction. This temperature is equal to the interfacial temperature between the thin and the thick domains. The thick domain energy equation is given as:

$$\alpha_1 \frac{\partial^2 T_1}{\partial x^2} = \frac{\partial T_1}{\partial t} \qquad in \quad 0 \le x \le a \qquad (2.26)$$

which assumes the following initial and boundary conditions:

$$T_1(x,0) = T_i \qquad (2.27)$$

$$T_1(0,t) = T_w \qquad (2.28)$$

$$-k_1 \frac{\partial T_1(a,t)}{\partial x} - \rho_2 c_2 (b-a) \frac{\partial T_1(a,t)}{\partial t} = 0.0$$

The second equation in (2.28) represents the generalized parabolic thermal boundary condition, which takes into account two thermal effects of the eliminated thin layer.

24

These two effects are the thermal storage of the thin layer and the thermal diffusion in the thin film transverse direction.

Using the following dimensionless parameter

$$\theta = \frac{T - T_w}{T_i - T_w}, \qquad \xi = \frac{x}{a}, \qquad \eta = \frac{\alpha_1 t}{a^2}$$

Equations (2.26), (2.27) and (2.28) become:

$$\frac{\partial^2 \theta_1}{\partial \xi^2} = \frac{\partial \theta_1}{\partial \eta} \qquad\qquad \text{in} \quad 0 \le \xi \le 1.0 \qquad\qquad (2.29)$$

$$\theta_1(\xi, 0) = 1.0 \qquad\qquad (2.30)$$

$$\theta_1(0, \eta) \qquad\qquad (2.31)$$

$$\frac{\partial \theta_1(1, \eta)}{\partial \xi} + H \frac{\partial \theta_1(1,, \eta)}{\partial \eta} = 0.0$$

where $H = \dfrac{K_r}{\alpha_r}(R - 1)$ and $R = b/a$. In a manner similar to what has been done previously, using Laplace transformation technique. Eqs. (2.29) and (2.31) assume the following solution in the Laplacian domain:

$$W_1(\xi, S) = A e^{\xi\sqrt{S}} + B e^{-\xi\sqrt{S}} + \frac{1}{S} \qquad\qquad (2.32)$$

where: $A = \dfrac{-\dfrac{1}{S}}{\left(1 + \dfrac{e^{-2\sqrt{S}}\left(1 - H\sqrt{S}\right)}{\left(1 + H\sqrt{S}\right)}\right)} \left(\dfrac{e^{-2\sqrt{S}}\left(1 - H\sqrt{S}\right)}{\left(1 + H\sqrt{S}\right)}\right)$ and $B = \dfrac{-\dfrac{1}{S}}{\left(1 + \dfrac{e^{-2\sqrt{S}}\left(1 - H\sqrt{S}\right)}{\left(1 + H\sqrt{S}\right)}\right)}$

Equation (2.32) is inverted numerically using a computer program based on Riemann-sum approximation as:

$$\theta_1(\xi, \eta) \cong \frac{e^{\gamma\eta}}{\eta}\left[\frac{1}{2}W_1(\xi, \gamma) + \mathrm{Re}\sum_{n=1}^{N} W_1\left(\xi, \gamma + \frac{in\pi}{\eta}\right)(-1)^n\right] \qquad\qquad (2.33)$$

Equation (3.33) represent the approximate temperature distribution in the thick domain.

25

experimentally the existence of thermal waves using super fluid liquid helium near absolute zero. Since then, the wave nature of heat propagation has been the subject of numerous investigations, (Kim *et al.*, 1990); (Vick and Ozisik, 1983); (Ozisik and Tzou, 1994).

The aim of this part of the present work is to derive a generalized thermal boundary condition for a given domain, which is in thermal contact with an adjacent thin layer. The thermal behavior of both domains is described by the hyperbolic energy equation. The generalized boundary condition is applied at the boundary of the adjacent domain and takes into account all thermal effects of the thin layer. These effects are the thermal capacity, enthalpy flow, thermal diffusion, viscous dissipation and other aspects of thermal interaction between the thin layer and both its surroundings and adjacent domain. The generalized thermal boundary condition is modified to describe situations in which the thermal contact between the thin layer and its adjacent domain is imperfect. An example is given to demonstrate the importance of the introduced generalized thermal boundary condition. The effects of different geometrical and thermophysical properties on the validity of the generalized thermal boundary condition are investigated.

3.2 Analysis

Consider a thin layer that is in perfect thermal contact with an adjacent domain as shown in Fig. 2.1 and follow the same procedure shown in chapter 2. Applying the balance of thermal energy on a differential element of the thin layer yields:

$$q_y^k dx - \frac{dq_x^k}{dx}dx\Delta y - \frac{dq_x^h}{dx}dx\Delta y - q^c dx + q^i dx = \rho_2 c_2 \frac{\partial T_2}{\partial t}dx\Delta y \qquad (3.1)$$

where q^k, q^c, q^h and q^i were defined in chapter 2. The constitution law which relates the conduction heat flux with temperature gradient is given by the classical thermal wave model proposed by (Cattaneo, 1958) and (Vernotte, 1961) as:

$$q_y^k + \widetilde{\tau}_1 \frac{\partial q_y^k}{\partial t} = -k_1 \frac{\partial T_1}{\partial y} \tag{3.2}$$

where $\widetilde{\tau}_1$ is the thermal relaxation time, which is the effective mean free path divided by the phonon speed. In the absence of the relaxation time, $\widetilde{\tau}_1 = 0$, Eq. (3.2) reduces to the classical Fourier's law.

Now substitute for q_y^k from Eq. (3.1) into (3.2) and express q_x^h and q^c by their constitutive laws after neglecting the axial diffusion within the thin layer, which is not significant in most applications, yields:

$$-k_1 \frac{\partial T_1(t,x,y_i)}{\partial y} = h_o(T_2(t,x,y_i) - f(t,x,y_i)) - q^i(t,x,y_i) + \rho_2 c_2 \Delta y u_x \frac{\partial T_2(t,x,y_i)}{\partial x}$$

$$+ \rho_2 c_2 \Delta y \frac{\partial T_2(t,x,y_i)}{\partial t} + \widetilde{\tau}_1 \frac{\partial}{\partial t} \{ h_o(T_2(t,x,y_i) - f(t,x,y_i)) - q^i(t,x,y_i) \} +$$

$$\widetilde{\tau}_1 \frac{\partial}{\partial t} \left(\rho_2 c_2 \Delta y u_x \frac{\partial T_2(t,x,y_i)}{\partial x} + \rho_2 c_2 \Delta y \frac{\partial T_2(t,x,y_i)}{\partial t} \right) \tag{3.3}$$

where subscripts 1 and 2 refer to the properties of the adjacent (thick) domain and the thin layer, respectively, and u_x refers to the velocity (in the x-direction) of the moving solid–skin or to the average velocity (in the x-direction) of the fluid flow within the thin film since the velocity distribution is assumed to be lumped in the transverse direction of the film. Also, $\Delta y (= y_o - y_i)$ is the thickness of the thin layer, $f(x,t)$ is a space-and time-dependent surface temperature and h_o is the heat transfer coefficient at the outer surface of the thin layer.

For thin layers having high thermal conductivity and in perfect thermal contact with their adjacent domains, the temperature of the thin layer is assumed to be lumped transversally and equal to the boundary temperature of the adjacent domain, and as a result, $T_1(t,x,y_i) = T_2(t,x,y_i)$. This reduces Eq. (3.3) to:

$$-k_1 \frac{\partial T_1(t,x,y_i)}{\partial y} =$$

$$h_o(T_1(t,x,y_i) - f(t,x,y_i)) - q^i(t,x,y_i) + \rho_2 c_2 \Delta y u_x \frac{\partial T_1(t,x,y_i)}{\partial x} + \rho_2 c_2 \Delta y \frac{\partial T_1(t,x,y_i)}{\partial t} +$$

$$\tilde{\tau}_1 \frac{\partial}{\partial t} \left\{ h_o(T_1(t,x,y_i) - f(t,x,y_i)) - q^i(t,x,y_i) + \rho_2 c_2 \Delta y \left(u_x \frac{\partial T_1(t,x,y_i)}{\partial x} + \frac{\partial T_1(t,x,y_i)}{\partial t} \right) \right\}$$

(3.4)

Equation (3.4) is generalized to three-dimensional cases as:

$$\pm k_1 \frac{\partial T_1(t,x,y_i)}{\partial y} = h_o(T_1(t,x,y_i,z) - f(t,x,y_i,z)) - q^i(t,x,y_i,z) - \Delta y \mu_2 \Phi$$

$$+ \rho_2 c_2 \Delta y \left[u_x \frac{\partial T_1(t,x,y_i,z)}{\partial x} + u_z \frac{\partial T_1(t,x,y_i,z)}{\partial z} \right] + \rho_2 c_2 \Delta y \frac{\partial T_1(t,x,y_i,z)}{\partial t} +$$

$$\tilde{\tau}_1 \frac{\partial}{\partial t} \left\{ h_o(T_1(t,x,y_i,z) - f(t,x,y_i,z)) - q^i(t,x,y_i,z) - \Delta y \mu_2 \Phi \right\} +$$

$$\tilde{\tau}_1 \frac{\partial}{\partial t} \left\{ \rho_2 c_2 \Delta y \left[u_x \frac{\partial T_1(t,x,y_i,z)}{\partial x} + u_z \frac{\partial T_1(t,x,y_i,z)}{\partial z} \right] + \rho_2 c_2 \Delta y \frac{\partial T_1(t,x,y_i,z)}{\partial t} \right\}$$

(3.5)

The first term in Eq. (3.5) has a negative sign when the outward drawn normal to the thin layers has the same direction as the positive y-direction, otherwise it has a positive sign. The term Φ represents the thermal energy generated within the flowing thin fluid film as a result of dissipation which is given as follows:

$$\Phi = 2 \left[\left(\frac{\partial u_x}{\partial x} \right)^2 + \left(\frac{\partial u_z}{\partial z} \right)^2 \right] + \left(\frac{\partial u_x}{\partial y} \right)^2 + \left(\frac{\partial u_z}{\partial y} \right)^2 + \left(\frac{\partial u_z}{\partial x} + \frac{\partial u_x}{\partial z} \right)^2$$

(3.6)

Where it is assumed that $u_y=0$ within the thin flowing film. Terms such as $\partial u_x/\partial y$ and $\partial u_z/\partial y$ may be given by their average values within the transverse direction of the flowing film. When the thin layer is a moving solid -skin, then $\Phi = 0$, and q^i will contain a term that represents the thermal energy generated as a result of

29

friction between the surface of the moving solid skin and that of the adjacent domain as follows:

$$q^i = \mu^* P\left[\sqrt{u_x^2 + u_z^2}\right] \tag{3.7}$$

where μ^* is the friction coefficient and P is the normal stress acting on the thin skin to maintain its contact with the adjacent domain. Equation (3.5) is reduced to:

$$\pm k_1 \frac{\partial T_1(t,x,y_i)}{\partial y} = h_o(T_1(t,x,y_i,z) - f(t,x,y_i,z)) - q^i(t,x,y_i,z) - \Delta y \mu_2 \Phi(t,x,y_i,z)$$

$$+ \rho_2 c_2 \Delta y\left[u_x \frac{\partial T_1(t,x,y_i,z)}{\partial x} + u_z \frac{\partial T_1(t,x,y_i,z)}{\partial z}\right] + \rho_2 c_2 \Delta y \frac{\partial T_1(t,x,y_i,z)}{\partial t} +$$

$$\tilde{\tau}_1 h_o\left(\frac{\partial T_1(t,x,y_i,z)}{\partial t} - \frac{\partial f(t,x,y_i,z)}{\partial t}\right) - \tilde{\tau}_1 \frac{\partial q^i(t,x,y_i,z)}{\partial t} - \tilde{\tau}_1 \Delta y \mu_2 \frac{\partial \Phi(t,x,y_i,z)}{\partial t}$$

$$\tilde{\tau}_1 \rho_2 c_2 \Delta y \frac{\partial}{\partial t}\left[u_x \frac{\partial T_1(t,x,y_i,z)}{\partial x} + u_z \frac{\partial T_1(t,x,y_i,z)}{\partial z}\right] + \tilde{\tau}_1 \rho_2 c_2 \Delta y \frac{\partial^2 T_1(t,x,y_i,z)}{\partial t^2} \tag{3.8}$$

Equation (3.8) is considered as the generalized thermal boundary condition for the hyperbolic energy equation at the interface between the thin layer and its adjacent domain, which can be used to solve the hyperbolic energy equation in the adjacent (thick) domain. The derived boundary condition takes into account all possible effects of the thin layer and its interaction with both the ambient conditions and the adjacent domain. These effects are the thermal capacity of the thin layer, thermal diffusion in different directions of the layer, enthalpy flow within the layer, friction and viscous dissipated energy, convective losses from the skin, and other forms of incident energy fluxes. Also, Eq. (3.8) takes into account the effect of time phase lag effect between the

conduction heat flux and the temperature gradient in both the thin layer and its adjacent

domain.

Six boundary conditions may be considered as special cases of Eq. (3.8). To

obtain these cases, rewrite Eq. (3.8) in the following form:

$$\pm F_1 k_1 \frac{\partial T_1(t,x,y_i)}{\partial y} =$$

$$F_2 h_o (T_1(t,x,y_i,z) - f(t,x,y_i,z)) - F_3 q'(t,x,y_i,z) - F_4 \Delta y \mu_2 \Phi(t,x,y_i,z)$$

$$+ F_5 \rho_2 c_2 \Delta y \left[u_x \frac{\partial T_1(t,x,y_i,z)}{\partial x} + u_z \frac{\partial T_1(t,x,y_i,z)}{\partial z} \right] + F_6 \rho_2 c_2 \Delta y \frac{\partial T_1(t,x,y_i,z)}{\partial t} +$$

$$F_2 \tilde{\tau}_1 h_o \left(\frac{\partial T_1(t,x,y_i,z)}{\partial t} - \frac{\partial f(t,x,y_i,z)}{\partial t} \right) - F_3 \tilde{\tau}_1 \frac{\partial q'(t,x,y_i,z)}{\partial t} - F_4 \tilde{\tau}_1 \Delta y \mu_2 \frac{\partial \Phi(t,x,y_i,z)}{\partial t}$$

$$F_5 \tilde{\tau}_1 \rho_2 c_2 \Delta y \frac{\partial}{\partial t} \left[u_x \frac{\partial T_1(t,x,y_i,z)}{\partial x} + u_z \frac{\partial T_1(t,x,y_i,z)}{\partial z} \right] + F_6 \tilde{\tau}_1 \rho_2 c_2 \Delta y \frac{\partial^2 T_1(t,x,y_i,z)}{\partial t^2}$$

$$(3.9)$$

where F_i , with i=1,2,3,............6, may have a value of 0 or 1 depending on the

particular case. The six special cases of Eq. (3.9) are given as follows:

1. **The first kind boundary condition.**

For this kind: F₁=F₃=F₄=F₅=F₆=0, and F₂=1, and as a result:

$$\tilde{\tau}_1 \frac{\partial T_1(t,x,y_i,z)}{\partial t} + T_1(t,x,y_i,z) = \tilde{\tau}_1 \frac{\partial f(t,x,y_i,z)}{\partial t} + f(t,x,y_i,z)$$
$$(3.10)$$

In the absence of thermal relaxation time, $\tilde{\tau}_1 = 0$, Eq. (3.10) is reduced to:

$$T_1(t,x,y_i,z) = f(t,x,z)$$

31

which is the classical thermal boundary condition of the first kind for the parabolic diffusion energy equation as in Eq. (2.8). The boundary condition given by the previous equation is also; known as Dirichlet boundary condition, which describes the behavior of a boundary maintained at a prescribed temperature $f(t,x,z)$.

2. The second kind boundary condition

For this kind: $F_2 = F_4 = F_5 = F_6 = 0$, and $F_1 = F_3 = 1$, and as a result:

$$\pm k_1 \frac{\partial T_1(t,x,y_i,z)}{\partial y} = \tilde{\tau}_1 \frac{\partial q^i(t,x,y_i,z)}{\partial t} + q^i(t,x,z) \tag{3.11}$$

The second kind boundary condition, which is called Neumann boundary condition, for the classical diffusion energy equation is obtained from Eq. (3.11), with $\tilde{\tau}_1 = 0$, as in Eq. (2.9):

$$\pm k_1 \frac{\partial T_1(t,x,y_i,z)}{\partial y} = q^i(t,x,z)$$

This boundary condition represents a prescribed heat flux q^i imposed on the boundary.

3. The third kind or Robin boundary condition:

For this kind: $F_3 = F_4 = F_5 = F_6 = 0$, and $F_1 = F_2 = 1$, and as a result:

$$\pm k_1 \frac{\partial T_1(t,x,y_i)}{\partial y} = h_o(T_1(t,x,y_i,z) - f(t,x,y_i,z)) + \tilde{\tau}_1 h_o \left(\frac{\partial T_1(t,x,y_i,z)}{\partial t} - \frac{\partial f(t,x,y_i,z)}{\partial t} \right)$$

$$\tag{3.12}$$

In the limit of zero thermal relaxation time, Eq. (3.12) is reduced to the classical Robin boundary condition derived for the parabolic energy equation as in Eq. (2.9):

$$\pm k_1 \frac{\partial T_1(t,x,y_i)}{\partial y} = h_o(T_1(t,x,y_i,z) - f(t,x,y_i,z))$$

This kind represents a convective heat transfer from the outer surface of the thin layer to a prescribed ambient temperature $f(t, x, z)$.

32

4. The fourth or Carslaw boundary condition:

For this kind: $F_2 = F_4 = F_5 = 0$, and $F_1 = F_3 = F_6 = 1$, and as a result:

$$\pm k_1 \frac{\partial T_1(t,x,y_i)}{\partial y} = -q^i(t,x,y_i,z) + \rho_2 c_2 \Delta y \frac{\partial T_1(t,x,y_i,z)}{\partial t} - \widetilde{\tau}_1 \frac{\partial q^i(t,x,y_i,z)}{\partial t} +$$

$$\widetilde{\tau}_1 \rho_2 c_2 \Delta y \frac{\partial^2 T_1(t,x,y_i,z)}{\partial t^2} \qquad (3.13)$$

In this kind of boundary condition, the heat capacity effect of the thin layer is taken into consideration. A physical example of this kind is heat transfer into a large ceramic object with a thin metal coating on the surface. The temperature distribution in the metal coating may be neglected across the small thickness Δy because the thermal conductivity of the metal is large far greater than that of ceramic, but storage of thermal energy in the metal coating may not be neglected. This boundary condition can also describe a surface film composed of a well-stirred fluid with heat capacity $\Delta y \rho_2 c_2$. For the parabolic energy equation, Eq. (3.13) is reduced to, Eq. (2.11):

$$\pm k_1 \frac{\partial T_1(t,x,y_i)}{\partial y} = -q^i(t,x,y_i,z) + \rho_2 c_2 \Delta y \frac{\partial T_1(t,x,y_i,z)}{\partial t}$$

which is known in the literature as Carslaw boundary condition.

5. The fifth kind or Jaeger boundary condition:

For this kind: $F_3 = F_4 = F_5 = 0$, and $F_1 = F_2 = F_6 = 1$. As a result:

$$\pm k_1 \frac{\partial T_1(t,x,y_i)}{\partial y} = h_o(T_1(t,x,y_i,z) - f(t,x,y_i,z)) + \rho_2 c_2 \Delta y \frac{\partial T_1(t,x,y_i,z)}{\partial t} +$$

$$\widetilde{\tau}_1 h_o \left(\frac{\partial T_1(t,x,y_i,z)}{\partial t} - \frac{\partial f(t,x,y_i,z)}{\partial t} \right) + \widetilde{\tau}_1 \rho_2 c_2 \Delta y \frac{\partial^2 T_1(t,x,y_i,z)}{\partial t^2} \qquad (3.14)$$

This kind of boundary condition takes into consideration heat losses from the film and it is physically identical to the fourth kind except that, instead of a specified heat flux on the outer surface of the thin layer, there is a specified heat transfer coefficient h_o. In the

33

limit of zero thermal relaxation time, Eq. (3.14) is reduced to the classical fifth kind, or Jaeger, boundary condition, which is given in Eq. (2.12):

$$\pm k_1 \frac{\partial T_1(t,x,y_i)}{\partial y} = h_o(T_1(t,x,y_i,z) - f(t,x,y_i,z)) + \rho_2 c_2 \Delta y \frac{\partial T_1(t,x,y_i,z)}{\partial t}$$

6. **The sixth kind boundary condition:**

For this kind: $F_1 = F_2 = F_3 = F_4 = F_5 = F_6 = 1$.

In addition to the above mentioned six kinds of boundary conditions, there is the zeroth kind boundary condition which can not be derived from the generalized kind given by Eq. (3.9). The reason for this is that the zeroth kind boundary condition has no physical content.

3.3 Generalized boundary condition for imperfect contact

When the thermal contact between the thin layer and its adjacent domain is imperfect, then $T_1(t,x,y_i,z) \neq T_2(t,x,y_i,z)$. The boundary condition for imperfect contact situations is obtained by applying the balance of thermal energy on a differential element of the thin layer, to obtain

$$h_i(T_1 - T_2) - h_o(T_2 - f) + q^i + \Delta y \mu_2 \Phi - \rho_2 c_2 \Delta y \left[u_x \frac{\partial T_2}{\partial x} + u_z \frac{\partial T_2}{\partial z} \right] - \rho_2 c_2 \Delta y \frac{\partial T_2}{\partial t} = 0$$

$$(3.15)$$

Also,

$$q_y^k = h_i(T_1 - T_2) \tag{3.16}$$

Substitute Eq. (3.16) into (3.2) to yield:

$$-k_1 \frac{\partial T_1}{\partial y} = h_i(T_1 - T_2) + \tilde{\tau}_1 \frac{\partial}{\partial t}[h_i(T_1 - T_2)] \tag{3.17}$$

Equation (3.15) and (3.17) are solved for T_2 to get:

$$h_o(T_2 - f) - q^i - \Delta y \mu_2 \Phi + \rho_2 c_2 \Delta y \left[u_x \frac{\partial T_2}{\partial x} + u_z \frac{\partial T_2}{\partial z} \right] + \rho_2 c_2 \Delta y \frac{\partial T_2}{\partial t} +$$

$$\tilde{\tau}_1 \frac{\partial}{\partial t} \left\{ h_o(T_2 - f) - q^i - \Delta y \mu_2 \Phi + \rho_2 c_2 \Delta y \left[u_x \frac{\partial T_2}{\partial x} + u_z \frac{\partial T_2}{\partial z} \right] + \rho_2 c_2 \Delta y \frac{\partial T_2}{\partial t} \right\} =$$

$$-k_1 \frac{\partial}{\partial y} \left\{ T_2 + \frac{h_o}{h_i}(T_2 - f) - \frac{q^i}{h_i} - \Delta y \mu_2 \frac{\Phi}{h_i} + \frac{\rho_2 c_2 \Delta y}{h_i} \left[u_x \frac{\partial T_2}{\partial x} + u_z \frac{\partial T_2}{\partial z} \right] + \frac{\rho_2 c_2 \Delta y}{h_i} \frac{\partial T_2}{\partial t} \right\}$$

$$(3.18)$$

A generalized thermal boundary condition for imperfect thermal contact is obtained after solving Eq. (3.18) for T_2 and substituting the obtained expression into Eq. (3.15) to get the desired thermal boundary condition in terms of T_1.

3.4 Case study

Consider the same case study as illustrated in Fig. 2.2(a). The elementary assumption here is that the heat propagates with a finite speed. This transforms the governing heat conduction equation from parabolic into hyperbolic equation. The classical Fourier's model for conduction may breakdown under situations involving very low temperature near absolute zero, extremely short transient duration, or very high heat flux. Under these circumstances, heat propagates with a finite speed. Thus, the hyperbolic heat conduction model is suitable for accounting for the phenomena concerning the finite propagation speed of the thermal wave.

3.4.1 Exact model

In this case, the energy equations coupled at the interface have to be solved. These equations are written as:

$$\rho_1 c_1 \frac{\partial T_1(x,t)}{\partial t} = -\frac{\partial q_1}{\partial x} \qquad (3.19)$$

$$\rho_2 c_2 \frac{\partial T_2(x,t)}{\partial t} = -\frac{\partial q_2}{\partial x} \qquad (3.20)$$

$$q_1 + \tilde{\tau}_{q,1} \frac{\partial q_1}{\partial t} = -k_1 \frac{\partial T_1}{\partial x} \qquad (3.21)$$

$$q_2 + \tilde{\tau}_{q,2} \frac{\partial q_2}{\partial t} = -k_2 \frac{\partial T_2}{\partial x} \qquad (3.22)$$

Combining Eqs. (3.19) and (3.21), (3.20) and (3.22), yields:

$$\tilde{\tau}_{q,1} \frac{\partial^2 T_1(x,t)}{\partial t^2} + \frac{\partial T_1(x,t)}{\partial t} = \alpha_1 \frac{\partial^2 T_1(x,t)}{\partial x^2} \qquad \text{in} \quad 0 \le x \le a \qquad (3.23)$$

$$\tilde{\tau}_{q,2} \frac{\partial^2 T_2(x,t)}{\partial t^2} + \frac{\partial T_2(x,t)}{\partial t} = \alpha_2 \frac{\partial^2 T_2(x,t)}{\partial x^2} \qquad \text{in} \quad a \le x \le b \qquad (3.24)$$

which assume the following initial and boundary conditions are:

$$T_1(x,0) = T_2(x,0) = T_i$$

$$(3.25)$$

$$\frac{\partial T_1(x,0)}{\partial t} = \frac{\partial T_2(x,0)}{\partial t} = 0.0$$

$$T_1(0,t) = T_w$$

$$\frac{\partial T_2(b,t)}{\partial x} = 0.0$$

$$(3.26)$$

$$T_1(a,t) = T_2(a,t)$$

$$q_1(a,t) = q_2(a,t)$$

Using the following dimensionless parameters

$$\theta = \frac{T - T_w}{T_i - T_w}, \qquad \xi = \frac{x}{a}, \qquad \eta = \frac{\alpha_1 t}{a^2}, \qquad \tau = \frac{\tilde{\tau} \alpha_1}{a^2}, \qquad Q = \frac{qa}{k_1 \Delta T}$$

36

Equations (3.19-3.24) and their initial and boundary conditions become:

$$\frac{\partial \theta_1}{\partial \eta} = -\frac{\partial Q_1}{\partial \xi} \tag{3.27}$$

$$\frac{\partial \theta_2}{\partial \eta} = -\frac{1}{C_R}\frac{\partial Q_2}{\partial \xi} \tag{3.28}$$

$$Q_1 + \tau_{q,1}\frac{\partial Q_1}{\partial \eta} = -\frac{\partial \theta_1}{\partial \xi} \tag{3.29}$$

$$Q_2 + \tau_{q,2}\frac{\partial Q_2}{\partial \eta} = -K_r\frac{\partial \theta_2}{\partial \xi} \tag{3.30}$$

$$\tau_{q,1}\frac{\partial^2 \theta_1}{\partial \eta^2} + \frac{\partial \theta_1}{\partial \eta} = \frac{\partial^2 \theta_1}{\partial \xi^2} \qquad 0 \le \xi \le 1.0 \tag{3.31}$$

$$\tau_{q,2}\frac{\partial^2 \theta_2}{\partial \eta^2} + \frac{\partial \theta_2}{\partial \eta} = \alpha_r\frac{\partial^2 \theta_2}{\partial \xi^2} \qquad 1.0 \le \xi \le R \tag{3.32}$$

$$\theta_1(\xi,0) = \theta_2(\xi,0) = 1.0$$

$$\frac{\partial \theta_1(\xi,0)}{\partial \eta} = \frac{\partial \theta_2(\xi,0)}{\partial \eta} = 0.0 \tag{3.33}$$

$$\theta_1(0,\eta) = 0.0$$

$$\frac{\partial \theta_2(R,\eta)}{\partial \xi} = 0.0$$

$$\theta_1(1,\eta) = \theta_2(1,\eta) \tag{3.34}$$

$$Q_1(1,\eta) = Q_2(1,\eta)$$

where $K_r = k_2/k_1$ is the thermal conductivity ratio, $\alpha_r = \alpha_2/\alpha_1$ is the thermal diffiusivity ratio, and $R=b/a$. From the definition of R, (R-1) represents the dimensionless thickness of the thin layer $(=\frac{b-a}{a})$. Now, with the notation that

$L\{\theta(\xi,\eta)\} = W(\xi,S)$, Laplace transformation of Eqs. (3.31) and (3.32), yields:

$$\frac{d^2W_1}{d\xi^2} - \left(\tau_{q,1}S^2 + S\right)W_1 = -\left(1 + \tau_{q,1}S\right) \tag{3.35}$$

$$\frac{d^2W_2}{d\xi^2} - \left(\frac{\tau_{q,2}S^2 + S}{\alpha_r}\right)W_2 = -\left(\frac{\tau_{q,2}S + 1}{\alpha_r}\right) \tag{3.36}$$

These two equations assume the following solutions:

$$W_1(\xi,S) = C_1e^{M_1\xi} + C_2e^{-M_1\xi} + \frac{1}{S} \tag{3.37}$$

$$W_2(\xi,S) = C_3e^{M_2\xi} + C_4e^{-M_2\xi} + \frac{1}{S} \tag{3.38}$$

where $M_1 = \sqrt{\left(\tau_{q,1}S^2 + S\right)}$ and $M_2 = \sqrt{\dfrac{\left(\tau_{q,2}S^2 + S\right)}{\alpha_r}}$.

Also, with the notation that $V = L\{Q\}$, Laplace transformation of Eq. (3.34) yields:

$$W_1(0,S) = 0.0$$

$$\frac{\partial W_2(R,S)}{\partial \xi} = 0.0$$

$$\tag{3.39}$$

$$W_1(1,S) = W_2(1,S)$$

$$V_1(1,S) = V_2(1,S)$$

From Eqs. (3.29) and (3.30) with $Q_1(\xi,0) = Q_2(\xi,0) = 0.0$ we have:

$$V_1 + \tau_{q,1}(SV_1) = -\frac{dW_1}{d\xi}$$

$$V_2 + \tau_{q,2}(SV_2) = -K_r\frac{dW_2}{d\xi}$$

with $V_1(1,S) = V_2(1,S)$, the second boundary condition at the interface becomes:

$$\frac{dW_1(1,S)}{d\xi} = \left(\frac{K_r\left(1 + \tau_{q,1}S\right)}{\left(1 + \tau_{q,2}S\right)}\right)\frac{dW_2(1,S)}{d\xi}$$

Insert Eqs. (3.37) and (3.38) into (3.39) and solve for $C_1, C_2, C_3,$ and C_4 to yield:

$$C_1 = \frac{\left(-\dfrac{1}{S}\right)\left\{\dfrac{e^{-2M_1}\left[\left(1+\dfrac{K_r}{\sqrt{\alpha_r}}\sqrt{\dfrac{\left(1+\tau_{q,1}S\right)}{\left(1+\tau_{q,2}S\right)}}\right)+\left(1-\dfrac{K_r}{\sqrt{\alpha_r}}\sqrt{\dfrac{\left(1+\tau_{q,1}S\right)}{\left(1+\tau_{q,2}S\right)}}\right)\left(e^{M_2(2R-2)}\right)\right]}{\left[\left(1-\dfrac{K_r}{\sqrt{\alpha_r}}\sqrt{\dfrac{\left(1+\tau_{q,1}S\right)}{\left(1+\tau_{q,2}S\right)}}\right)+\left(1+\dfrac{K_r}{\sqrt{\alpha_r}}\sqrt{\dfrac{\left(1+\tau_{q,1}S\right)}{\left(1+\tau_{q,2}S\right)}}\right)\left(e^{M_2(2R-2)}\right)\right]}\right\}}{\left\{1+\dfrac{e^{-2M_1}\left[\left(1+\dfrac{K_r}{\sqrt{\alpha_r}}\sqrt{\dfrac{\left(1+\tau_{q,1}S\right)}{\left(1+\tau_{q,2}S\right)}}\right)+\left(1-\dfrac{K_r}{\sqrt{\alpha_r}}\sqrt{\dfrac{\left(1+\tau_{q,1}S\right)}{\left(1+\tau_{q,2}S\right)}}\right)\left(e^{M_2(2R-2)}\right)\right]}{\left[\left(1-\dfrac{K_r}{\sqrt{\alpha_r}}\sqrt{\dfrac{\left(1+\tau_{q,1}S\right)}{\left(1+\tau_{q,2}S\right)}}\right)+\left(1+\dfrac{K_r}{\sqrt{\alpha_r}}\sqrt{\dfrac{\left(1+\tau_{q,1}S\right)}{\left(1+\tau_{q,2}S\right)}}\right)\left(e^{M_2(2R-2)}\right)\right]}\right\}},$$

$$C_2 = \frac{-1/S}{\left\{1+\dfrac{e^{-2M_1}\left[\left(1+\dfrac{K_r}{\sqrt{\alpha_r}}\sqrt{\dfrac{\left(1+\tau_{q,1}S\right)}{\left(1+\tau_{q,2}S\right)}}\right)+\left(1-\dfrac{K_r}{\sqrt{\alpha_r}}\sqrt{\dfrac{\left(1+\tau_{q,1}S\right)}{\left(1+\tau_{q,2}S\right)}}\right)\left(e^{M_2(2R-2)}\right)\right]}{\left[\left(1-\dfrac{K_r}{\sqrt{\alpha_r}}\sqrt{\dfrac{\left(1+\tau_{q,1}S\right)}{\left(1+\tau_{q,2}S\right)}}\right)+\left(1+\dfrac{K_r}{\sqrt{\alpha_r}}\sqrt{\dfrac{\left(1+\tau_{q,1}S\right)}{\left(1+\tau_{q,2}S\right)}}\right)\left(e^{M_2(2R-2)}\right)\right]}\right\}},$$

$$C_3 = \frac{C_1 e^{M_1} + C_2 e^{M_1}}{e^{M_2}\left(1+e^{M_2(2R-2)}\right)}$$

and $\quad C_4 = \left\{\dfrac{C_1 e^{M_1} + C_2 e^{M_1}}{e^{M_2}\left(1+e^{M_2(2R-2)}\right)}\right\} e^{2RM_2}$

Equations (3.37) and (3.38) are inverted numerically using a computer program based on Riemann-sum approximation as:

$$\theta_k(\xi,\eta) \cong \frac{e^{\gamma\eta}}{\eta}\left[\frac{1}{2}W_k(\xi,\gamma) + \mathrm{Re}\sum_{n=1}^{N} W_k\left(\xi,\gamma+\frac{in\pi}{\eta}\right)(-1)^n\right] \qquad (3.40)$$

Equation (3.40) yields the exact temperature distribution in both domains for the perfect contact hyperbolic heat conduction model case.

39

3.4.2 Approximate model

In this case, we intend to solve one energy equation in the thick domain (domain 1) and ignore the existence of the thin layer and replace its thermal effect by using the generalized thermal boundary condition at the thick domain interfacial boundary with the thin domain. It will be assumed that the two layers are in perfect thermal contact and the thin layer is thin enough so it has the same lumped temperature in its transverse direction. This temperature is equal to the temperature at the interface between the thin and the thick domains. The thick domain energy equation is given as:

$$\tilde{\tau}_{q,1}\frac{\partial^2 T_1}{\partial t^2}+\frac{\partial T_1}{\partial t}=\alpha_1\frac{\partial^2 T_1}{\partial x^2} \qquad in \quad 0\leq x\leq a \qquad (3.41)$$

which assumes the following initial and boundary conditions:

$$T_1(x,0)=T_i$$

$$\frac{\partial T_1(x,0)}{\partial \eta}=0.0 \qquad\qquad (3.42)$$

$$T_1(0,t)=T_w$$

$$\qquad\qquad (3.43)$$

$$-k_1\frac{\partial T_1(a,t)}{\partial x}-\rho_2 c_2(b-a)\frac{\partial T_1(a,t)}{\partial t}-\tilde{\tau}_{q,1}\rho_2 c_2(b-a)\frac{\partial^2 T_1(a,t)}{\partial t^2}=0.0$$

The second equation in (3.43) represents the generalized hyperbolic thermal boundary condition, which takes into account three thermal effects of the eliminated thin layer. These three effects are the thermal storage of the thin layer, thermal diffusion in the thin film transverse direction and the time phase lag effect between the conduction heat flux and the temperature gradient in both the thin layer and its adjacent domain. Using the following dimensionless parameters.

$$\theta=\frac{T-T_w}{T_i-T_w}, \qquad \xi=\frac{x}{a}, \qquad \eta=\frac{\alpha_1 t}{a^2}, \qquad \tau=\frac{\tilde{\tau}\alpha_1}{a^2}$$

Equations (3.41), (3.42) and (3.43) become:

40

$$\tau_{q,1}\frac{\partial^2\theta_1(\xi,\eta)}{\partial\eta^2}+\frac{\partial\theta_1(\xi,\eta)}{\partial\eta}=\frac{\partial^2\theta_1(\xi,\eta)}{\partial\xi^2} \qquad \text{in} \quad 0\le\xi\le1.0 \tag{3.44}$$

$$\theta_1(\xi,0)=1.0 \tag{3.45}$$

$$\frac{\partial\theta_1(\xi,0)}{\partial\eta}=0.0$$

$$\theta_1(0,\eta)=0.0$$

$$\frac{\partial\theta_1(1,\eta)}{\partial\xi}+H\left(\frac{\partial\theta_1(1,,\eta)}{\partial\eta}+\tau_{q,1}\frac{\partial^2\theta_1(1,,\eta)}{\partial\eta^2}\right)=0.0 \tag{3.46}$$

where $H=\dfrac{K_r}{\alpha_r}(R-1)$ and $R=b/a$. In a manner similar to what has been done previously, using Laplace transformation technique, Eqs. (3.44) and (3.46) assume the following solution in the Laplacian domain.

$$W_1(\xi,S)=Ae^{M_1\xi}+Be^{-M_1\xi}+\frac{1}{S} \tag{3.47}$$

where $M_1=\sqrt{\left(\tau_{q,1}S^2+S\right)}$,

$$A=\frac{-\dfrac{1}{S}}{\left[1+\dfrac{e^{-2M_1}\left(1-H\sqrt{\left(\tau_{q,1}S^2+S\right)}\right)}{\left(1+H\sqrt{\left(\tau_{q,1}S^2+S\right)}\right)}\right]}\left[\frac{e^{-2M_1}\left(1-H\sqrt{\left(\tau_{q,1}S^2+S\right)}\right)}{\left(1+H\sqrt{\left(\tau_{q,1}S^2+S\right)}\right)}\right] \text{ and}$$

$$B=\frac{-\dfrac{1}{S}}{\left[1+\dfrac{e^{-2M_1}\left(1-H\sqrt{\left(\tau_{q,1}S^2+S\right)}\right)}{\left(1+H\sqrt{\left(\tau_{q,1}S^2+S\right)}\right)}\right]}.$$

Equation (3.47) is inverted numerically using a computer program based on Riemann-sum approximation as:

$$\theta_1(\xi,\eta)\cong\frac{e^{\gamma\eta}}{\eta}\left[\frac{1}{2}W_1(\xi,\gamma)+\text{Re}\sum_{n=1}^{N}W_1\left(\xi,\gamma+\frac{in\pi}{\eta}\right)(-1)^n\right] \tag{3.48}$$

Equation (3.48) represents the approximate temperature distribution in the thick domain.

4- DUAL PHASE MODEL

4.1 Introduction

The Cattaneo and Vernotte wave model assumes an instantaneous heat flow. The temperature gradient is always the cause for the heat transfer, while the heat flux vector is always the effect. The dual-phase-lag model aims to remove the precedence assumption made in the thermal wave model. It allows either the temperature gradient (cause) to precede the heat flux vector (effect) or the heat flux vector (cause) to precede the temperature gradient (effect). Mathematically, Tzou (1995a- c) represents this model as:

$$q(x, t + \tilde{\tau}_q) = -k \nabla T(x, t + \tilde{\tau}_T) \tag{4.1}$$

where $\tilde{\tau}_T$ is the phase lag of the temperature gradient and $\tilde{\tau}_q$ is the phase lag of the heat flux vector. For the case $\tilde{\tau}_T > \tilde{\tau}_q$, the temperature gradient established across a material volume is a result of the heat flow, implying that the heat flux vector is the cause and the temperature gradient is the effect. For $\tilde{\tau}_T < \tilde{\tau}_q$, on the other hand, heat flow is induced by the temperature gradient established at an earlier time, implying that the temperature gradient is the cause, while the heat flux vector is the effect.

4.2 Mathematical formulation

The case study shown in Fig. (2.2a) is considered here. In this case, the energy equations coupled at the interface have to be solved. These equations are written as:

$$\rho_1 c_1 \frac{\partial T_1}{\partial t} = -\frac{\partial q_1}{\partial x} + g_1 \tag{4.2}$$

$$\rho_2 c_2 \frac{\partial T_2}{\partial t} = -\frac{\partial q_2}{\partial x} + g_2 \tag{4.3}$$

$$q_1 + \widetilde{\tau}_{q,1} \frac{\partial q_1}{\partial t} = -\kappa_1 \frac{\partial T_1}{\partial x} - \kappa_1 \widetilde{\tau}_{T,1} \frac{\partial^2 T_1}{\partial t \partial x} \tag{4.4}$$

$$q_2 + \widetilde{\tau}_{q,2} \frac{\partial q_2}{\partial t} = -\kappa_2 \frac{\partial T_2}{\partial x} - \kappa_2 \widetilde{\tau}_{T,2} \frac{\partial^2 T_2}{\partial t \partial x} \tag{4.5}$$

When Eqs. (4.2) and (4.4), (4.3) and (4.5), are combined yield:

$$\frac{\partial^2 T_1}{\partial x^2} + \widetilde{\tau}_{T,1} \frac{\partial^3 T_1}{\partial t \partial x^2} + \frac{1}{\kappa_1}\left[g_1 + \widetilde{\tau}_{q,1} \frac{\partial g_1}{\partial t} \right] = \frac{1}{\alpha_1} \frac{\partial T_1}{\partial t} + \frac{\widetilde{\tau}_{q,1}}{\alpha_1} \frac{\partial^2 T_1}{\partial t^2} \tag{4.6}$$

$$\frac{\partial^2 T_2}{\partial x^2} + \widetilde{\tau}_{T,2} \frac{\partial^3 T_2}{\partial t \partial x^2} + \frac{1}{\kappa_2}\left[g_2 + \widetilde{\tau}_{q,2} \frac{\partial g_2}{\partial t} \right] = \frac{1}{\alpha_2} \frac{\partial T_2}{\partial t} + \frac{\widetilde{\tau}_{q,2}}{\alpha_2} \frac{\partial^2 T_2}{\partial t^2} \tag{4.7}$$

Initial and boundary conditions:

$$T_1(x,0) = T_2(x,0) = T_i$$

$$\frac{\partial T_1}{\partial t}(x,0) = \frac{\partial T_2}{\partial t}(x,0) = 0 \tag{4.8}$$

$$T_1(0,t) = T_w$$

$$\frac{\partial T_2}{\partial x}(b,t) = 0 \tag{4.9}$$

$$T_1(a,t) = T_2(a,t)$$

$$q_1(a,t) = q_2(a,t)$$

using the following dimensionless parameters

$$\xi = \frac{x}{a} \quad , \quad \theta = \frac{T - T_w}{T_i - T_w} \quad , \quad \eta = \frac{t\,\alpha_1}{a^2} \quad , \quad \tau = \frac{\tilde{\tau}\,\alpha_1}{a^2} \quad , \quad Q = \frac{q\,a}{k_1 \Delta T}$$

Equations (4.2), (4.3), (4.4) and (4.5) in dimensionless form become:

$$\frac{\partial \theta_1}{\partial \eta} = -\frac{\partial Q_1}{\partial \xi} + G_1 \tag{4.10}$$

$$\frac{\partial \theta_2}{\partial \eta} = -\frac{1}{C_R}\frac{\partial Q_2}{\partial \xi} + G_2 \tag{4.11}$$

$$Q_1 + \tau_{q,1}\frac{\partial Q_1}{\partial \eta} = -\frac{\partial \theta_1}{\partial \xi} - \tau_{T,1}\frac{\partial \theta_1}{\partial \eta \partial \xi^2} \tag{4.12}$$

$$Q_2 + \tau_{q,2}\frac{\partial Q_2}{\partial \eta} = K_r\left[-\frac{\partial \theta_2}{\partial \xi} - \tau_{T,2}\frac{\partial \theta_2}{\partial \eta \partial \xi^2} \right] \tag{4.13}$$

equations (4.6) and (4.7) are reduced to:

$$\frac{\partial^2 \theta_1}{\partial \xi^2} + \tau_{T,1}\frac{\partial^3 \theta_1}{\partial \eta \partial \xi^2} + \left[G_1 + \tau_{q,1}\frac{\partial G_1}{\partial \eta} \right] = \frac{\partial \theta_1}{\partial \eta} + \tau_{q,1}\frac{\partial^2 \theta_1}{\partial \eta^2} \tag{4.14}$$

$$\frac{\partial^2 \theta_2}{\partial \xi^2} + \tau_{T,2}\frac{\partial^3 \theta_2}{\partial \eta \partial \xi^2} + \frac{C_R}{K_r}\left[G_2 + \tau_{q,2}\frac{\partial G_2}{\partial \eta} \right] = \frac{C_R}{K_r}\left[\frac{\partial \theta_2}{\partial \eta} + \tau_{q,2}\frac{\partial^2 \theta_2}{\partial \eta^2} \right] \tag{4.15}$$

where $\qquad \dfrac{C_R}{K_r} = \dfrac{\alpha_1}{\alpha_2} = \dfrac{1}{\alpha_r}$

Initial and boundary conditions

$$\theta_1(\xi,0) = \theta_2(\xi,0) = 1.0$$

$$\tag{4.16}$$

$$\frac{\partial \theta_1}{\partial \eta}(\xi,0) = \frac{\partial \theta_2}{\partial \eta}(\xi,0) = 0.0$$

45

$$\theta_1(0,\eta) = 0.0$$

$$\frac{\partial \theta_2}{\partial \xi}(R,\eta) = 0.0$$

(4.17)

$$\theta_1(1,\eta) = \theta_2(1,\eta)$$

$$Q_1(1,\eta) = Q_2(1,\eta)$$

Now, assume there is no heating source $(G_1 = G_2 = 0.0))$ with the notation that $W(\xi, S) = L\{\theta(\xi,\eta)\}$, Laplace transformation of Eqs. (4.14) and (4.15), yield:

$$\frac{d^2 W_1}{d\xi^2} + \tau_{T,1}\left(S \frac{d^2 W_1}{d\xi^2}\right) = S W_1 - 1 + \tau_{q,1}\left(S^2 W_1 - S\right)$$

In other form:

$$\frac{d^2 W_1}{d\xi^2} - \left(\frac{S + \tau_{q,1} S^2}{1 + \tau_{T,1} S}\right) W_1 = -\left(\frac{1 + \tau_{q,1} S}{1 + \tau_{T,1} S}\right)$$

(4.18)

Also,

$$\frac{d^2 W_2}{d\xi^2} + \tau_{T,2}\left(S \frac{d^2 W_2}{d\xi^2}\right) = \frac{1}{\alpha_r}(S W_2 - 1) + \frac{\tau_{q,2}}{\alpha_r}\left(S^2 W_2 - S\right)$$

In other form:

$$\frac{d^2 W_2}{d\xi^2} - \left(\frac{S + \tau_{q,1} S^2}{(1 + \tau_{T,1} S)\alpha_r}\right) W_2 = -\left(\frac{1 + \tau_{q,1} S}{(1 + \tau_{T,1} S)\alpha_r}\right)$$

(4.19)

equations (4.18) and (4.19) assume the following solutions:

$$W_1 = C_1 e^{\xi \lambda_1} + C_2 e^{-\xi \lambda_1} + \frac{1}{S}$$

(4.20)

$$W_2 = C_3 e^{\xi \lambda_2} + C_4 e^{-\xi \lambda_2} + \frac{1}{S}$$

(4.21)

where $\lambda_1 = \sqrt{\left(\frac{S + \tau_{q,1} S^2}{1 + \tau_{T,1} S}\right)}$ and $\lambda_2 = \sqrt{\frac{(S + \tau_{q,2} S^2)}{(1 + \tau_{T,2} S)\alpha_r}}$.

46

Also, with the notation that $V = L\{Q\}$, Laplace transformation of Eq. (4.17), yields:

$$W_1(0,S) = 0.0$$

$$\frac{dW_2}{\partial \xi}(R,S) = 0.0$$

$$\quad (4.22)$$

$$W_1(1,S) = W_2(1,S)$$

$$V_1(1,S) = V_2(1,S)$$

From Eqs. (4.12) and (4.13) with $Q_1(\xi,0) = Q_2(\xi,0) = 0.0$, we have:

$$V_1 + \tau_{q,1}(SV_1) = -\frac{dW_1}{d\xi} - \tau_{T,1}\left(S\frac{dW_1}{d\xi}\right)$$

$$V_2 + \tau_{q,2}(SV_2) = k_r\left[-\frac{dW_2}{d\xi} - \tau_{T,2}\left(S\frac{dW_2}{d\xi}\right)\right]$$

V_1 and V_2 can be expressed as:

$$V_1(\xi,S) = -\left(\frac{1+\tau_{T,1}S}{1+\tau_{q,1}S}\right)\left(\frac{dW_1}{d\xi}\right) \quad (4.23a)$$

$$V_2(\xi,S) = -K_r\left(\frac{1+\tau_{T,2}S}{1+\tau_{q,2}S}\right)\left(\frac{dW_2}{d\xi}\right) \quad (4.23b)$$

with $V_1(1,S) = V_2(1,S)$, the second boundary condition at the interface becomes:

$$\left(\frac{dW_1(1,S)}{d\xi}\right) = \Psi\left(\frac{dW_2(1,S)}{d\xi}\right)$$

where $\Psi = \left[\frac{K_r(1+\tau_{T,2}S)}{(1+\tau_{q,2}S)}\frac{(1+\tau_{q,1}S)}{(1+\tau_{T,1}S)}\right]$

Insert Eqs. (4.20) and (4.21) into (4.22) and solve for C_1, C_2, C_3, and C_4 to yield:

47

$$C_1 = \cfrac{\left(-\dfrac{1}{S}\right)\left\{\dfrac{e^{-2\lambda_1}\left[\left(1+\Psi\dfrac{\lambda_2}{\lambda_1}\right)+\left(1-\Psi\dfrac{\lambda_2}{\lambda_1}\right)e^{\lambda_2(2R-2)}\right]}{\left[\left(1-\Psi\dfrac{\lambda_2}{\lambda_1}\right)+\left(1+\Psi\dfrac{\lambda_2}{\lambda_1}\right)e^{\lambda_2(2R-2)}\right]}\right\}}{\left\{1+\dfrac{e^{-2\lambda_1}\left[\left(1+\Psi\dfrac{\lambda_2}{\lambda_1}\right)+\left(1-\Psi\dfrac{\lambda_2}{\lambda_1}\right)e^{\lambda_2(2R-2)}\right]}{\left[\left(1-\Psi\dfrac{\lambda_2}{\lambda_1}\right)+\left(1+\Psi\dfrac{\lambda_2}{\lambda_1}\right)e^{\lambda_2(2R-2)}\right]}\right\}}$$

$$C_2 = \cfrac{-\dfrac{1}{S}}{\left\{1+\dfrac{e^{-2\lambda_1}\left[\left(1+\Psi\dfrac{\lambda_2}{\lambda_1}\right)+\left(1-\Psi\dfrac{\lambda_2}{\lambda_1}\right)e^{\lambda_2(2R-2)}\right]}{\left[\left(1-\Psi\dfrac{\lambda_2}{\lambda_1}\right)+\left(1+\Psi\dfrac{\lambda_2}{\lambda_1}\right)e^{\lambda_2(2R-2)}\right]}\right\}}$$

$$C_3 = \frac{C_1 e^{\lambda_1}+C_2 e^{-\lambda_1}}{e^{\lambda_2}\left(1+e^{\lambda_2(2R-2)}\right)}$$

and $\quad C_4 = \dfrac{C_1 e^{\lambda_1}+C_2 e^{-\lambda_1}}{e^{\lambda_2}\left(1+e^{\lambda_2(2R-2)}\right)}e^{2\lambda_2 R}$

where $\quad \Psi\dfrac{\lambda_2}{\lambda_1} = \sqrt{\dfrac{\left(1+\tau_{T,2}S\right)\left(1+\tau_{q,1}S\right)}{\left(1+\tau_{T,1}S\right)\left(1+\tau_{q,2}S\right)}}$

Equations (4.20) and (4.21) are inverted using a computer program based on Riemann-sum approximation as:

$$\theta_k(\xi,\eta) \cong \frac{e^{r\eta}}{\eta}\left[\frac{1}{2}W_k(\xi,\gamma)+\mathrm{Re}\sum_{n=1}^{N}W_k\left(\xi,\gamma+\frac{in\pi}{\eta}\right)(-1)^n\right] \qquad (2.24)$$

Equation (2.24) yields the exact temperature distribution in both domains for the perfect contact dual phase heat conduction model case.

48

4.3 Heat flux calculations

To find the heat flux in the two domains Eqs. (4.23a) and (4.23b) are inverted using a computer program based on Riemann-sum approximation as:

$$Q_k(\xi,\eta) \cong \frac{e^{r\eta}}{\eta}\left[\frac{1}{2}V_k(\xi,\gamma) + \mathrm{Re}\sum_{n=1}^{N} V_k\left(\xi,\gamma + \frac{in\pi}{\eta}\right)(-1)^n\right] \qquad (4.25)$$

Equation (2.25) yields the exact heat flux in both domains for the perfect contact dual phase heat conduction model case. The computer model results with changing thickness ratios, thermal diffusivity ratios, thermal conductivity ratios and thermal relaxation time were exhibited in the figures in chapter 7, which will be analyzed later.

5- PARABOLIC, HYPERBOLIC AND DUAL PHASE MODELS FOR IMPERFECT CONTACT

5.1 Introduction

Although neglected until now, it is important to recognize that, in composite systems, the temperature drop across the interface between materials may be appreciable. This temperature change is attributed to what is known as the thermal contact resistance, $R_{t,c}$. The effect is shown in Fig. 5.1, and for a unit area of the interface, the resistance is defined as

$$R^{"}_{t,c} = \frac{T_A - T_B}{q^{"}_x} \tag{5.1}$$

The existence of a finite contact resistance is due principally to surface roughness effect. Contact spots are interspersed with gaps that are, in most instances, air filled. Heat transfer is therefore due to conduction across the actual contact area and to conduction and/or radiation across the gaps. The contact resistance may be viewed as two parallel resistances: that due to the contact spots and that due to the gaps. The contact area is typically small, and especially for rough surfaces, the major contribution to the resistance is made by the gaps.

For solids whose thermal conductivity exceeds that of the interfacial fluid, the contact resistance may be reduced by increasing the area of the contact spots. Such an increase may be effected by increasing the joint pressure and/or by reducing the roughness of the mating surfaces. Selecting an interfacial fluid of large thermal conductivity may also reduce the contact resistance. In this respect, no fluid (an

50

evacuated interface) eliminates conduction across the gap, thereby increasing the

contact resistance.
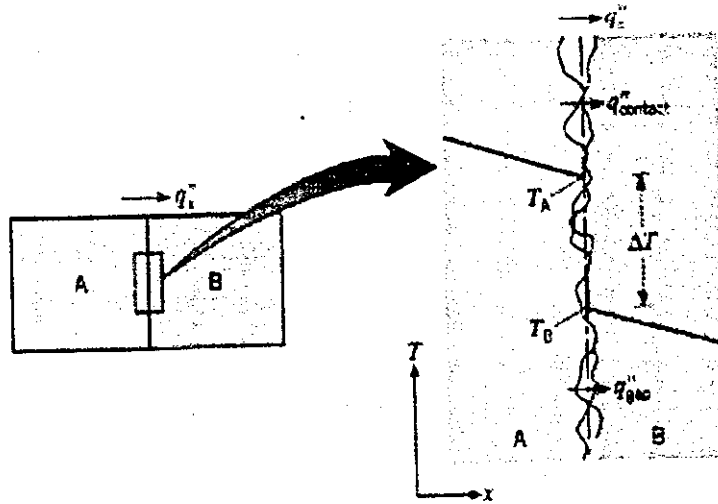
Figure 5.1: Temperature drop due to thermal contact resistance.

5.2 Parabolic heat conduction model for imperfect contact

In a manner similar to what has been done for perfect contact, two energy

equations coupled at the interface have to be solved with different interfacial boundary

conditions. In the case of perfect contact the temperatures at the interface are equal

while in this case the temperatures at the interface are related as:

$$q_1(1,\eta) = h[T_1(1,\eta) - T_2(1,\eta)]$$

where 1 and 2 refer to domain A and B respectively and h is the interfacial convective

heat transfer coefficient. The energy equations in dimensionless form are given as:

$$\frac{\partial^2 \theta_1}{\partial \xi^2} = \frac{\partial \theta_1}{\partial \eta} \qquad \text{in} \quad 0 \le \xi \le 1.0 \qquad (5.2)$$

$$\frac{\partial^2 \theta_2}{\partial \xi^2} = \frac{1}{\alpha_r} \frac{\partial \theta_2}{\partial \eta} \qquad \text{in} \quad 1.0 \le \xi \le R \qquad (5.3)$$

51

Subject to the following initial and boundary conditions:

$$\theta_1(\xi,0) = \theta_2(\xi,0) = 1.0 \tag{5.4}$$

$$\theta_1(0,\eta) = 0.0$$

$$\frac{\partial\theta_2(R,\eta)}{\partial\xi} = 0.0$$

$$\tag{5.5}$$

$$Q_1(1,\eta) = Q_2(1,\eta)$$

$$Q_1(1,\eta) = Bi(\theta_1(1,\eta) - \theta_2(1,\eta)),$$

where $\quad Q_1 = -\dfrac{\partial\theta_1}{\partial\xi}$

The first boundary condition at the interface yields:

$$\frac{\partial\theta_1(1,\eta)}{\partial\xi} = K_r\frac{\partial\theta_2(1,\eta)}{\partial\xi}$$

where Bi is *Biot number* defined as ha/k_1 .

Now, with the notation that $L\{\theta(\xi,\eta)\} = W(\xi,S)$, Laplace transformation of Eqs. (5.2)

and (5.3) yields:

$$\frac{d^2W_1}{d\xi^2} - SW_1 = -1$$

$$\frac{d^2W_2}{d\xi^2} - \frac{S}{\alpha_r}W_2 = -\frac{1}{\alpha_r}$$

These equations assume the following solutions:

$$W_1(\xi,S) = C_1e^{\xi\sqrt{S}} + C_2e^{-\xi\sqrt{S}} + \frac{1}{S} \tag{5.6}$$

$$W_2(\xi,S) = C_3e^{\xi\sqrt{S/\alpha_r}} + C_4e^{-\xi\sqrt{S/\alpha_r}} + \frac{1}{S} \tag{5.7}$$

Also, with the notation that $V = L\{Q\}$, Laplace transformation of Eq. (5.5) yields:

52

$$W_1(0,S) = 0.0$$

$$\frac{dW_2(R,S)}{\partial \xi} = 0.0$$

<div align="right">(5.8)</div>

$$\frac{dW_1(1,S)}{\partial \xi} = K_r \frac{dW_2(1,S)}{\partial \xi}$$

$$V_1(1,S) = Bi\left(W_1(1,S) - W_2(1,S)\right)$$

where $V_1(1,S) = -\left(\dfrac{dW_1(1,S)}{d\xi}\right)$

Insert Eqs. (5.6) and (5.7) into (5.8) and solve for $C_1, C_2, C_3,$ and C_4 to yield:

$$C_1 = \frac{\left(-\dfrac{1}{S}\right)\left\{\dfrac{e^{-2\sqrt{S}}\left\{\left(Bi - \dfrac{K_r\left(\sqrt{S} - Bi\right)}{\sqrt{\alpha_r}}\right) + \left(e^{(2R-2)\sqrt{S/\alpha_r}}\right)\left(Bi + \dfrac{K_r\left(\sqrt{S} - Bi\right)}{\sqrt{\alpha_r}}\right)\right\}}{\left\{\left(Bi - \dfrac{K_r\left(\sqrt{S} + Bi\right)}{\sqrt{\alpha_r}}\right) + \left(e^{(2R-2)\sqrt{S/\alpha_r}}\right)\left(Bi + \dfrac{K_r\left(\sqrt{S} + Bi\right)}{\sqrt{\alpha_r}}\right)\right\}}\right\}}{\left\{1 + \dfrac{e^{-2\sqrt{S}}\left\{\left(Bi - \dfrac{K_r\left(\sqrt{S} - Bi\right)}{\sqrt{\alpha_r}}\right) + \left(e^{(2R-2)\sqrt{S/\alpha_r}}\right)\left(Bi + \dfrac{K_r\left(\sqrt{S} - Bi\right)}{\sqrt{\alpha_r}}\right)\right\}}{\left\{\left(Bi - \dfrac{K_r\left(\sqrt{S} + Bi\right)}{\sqrt{\alpha_r}}\right) + \left(e^{(2R-2)\sqrt{S/\alpha_r}}\right)\left(Bi + \dfrac{K_r\left(\sqrt{S} + Bi\right)}{\sqrt{\alpha_r}}\right)\right\}}\right\}},$$

$$C_2 = \frac{-\dfrac{1}{S}}{\left\{1 + \dfrac{e^{-2\sqrt{S}}\left\{\left(Bi - \dfrac{K_r\left(\sqrt{S} - Bi\right)}{\sqrt{\alpha_r}}\right) + \left(e^{(2R-2)\sqrt{S/\alpha_r}}\right)\left(Bi + \dfrac{K_r\left(\sqrt{S} - Bi\right)}{\sqrt{\alpha_r}}\right)\right\}}{\left\{\left(Bi - \dfrac{K_r\left(\sqrt{S} + Bi\right)}{\sqrt{\alpha_r}}\right) + \left(e^{(2R-2)\sqrt{S/\alpha_r}}\right)\left(Bi + \dfrac{K_r\left(\sqrt{S} + Bi\right)}{\sqrt{\alpha_r}}\right)\right\}}\right\}},$$

$$C_3 = \frac{C_1\left(\sqrt{S} + Bi\right)e^{\sqrt{S}} - C_2\left(\sqrt{S} - Bi\right)e^{-\sqrt{S}}}{Bi\,e^{\sqrt{S/\alpha_r}}\left(1 + e^{\sqrt{S/\alpha_r}(2R-2)}\right)}$$

and $C_4 = \left\{\dfrac{C_1\left(\sqrt{S} + Bi\right)e^{\sqrt{S}} - C_2\left(\sqrt{S} - Bi\right)e^{-\sqrt{S}}}{Bi\,e^{\sqrt{S/\alpha_r}}\left(1 + e^{\sqrt{S/\alpha_r}(2R-2)}\right)}\right\} e^{2RM_2}.$

Equations (5.6) and (5.7) are inverted using a computer program based on Riemann-sum approximation as:

$$O_k(\xi,\eta) \cong \frac{e^{r\eta}}{\eta}\left[\frac{1}{2}W_k(\xi,\gamma) + \mathrm{Re}\sum_{n=1}^{N} W_k\left(\xi,\gamma + \frac{in\pi}{\eta}\right)(-1)^n\right] \tag{5.9}$$

Equation (5.9) yields the exact temperature distribution in both domains for the imperfect contact parabolic heat conduction model case.

5.2 Hyperbolic model for imperfect contact

In a manner similar to what has been done for perfect contact, the energy equations coupled at the interface have to be solved with different interfacial boundary conditions. In the case of perfect contact the temperatures at the interface are equaled while in this case the temperatures at the interface are related as:

$$q_1(1,\eta) = h[T_1(1,\eta) - T_2(1,\eta)]$$

The energy equations in dimensionless form are given as:

$$\frac{\partial \theta_1}{\partial \eta} = -\frac{\partial Q_1}{\partial \xi} \tag{5.10}$$

$$\frac{\partial \theta_2}{\partial \eta} = -\frac{1}{C_R}\frac{\partial Q_2}{\partial \xi} \tag{5.11}$$

$$Q_1 + \tau_{q,1}\frac{\partial Q_1}{\partial \eta} = -\frac{\partial \theta_1}{\partial \xi} \tag{5.12}$$

$$Q_2 + \tau_{q,2}\frac{\partial Q_2}{\partial \eta} = -K_r\frac{\partial \theta_2}{\partial \xi} \tag{5.13}$$

Eqs. (5.10) and (5.12), (5.11) and (5.13), are combined to yield:

$$\tau_{q,1}\frac{\partial^2 O_1}{\partial \eta^2} + \frac{\partial O_1}{\partial \eta} = \frac{\partial^2 O_1}{\partial \xi^2} \qquad 0 \leq \xi \leq 1.0 \tag{5.14}$$

$$\tau_{q,2}\frac{\partial^2 O_2}{\partial \eta^2} + \frac{\partial O_2}{\partial \eta} = \alpha_r\frac{\partial^2 O_2}{\partial \xi^2} \qquad 1.0 \leq \xi \leq R \tag{5.15}$$

54

Subject to the following initial and boundary conditions:

$$\theta_1(\xi,0) = \theta_2(\xi,0) = 1.0$$

(5.16)

$$\frac{\partial\theta_1(\xi,0)}{\partial\eta} = \frac{\partial\theta_2(\xi,0)}{\partial\eta} = 0.0$$

$$\theta_1(0,\eta) = 0.0$$

$$\frac{\partial\theta_2(R,\eta)}{\partial\xi} = 0.0$$

(5.17)

$$Q_1(1,\eta) = Q_2(1,\eta)$$

$$Q_1(1,\eta) = Bi(\theta_1(1,\eta) - \theta_2(1,\eta))$$

Laplace transformation of Eqs. (5.14) and (5.15), yields:

$$\frac{d^2W_1}{d\xi^2} - (\tau_{q,1}S^2 + S)W_1 = -(1 + \tau_{q,1}S)$$

(5.18)

$$\frac{d^2W_2}{d\xi^2} - \left(\frac{\tau_{q,2}S^2 + S}{\alpha_r}\right)W_2 = -\left(\frac{\tau_{q,2}S + 1}{\alpha_r}\right)$$

(5.19)

These two equations assume the following solutions:

$$W_1(\xi,S) = C_1e^{M_1\xi} + C_2e^{-M_1\xi} + \frac{1}{S}$$

(5.20)

$$W_2(\xi,S) = C_3e^{M_2\xi} + C_4e^{-M_2\xi} + \frac{1}{S}$$

(5.21)

where $M_1 = \sqrt{(\tau_{q,1}S^2 + S)}$ and $M_2 = \sqrt{\frac{(\tau_{q,2}S^2 + S)}{\alpha_r}}$.

Also, with the notation that $V = L\{Q\}$, Laplace transformation of Eq. (5.17) yields:

$$W_1(0,S) = 0.0$$

(5.22a)

$$\frac{dW_2(R,S)}{\partial\xi} = 0.0$$

(5.22b)

$$V_1(1,S) = V_2(1,S)$$

55

From Eqs. (5.12) and (5.13) with $Q_1(\xi,0) = Q_2(\xi,0) = 0.0$ and $V_1(1,S) = V_2(1,S)$, we obtain:

$$\frac{dW_1(1,S)}{d\xi} = \left(\frac{K_r(1+\tau_{q,1}S)}{(1+\tau_{q,2}S)}\right)\frac{dW_2(1,S)}{d\xi} \tag{5.22c}$$

Also, the second interfacial boundary condition becomes:

$$\frac{dW_1(1,S)}{d\xi} = -Bi(1+\tau_{q,1}S)[W_1(1,S) - W_2(1,S)] \tag{5.22d}$$

Insert Eqs. (5.20) and (5.21) into (5.22a-5.22d) and solve theses equations for C_1, C_2, C_3 and C_4 to yield:

$$C_1 = \frac{\left(-\dfrac{1}{S}\right)\left\{\dfrac{e^{-2M_1}\left[\beta\left(1+e^{M_2(2R-2)}\right)+\dfrac{K_r(M_1-\beta)}{\sqrt{\alpha_r}}\sqrt{\dfrac{(1+\tau_{q,1}S)}{(1+\tau_{q,2}S)}}\left(e^{M_2(2R-2)}-1\right)\right]}{\left[\dfrac{K_r(M_1+\beta)}{\sqrt{\alpha_r}}\sqrt{\dfrac{(1+\tau_{q,1}S)}{(1+\tau_{q,2}S)}}\left(e^{M_2(2R-2)}-1\right)+\beta\left(1+e^{M_2(2R-2)}\right)\right]}\right\}}{\left\{1+\dfrac{e^{-2M_1}\left[\beta\left(1+e^{M_2(2R-2)}\right)+\dfrac{K_r(M_1-\beta)}{\sqrt{\alpha_r}}\sqrt{\dfrac{(1+\tau_{q,1}S)}{(1+\tau_{q,2}S)}}\left(e^{M_2(2R-2)}-1\right)\right]}{\left[\dfrac{K_r(M_1+\beta)}{\sqrt{\alpha_r}}\sqrt{\dfrac{(1+\tau_{q,1}S)}{(1+\tau_{q,2}S)}}\left(e^{M_2(2R-2)}-1\right)+\beta\left(1+e^{M_2(2R-2)}\right)\right]}\right\}},$$

$$C_2 = \frac{-\dfrac{1}{S}}{\left\{1+\dfrac{e^{-2M_1}\left[\beta\left(1+e^{M_2(2R-2)}\right)+\dfrac{K_r(M_1-\beta)}{\sqrt{\alpha_r}}\sqrt{\dfrac{(1+\tau_{q,1}S)}{(1+\tau_{q,2}S)}}\left(e^{M_2(2R-2)}-1\right)\right]}{\left[\dfrac{K_r(M_1+\beta)}{\sqrt{\alpha_r}}\sqrt{\dfrac{(1+\tau_{q,1}S)}{(1+\tau_{q,2}S)}}\left(e^{M_2(2R-2)}-1\right)+\beta\left(1+e^{M_2(2R-2)}\right)\right]}\right\}},$$

$$C_3 = \frac{C_1(M_1+\beta)e^{-M_1} - C_2(M_1-\beta)e^{-M_1}}{\beta e^{-M_1}\left(1+e^{M_2(2R-2)}\right)} \quad \text{and}$$

$$C_4 = \left\{\frac{C_1(M_1+\beta)e^{-M_1} - C_2(M_1-\beta)e^{-M_1}}{\beta e^{-M_1}\left(1+e^{M_2(2R-2)}\right)}\right\} e^{2RM_2} \quad .$$

56

where $\beta = -Bi\left(1 + \tau_{q,1} S\right)$

Equations (5.20) and (5.21) are inverted using a computer program based on Riemann-sum approximation as:

$$\theta_k(\xi,\eta) \cong \frac{e^{\gamma\eta}}{\eta}\left[\frac{1}{2}W_k(\xi,\gamma) + \text{Re}\sum_{n=1}^{N} W_k\left(\xi,\gamma + \frac{in\pi}{\eta}\right)(-1)^n\right]$$

This equation yields the exact temperature distribution in both domains for the imperfect contact hyperbolic heat conduction model case.

5.4 Dual phase model for imperfect contact

In this case the temperatures at the interface are related as:

$$q_1(1,\eta) = h\left[T_1(1,\eta) - T_2(1,\eta)\right]$$

The energy equations in dimensionless form are given as:

$$\frac{\partial\theta_1}{\partial\eta} = -\frac{\partial Q_1}{\partial\xi} + G_1 \tag{5.23}$$

$$\frac{\partial\theta_2}{\partial\eta} = -\frac{1}{C_R}\frac{\partial Q_2}{\partial\xi} + G_2 \tag{5.24}$$

$$Q_1 + \tau_{q,1}\frac{\partial Q_1}{\partial\eta} = -\frac{\partial\theta_1}{\partial\xi} - \tau_{T,1}\frac{\partial\theta_1}{\partial\eta\partial\xi^2} \tag{5.25}$$

$$Q_2 + \tau_{q,2}\frac{\partial Q_2}{\partial\eta} = K_r\left[-\frac{\partial\theta_2}{\partial\xi} - \tau_{T,2}\frac{\partial\theta_2}{\partial\eta\partial\xi^2}\right] \tag{5.26}$$

Combine Eqs. (5.23) and (5.25), (5.24) and (5.26), to get:

$$\frac{\partial^2\theta_1}{\partial\xi^2} + \tau_{T,1}\frac{\partial^3\theta_1}{\partial\eta\partial\xi^2} + \left[G_1 + \tau_{q,1}\frac{\partial G_1}{\partial\eta}\right] = \frac{\partial\theta_1}{\partial\eta} + \tau_{q,1}\frac{\partial^2\theta_1}{\partial\eta^2} \tag{5.27}$$

$$\frac{\partial^2\theta_2}{\partial\xi^2} + \tau_{T,2}\frac{\partial^3\theta}{\partial\eta\partial\xi^2} + \frac{C_R}{K_r}\left[G_2 + \tau_{q,2}\frac{\partial G_2}{\partial\eta}\right] = \frac{C_R}{K_r}\left[\frac{\partial\theta_2}{\partial\eta} + \tau_{q,2}\frac{\partial^2\theta_2}{\partial\eta^2}\right] \tag{5.28}$$

where $\qquad \dfrac{C_R}{K_r} = \dfrac{\alpha_1}{\alpha_2} = \dfrac{1}{\alpha_r}$

57

Subject to the following initial and boundary conditions

$$\theta_1(\xi,0) = \theta_2(\xi,0) = 1.0$$

(5.29)

$$\frac{\partial \theta_1}{\partial \eta}(\xi,0) = \frac{\partial \theta_2}{\partial \eta}(\xi,0) = 0.0$$

$$\theta_1(0,\eta) = 0.0$$

$$\frac{\partial \theta_2}{\partial \xi}(R,\eta) = 0.0$$

(5.30)

$$Q_1(1,\eta) = Q_2(1,\eta)$$

$$Q_1(1,\eta) = Bi\left[\theta_1(1,\eta) - \theta_2(1,\eta)\right]$$

Now, assume there is no heating source $(G_1 = G_2 = 0.0)$ with the notation that

$W(\xi,S) = L\{\theta(\xi,\eta)\}$, Laplace transformation of Eqs. (5.27) and (5.28), yields:

$$\frac{d^2 W_1}{d\xi^2} - \left(\frac{S + \tau_{q,1} S^2}{1 + \tau_{T,1} S}\right) W_1 = -\left(\frac{1 + \tau_{q,1} S}{1 + \tau_{T,1} S}\right)$$

(5.31)

$$\frac{d^2 W_2}{d\xi^2} - \left(\frac{S + \tau_{q,1} S^2}{(1 + \tau_{T,1} S)\alpha_r}\right) W_2 = -\left(\frac{1 + \tau_{q,1} S}{(1 + \tau_{T,1} S)\alpha_r}\right)$$

(5.32)

Equations (5.31) and (5.32) assume the following solutions:

$$W_1 = C_1 e^{\xi \lambda_1} + C_2 e^{-\xi \lambda_1} + \frac{1}{S}$$

(5.33)

$$W_2 = C_3 e^{\xi \lambda_2} + C_4 e^{-\xi \lambda_2} + \frac{1}{S}$$

(5.34)

where $\lambda_1 = \sqrt{\left(\dfrac{S + \tau_{q,1} S^2}{1 + \tau_{T,1} S}\right)}$ and $\lambda_2 = \sqrt{\dfrac{\left(S + \tau_{q,2} S^2\right)}{(1 + \tau_{T,2} S)\alpha_r}}$.

Also, with the notation that $V = L\{Q\}$, Laplace transformation of Eq. (5.30), yields:

$$W_1(0,S) = 0.0$$

58

$$\frac{dW_2}{\partial \xi}(R,S) = 0.0 \tag{5.35a}$$

$$V_1(1,S) = V_2(1,S)$$

From Eqs. (5.27) and (5.28) with $Q_1(\xi,0) = Q_2(\xi,0) = 0.0$ and $V_1(1,S) = V_2(1,S)$, we have:

$$\left(\frac{dW_1(1,S)}{d\xi}\right) = \left[\frac{K_r(1+\tau_{T,2}S)(1+\tau_{q,1}S)}{(1+\tau_{q,2}S)(1+\tau_{T,1}S)}\right]\left(\frac{dW_2(1,S)}{d\xi}\right) \tag{5.35b}$$

let $\Psi = \left[\dfrac{K_r(1+\tau_{T,2}S)(1+\tau_{q,1}S)}{(1+\tau_{q,2}S)(1+\tau_{T,1}S)}\right]$

Equation (5.35b) is expressed as:

$$\left(\frac{dW_1(1,S)}{d\xi}\right) = \Psi\left(\frac{dW_2(1,S)}{d\xi}\right)$$

Also, the second interfacial boundary condition becomes:

$$\frac{dW_1(1,S)}{d\xi} = -Bi\left(\frac{1+\tau_{q,1}S}{1+\tau_{T,1}S}\right)[W_1(1,S)-W_2(1,S)] \tag{5.35c}$$

let $\Phi = \left(\dfrac{1+\tau_{q,1}S}{1+\tau_{T,1}S}\right)$

Equation (5.35c) is expressed as:

$$\frac{dW_1(1,S)}{d\xi} = -Bi\,\Phi[W_1(1,S)-W_2(1,S)] \tag{5.35d}$$

Insert Eqs. (5.33) and (5.34) into (5.35a-5.35d) and solve these equations for C_1, C_2, C_3 and C_4 to yield:

59

$$C_1 = \cfrac{\left(-\dfrac{1}{S}\right)\left\{\cfrac{e^{2\lambda_1}\left[\left(Bi\,\Phi - \Psi\dfrac{\lambda_2}{\lambda_1}(\lambda_1 - Bi\,\Phi)\right)+\left(Bi\,\Phi + \Psi\dfrac{\lambda_2}{\lambda_1}(\lambda_1 - Bi\,\Phi)\right)e^{\lambda_2(2R-2)}\right]}{\left[\left(Bi\,\Phi - \Psi\dfrac{\lambda_2}{\lambda_1}(\lambda_1 + Bi\,\Phi)\right)+\left(Bi\,\Phi + \Psi\dfrac{\lambda_2}{\lambda_1}(\lambda_1 + Bi\,\Phi)\right)e^{\lambda_2(2R-2)}\right]}\right\}}{\left\{1+\cfrac{e^{2\lambda_1}\left[\left(Bi\,\Phi - \Psi\dfrac{\lambda_2}{\lambda_1}(\lambda_1 - Bi\,\Phi)\right)+\left(Bi\,\Phi + \Psi\dfrac{\lambda_2}{\lambda_1}(\lambda_1 - Bi\,\Phi)\right)e^{\lambda_2(2R-2)}\right]}{\left[\left(Bi\,\Phi - \Psi\dfrac{\lambda_2}{\lambda_1}(\lambda_1 + Bi\,\Phi)\right)+\left(Bi\,\Phi + \Psi\dfrac{\lambda_2}{\lambda_1}(\lambda_1 + Bi\,\Phi)\right)e^{\lambda_2(2R-2)}\right]}\right\}},$$

$$C_2 = \cfrac{-\dfrac{1}{S}}{\left\{1+\cfrac{e^{2\lambda_1}\left[\left(Bi\,\Phi - \Psi\dfrac{\lambda_2}{\lambda_1}(\lambda_1 - Bi\,\Phi)\right)+\left(Bi\,\Phi + \Psi\dfrac{\lambda_2}{\lambda_1}(\lambda_1 - Bi\,\Phi)\right)e^{\lambda_2(2R-2)}\right]}{\left[\left(Bi\,\Phi - \Psi\dfrac{\lambda_2}{\lambda_1}(\lambda_1 + Bi\,\Phi)\right)+\left(Bi\,\Phi + \Psi\dfrac{\lambda_2}{\lambda_1}(\lambda_1 + Bi\,\Phi)\right)e^{\lambda_2(2R-2)}\right]}\right\}},$$

$$C_3 = \frac{C_1(\lambda_1 + Bi\,\Phi)e^{\lambda_1} - C_2(\lambda_1 - Bi\,\Phi)e^{-\lambda_1}}{Bi\,\Phi\,e^{\lambda_2}\left(1 + e^{\lambda_2(2R-2)}\right)} \quad \text{and}$$

$$C_4 = \left\{\frac{C_1(\lambda_1 + Bi\,\Phi)e^{\lambda_1} - C_2(\lambda_1 - Bi\,\Phi)e^{-\lambda_1}}{Bi\,\Phi\,e^{\lambda_2}\left(1 + e^{\lambda_2(2R-2)}\right)}\right\}e^{2\lambda_2 R}.$$

where $\quad \Psi\dfrac{\lambda_2}{\lambda_1} = \sqrt{\dfrac{(1 + \tau_{T,2}S)(1 + \tau_{q,1}S)}{(1 + \tau_{T,1}S)(1 + \tau_{q,2}S)}}$

Equations (5.33) and (5.34) are inverted using a computer program based on Riemann-sum approximation as:

$$\theta_k(\xi,\eta) \cong \frac{e^{r\eta}}{\eta}\left[\frac{1}{2}W_k(\xi,\gamma) + \operatorname{Re}\sum_{n=1}^{N} W_k\left(\xi,\gamma + \frac{in\pi}{\eta}\right)(-1)^n\right] \tag{5.36}$$

Equation (5.36) yields the exact temperature distribution in both domains for the imperfect contact dual phase heat conduction model case.

6- PERTURBATION TECHNIQUE

6.1 Introduction

Knowledge of transient convective heat transfer is of importance in a number of different physical situations such as the starting, ending and change in power level transients in gas turbine engines, recuperative and regenerative heat exchangers, and cooling passages in nuclear power reactors. Practically speaking, most problems of this type are conjugated problems, that is., the temperature distribution in the moving fluid is mutually coupled to the temperature distribution in the solid body over, or through, which the fluid flows.

The behavior of forced convection conjugated heat transfer problems is described using two energy equations coupled at the interface between the solid and the fluid domains. It is not easy to solve the coupled energy equations, even after eliminating the coupling between them. The elimination of the coupling between the two equations yields a single equation, which contains higher-order mixed derivatives in both time and space. The appearance of such terms complicates the solution methodology. However, there are certain applications in which the convective heat transfer coefficient between the flowing fluid and the solid wall is high. As the convective heat transfer coefficient increases, the normalized temperature difference between the fluid and the solid-wall becomes small, but not negligible. This small temperature difference between the fluid and the solid domains is observed, especially in applications having high convective heat transfer coefficients or in applications having small fluid flow rates. A small fluid flow rate gives the fluid enough time to exchange its energy with the solid domain, and as a result the fluid temperature

61

approaches that of the solid domain. When the temperature difference between the fluid and the solid domains becomes small enough, then this difference may be normalized in the form of a perturbed quantity. As a result, a perturbation technique may be used to eliminate the coupling between the two energy equations. The elimination of this coupling produces two uncoupled partial differential equations which have the same order as the original coupled partial differential equations and which do not contain any mixed derivative terms.

The aim of the present work is to present a simplified perturbation technique to reformulate the two coupled energy equations of both the solid and the fluid domains. As an example, we consider a simple problem, which is solved numerically, using the proposed perturbation technique and the results are compared with the exact solution.

6.2 Analysis

Consider the transient conjugate forced convection heat transfer problem in circular channel of finite wall thickness as shown in Fig. 6.1. The flowing fluid in this channel is a steady slug flow of constant velocity with constant physical properties. The transient aspects in the thermal behavior of the channel are produced from the unsteadiness in the inlet fluid temperature, ambient conditions and fluid flow rate. The thermal behavior of the channel is assumed to be lumped radially. Also, it is assumed that there is no heat generation within the fluid and solid domains and there is no imposed heat flux on the outer boundary of the solid wall. As the result, the problem is described by the following two energy equations for the fluid and solid wall, respectively, (Al-Nimr and El-Shaarawi, 1992).
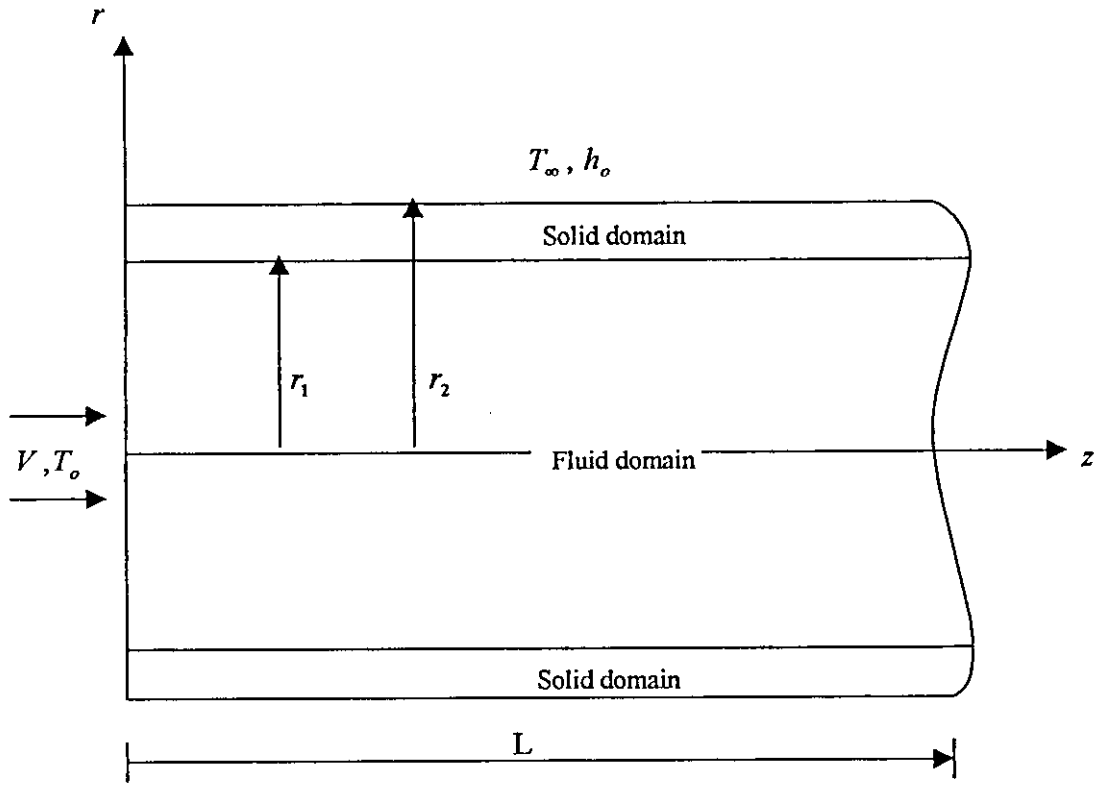
Figure 6.1: Schematic diagram of the problem

$$\frac{\partial T_f}{\partial t} + V \frac{\partial T_f}{\partial z} + b_1 \left(T_f - T_s \right) - b_2 \frac{\partial^2 T_f}{\partial z^2} = 0 \tag{6.1}$$

$$\frac{\partial T_s}{\partial t} - b_3 \left(T_f - T_s \right) + b_4 \left(T_s - T_\infty \right) - b_5 \frac{\partial^2 T_s}{\partial z^2} = 0 \tag{6.2}$$

where $b_1 = \dfrac{2 h_i}{\rho_f c_f r_1}$, $\qquad b_2 = \dfrac{k_f}{\rho_f c_f r_1^2}$, $\qquad b_3 = \dfrac{2 h_i r_1}{\rho_s c_s \left(r_2^2 - r_1^2 \right)}$,

$\qquad b_4 = \dfrac{2 h_o r_2}{\rho_s c_s \left(r_2^2 - r_1^2 \right)}$ and $\qquad b_5 = \dfrac{k_s}{\rho_s c_s r_1^2}$

The energy equations in dimensionless form for the fluid and solid wall respectively, are:

$$\frac{\partial \theta_f}{\partial \eta} + \frac{\partial \theta_f}{\partial \xi} + H_1(\theta_f - \theta_s) - H_2 \frac{\partial^2 \theta_f}{\partial \xi^2} = 0.0 \qquad (6.3)$$

$$\frac{\partial \theta_s}{\partial \eta} - H_3(\theta_f - \theta_s) + H_4(\theta_s - \theta_\infty) - H_5 \frac{\partial^2 \theta_s}{\partial \xi^2} = 0.0 \qquad (6.4)$$

where the dimensionless parameters are defined as:

$$\theta = \frac{T - T_\infty}{T_o - T_\infty}, \qquad \xi = \frac{z}{r_1}, \qquad \eta = \frac{tV}{r_1}$$

In the above dimensionless parameters, T_∞ and T_o are selected as a reference ambient and inlet fluid temperatures, respectively, and V is a given velocity. The different parameters, which appear in Eqs. (6.3) and (6.4) are defined as:

$$H_1 = \frac{2h_i}{V\rho_f c_f}, \; H_2 = \frac{\alpha_f}{V r_1}, \; H_3 = \frac{2h_i r_1^2}{V\rho_s c_s (r_2^2 - r_1^2)}, \; H_4 = \frac{2h_o r_2 r_1}{V\rho_s c_s (r_2^2 - r_1^2)} \text{ and } H_5 = \frac{\alpha_s}{V r_1}$$

where (h_i, h_o) are the inside and outside thermal conductivity, (r_1, r_2) are the inner and outer radius of the channel and $(\rho_f c_f)$, $(\rho_s c_s)$ are the density and specific heat of the fluid and the solid wall respectively.

The assumption that the thermal behavior of the channel is lumped radially is justified in channels having $r_1/L \ll 1$, and Pe <50, especially for locations far from the entrance of the channel, (Al-Nimr, 1993). Analytical or numerical solutions of Eqs. (6.3) and (6.4) are not an easy matter, and if it is obtained, it will have a complicated form. The reason for this is that Eqs. (6.3) and (6.4) are two coupled partial differential equations which are second order in space and first order in time. Eliminating the coupling between these equations yields a mixed-derivative partial differential equation, which is fourth order in space and second order in time. The higher order and mixed-derivative terms that appear in the resulting equations raise the difficulty of solving such problems. However, in many applications, the coupling between the two energy Eqs.

(6.3) and (6.4) may be eliminated without raising the order of the resulting partial differential equations and without the appearance of mixed-derivative terms. These applications involve situations in which the convective heat transfer coefficient between the flowing fluid and the solid-wall is large. In these applications, the difference between the solid and fluid temperatures may be normalized in the form of a small-perturbed quantity. This difference may be written as:

$$\theta_s(\xi,\eta) = \theta_f(\xi,\eta) + \varepsilon\,\Delta(\xi,\eta) \tag{6.5}$$

where $\Delta(\xi,\eta)$ is a function of space and time, and $\varepsilon = 1/H_3$ is a dimensionless small parameter.

Consider, for an example, flowing mercury in a finite wall thickness duct. The mercury has small velocity $(V=0.001\ m/s)$ and the interface heat transfer coefficient h_i between the liquid metal and the solid wall varies in the rage 50-20000 $W/m^2 k$. As a result, $\varepsilon = 0.03$, which is small enough to be considered as a perturbed quantity. Now, Eqs. (6.3) and (6.4) can be written as:

$$\frac{\partial^2 \theta_f}{\partial \xi^2} - M_1 \frac{\partial \theta_f}{\partial \xi} - M_2 \frac{\partial \theta_f}{\partial \eta} - M_3(\theta_f - \theta_\infty) = O(\varepsilon) \tag{6.6}$$

$$\Delta(\xi,\eta) = \frac{H_3}{H_1}\left(\frac{\partial \theta_f}{\partial \eta} + \frac{\partial \theta_f}{\partial \xi} - H_2 \frac{\partial^2 \theta_f}{\partial \xi^2}\right) \tag{6.7}$$

where:

$$M_1 = \frac{1}{H_1(H_2/H_1 + H_5/H_3)}, \qquad M_2 = \frac{(1/H_1 + 1/H_3)}{(H_2/H_1 + H_5/H_3)} \quad \text{and}$$

$$M_3 = \frac{H_4}{H_3(H_2/H_1 + H_5/H_3)}$$

Equation (6.6) is obtained by combining Eqs. (6.3) and (6.4) and Eq. (6.7) is obtained from Eq. (6.3) taking recourse to Eq. (6.5). It is clear that Eq. (6.6) is simple partial

65

differential equation which has the same order as that of the original governing Eqs. (6.3) and (6.4) and which has no mixed-derivative terms. It is worth mentioning that the previous analysis is valid even if the original governing Eqs. (6.3) and (6.4) contain temperature-dependent thermal properties.

6.3 Case study

Consider the case in which a steady slug flow of constant velocity (V) flowing into a semi-infinite channel having finite wall thickness. The semi-infinite length assumption is found to be true if Fo(1+Pe)<<1, as reported by (Issa and AL-Nimr, 1989). This condition requires that the sum of the energy transferred by conduction and convection is much less than the energy stored in the fluid. Also, it is assumed that there is no heat generation within the fluid and solid domains, the axial conduction both in the fluid and in the solid wall is negligible and there is no imposed heat flux on the outer boundary of the solid wall. Initially, both domains of the channel are in the thermal equilibrium with a constant ambient condition T_∞. Suddenly, a fluid having temperature T_o, different from the ambient one, starts entering the channel causing the unsteadiness in the thermal behavior of the channel. The thermal behavior of the channel as described by the exact and approximate perturbation models is given in the following two parts.

6.3.1 Exact model

In this case, two energy equations coupled at the interface have to be solved. As a result of the above assumptions, Eqs. (6.3) and (6.4) are reduced to:

$$\frac{\partial \theta_f}{\partial \eta} + \frac{\partial \theta_f}{\partial \xi} + H_1\left(\theta_f - \theta_s\right) = 0.0 \tag{6.8}$$

$$\frac{\partial \theta_s}{\partial \eta} - H_3\left(\theta_f - \theta_s\right) + H_4\left(\theta_s - \theta_\infty\right) = 0.0 \tag{6.9}$$

66

Subject to the following initial and boundary conditions

$$\theta_f(\xi,0) = \theta_s(\xi,0) = 0.0 \qquad (6.10)$$

$$\theta_f(0,\eta) = 1.0 \qquad (6.11)$$

Now, with the notation that $L\{\theta_f(\xi,\eta)\} = W_f(\xi,S)$, Laplace transformation of Eqs. (6.8)

and (6.9), yields:

$$SW_f + \frac{dW_f}{d\xi} + H_1(W_f - W_s) = 0.0$$

$$\frac{dW_f}{d\xi} + (H_1 + S)W_f - H_1 W_s = 0.0 \qquad (6.12)$$

$$SW_s - H_3(W_f - W_s) + H_4 W_s = 0.0$$

$$W_s = \frac{H_3 W_f}{(S + H_3 + H_4)} \qquad (6.13)$$

Substitute (6.13) into (6.12) yields

$$\frac{dW_f}{d\xi} + \left[(H_1 + S) - \frac{H_1 H_3}{(S + H_3 + H_4)}\right]W_f = 0.0 \qquad (6.14)$$

This equation assumes the following solution

$$W_f = C e^{-\sigma_1 \xi} \qquad (6.15)$$

where $\sigma_1 = \left[(H_1 + S) - \frac{H_1 H_3}{(S + H_3 + H_4)}\right]$

Also, Laplace transformation of Eq. (6.11) yields:

$$W_f(0,S) = \frac{1}{S} \qquad (6.16)$$

In term of Eq.(6.16), Eq.(6.15) is rewritten as:

$$W_f(\xi,S) = \frac{1}{S} e^{-\sigma_1 \xi} \qquad (6.17)$$

Equation (6.17) is inverted numerically using Riemann-sum approximation as:

67

$$\theta_f(\xi,\eta) \cong \frac{e^{\gamma\eta}}{\eta}\left[\frac{1}{2}W_f(\xi,\gamma) + \mathrm{Re}\sum_{n=1}^{N} W_f\left(\xi,\gamma + \frac{in\pi}{\eta}\right)(-1)^n\right] \qquad (6.18)$$

Equation (6.18) yields the exact temperature distribution in the fluid domain. The computer model results with changing the $H_1, H_2, and\, H_3$ parameters were exhibited in the figures in chapter 7, which will be analyzed later.

6.3.2 Approximate model

In this case, we intend to solve one energy equation in the fluid domain.

$$\frac{\partial\theta_f}{\partial\eta} + N_1\frac{\partial\theta_f}{\partial\xi} + N_2\theta_f = O(\varepsilon) \qquad (6.19)$$

where $N_1 = \dfrac{H_3}{H_3 + H_1}$, $\quad N_2 = \dfrac{H_1 H_4}{H_3 + H_1}$ and the temperature difference is obtained in terms of θ_f as:

$$\Delta(\xi,\eta) = \frac{H_3}{H_1}\left(\frac{\partial\theta_f}{\partial\eta} + \frac{\partial\theta_f}{\partial\xi}\right) \qquad (6.20)$$

Equation (6.19) has the following initial and boundary conditions:

$$\theta_f(\xi,0) = 0.0 \qquad (6.21)$$

$$\theta_f(0,\eta) = 1.0 \qquad (6.22)$$

Laplace transformation of Eqs. (6.19) and (6.22), with the notation that $L\{\theta_f(\xi,\eta)\} = W_f(\xi,S)$ yields the following equations:

$$\frac{dW_f}{d\xi} + \left(\frac{N_2 + S}{N_1}\right)W_f = 0.0 \qquad (6.23)$$

$$W_f(0,S) = \frac{1}{S} \qquad (6.24)$$

In a manner similar to what has been done previously, using Laplace transformation technique, Eqs. (6.23) and (6.24) assume the following solution in the Laplacian domain:

$$W_f(\xi, S) = \frac{1}{S} e^{-\sigma_2 \xi} \qquad (6.25)$$

where $\sigma_2 = \dfrac{(N_2 + S)}{N_1}$

Equation (6.25) is inverted numerically using a computer program based on Riemann-sum approximation as:

$$\theta_f(\xi, \eta) \cong \frac{e^{\gamma \eta}}{\eta} \left[\frac{1}{2} W_f(\xi, \gamma) + \mathrm{Re} \sum_{n=1}^{N} W_f\left(\xi, \gamma + \frac{in\pi}{\eta}\right)(-1)^n \right] \qquad (6.26)$$

Equation (6.26) yields the approximate temperature distribution in the fluid domain.

69

7- RESULTS AND DISCUSIONS

7.1 Generalized boundary condition for the parabolic heat conduction model

The mathematical models described in the previous chapters were solved in a computer simulation program and the results are illustrated in Figs. 7.1 through 7.53. Figures (7.1-7.3) show the exact and the approximate transient temperature variation in the thick domain for certain values of thickness ratio, thermal diffusivity ratio and thermal conductivity ratio. These figures demonstrate that both models give almost the same predictions according to the values summarized in Table (7.1).

Figures (7.4-7.6) show the effect of α_r and K_r on the transient temperature difference at different thickness ratio (R). Therefore, from these figures the difference in the dimensionless temperature between the exact and the approximate models does not exceed 0.035. Fig. (7.7) shows the effect of α_r and K_r on the percentage transient temperature difference between the exact and the approximate models $\left| \dfrac{\theta_{exact} - \theta_{approximate}}{\theta_{exact}} \right| *100\%$ .Figures (7.8 and 7.9) show clearly the effect of α_r on the transient temperature variation for both models. It is obvious that when α_r increases above the values shown in Table (7.1) at any R, the deviation between both models decreases and when α_r decreases the deviation between both models increases. Figure (7.10) shows comparisons between the exact and the approximate transient temperature distributions at different thermal conductivity ratios. The approximate temperature distribution is obtained by solving the thick domain energy equation using the appropriate generalized thermal boundary condition. Figures (7.11 and 7.12) show a

comparison between the exact and the approximate transient temperature distributions at different thickness ratio (R). The approximate temperature distribution is obtained by solving the thick domain energy equation using the appropriate generalized thermal boundary condition. These figures show that the deviation in the transient temperature distribution between both models decreases as R decreases and the deviation increases as R increases.

Figures (7.13-7.18) show the effect of α_r, K_r and R on the dimensionless temperature difference which is defined as $\left|\theta_{exact} - \theta_{approximate}\right|$. Figures (7.13 and 7.14) show the effect of α_r on the temperature difference between the predictions of the exact and the approximate models. It is obvious that the validity of using the generalized boundary condition is secured as α_r increases. Using thin film of large α_r implies that the thin film has high α_2 or the thick domain has low α_1. The thin film thermal diffusivity α_2 may be increased by increasing its thermal conductivity k_2 or by decreasing its thermal capacity $(\rho_2 c_2)$. The ability of the thin film to store energy decreases as its thermal capacity $(\rho_2 c_2)$ decreases. Also, thermal resistance of the thin layer decreases as its thermal conductivity k_2 increases. As a result, the thick domain interaction with its surrounding is not affected by the presence of the thin layer as α_r increases and this implies that the predictions of both models become very close to each other. Figure (7.13) clearly portrays that the deviation between the predictions of both models decreases as time proceeds. This is predicted since both models show that $\theta \to 0$ as $\eta \to \infty$. Also, low thermal diffusivity α_1 implies that the thick domain has law thermal conductivity or large thermal capacity ratios. If the thick domain has low thermal conductivity then its interaction with the thin domain is week and as a result, the thick domain is not aware of the existence of the thin layer. On the other hand, if the

71

thick domain thermal capacity is large, then the thermal effects of the thin layer can not cause significant thermal changes in the thick domain.

Figures (7.15 and 7.16) show the effect of K_r on the validity of using the generalized thermal boundary condition. The effect of K_r on the validity of the generalized boundary condition is insignificant. As an example, the temperature difference does not exceed 0.035 for any K_r used. But relatively as K_r increases, then both models will obtain a better agreement. As the thin film thermal conductivity k_2 increases, then the thick domain can feel the external thermal effects of the surrounding perfectly as if the thin layer is in non-existence. Also, if the thick domain thermal conductivity decreases, then the existence of the thin layer does not affect the thermal interaction of the thick domain with the external boundary. As a result, the thick domain behaves as if the thin layer, again, is in non-existence.

Figures (7.17 and 7.18) show the effect of the thickness ratio (R) on the dimensionless temperature difference. The validity of using the generalized boundary condition is secured as R decreases. This was expected since decreasing R decreases the total thermal capacity of the thin layer and this in turns decreases the thin layer ability to store energy. Also, as R decreases the thin layer thermal resistance decreases and this in turns justifies the replacement of the thin layer by its equivalence generalized thermal boundary condition. In the limit as the layer thickness (R-1) approaches 0.0, the interaction of the thick domain with its surrounding is not affected by the presence of the thin layer. As mentioned previously, the approximate model ignores the presence of the thin layer and replaces its effect by using the generalized thermal boundary condition. This replacement becomes more accurate when the thin layer gets insignificant effect. This is satisfied when the thin layer has very small thickness, density, specific heat and high thermal conductivity.

72

Figures (7.19 and 7.20) show the exact and the approximate transient temperature variation in the thick domain for certain values of thickness ratio, thermal diffusivity ratio, thermal conductivity ratio and different dimensionless distance in the thick domain. Evident from these figures that both models give almost the same predictions at any location in the thick domain according to the values summarized in Table (7.1). Figure (7.21) shows the exact and the approximate temperature distribution in the thick domain for certain values of thickness ratio, thermal diffusivity ratio, thermal conductivity ratio and different dimensionless time. This figure depicts that both models give almost the same predictions at any time in the thick domain according to the values summarized in Table (7.1).

Figure (7.22) shows a map for the validity of using the generalized boundary condition. The valid region, within which using the generalized boundary condition is secured, increases as α_r increases and R decreases. It is found that this map is insensitive to the changes in K_r. But relatively for very high values of K_r the temperature difference between the exact and approximate models become very small as shown in Fig. (7.15).

Table (7.1) summarizes the ranges of α_r within which the generalized thermal boundary condition yields accurate predictions. What is shown here is that the ranges of α_r become narrower as R increases. As an example, when R=1.01, the generalized thermal boundary condition may be used over the entire ranges of α_r. On the other hand when R=1.5, the generalized boundary condition is secured when α_r is greater than 0.9.

7.2 Generalized boundary condition for the hyperbolic heat conduction model

Figures (7.23 and 7.24) show the exact temperature distributions in both domains under the effect of the parabolic and hyperbolic heat conduction models. From these figures, it is shown that both models give almost the same predictions since the values of $\tau_{q,1}$ and $\tau_{q,2}$ are relatively small. This implies that the phase-lag concept has insignificant effect on the predictions of the parabolic heat conduction model when $\tau_{q,1}$ and $\tau_{q,2}$ are less than 0.01. Consequently as $\tau_{q,1}$ or $\tau_{q,2}$ increases, the deviation between both models increases. Figures (7.25-7.27) show a comparison between the exact and the approximate model. The approximate model uses the generalized hyperbolic boundary condition. Both figures show that the generalized boundary condition gives a very good prediction for the layers thermal behavior.

Figure (7.28) shows the effect of the thermal diffusivity ratio (α_r) on the predictions of the generalized boundary condition as compared to the predictions of the exact model. Therefore, from this figure, the validity of using the generalized boundary is secured as α_r increases. Using thin film of large α_r implies that the thin film has high α_2 or the thick domain has low α_1. The thin film thermal diffusivity α_2 may be increased by increasing its thermal conductivity k_2 or by decreasing its thermal capacity $(\rho_2 c_2)$. The ability of the thin film to store energy decreases as its thermal capacity $(\rho_2 c_2)$ decreases. Also, thermal resistance of the thin layer decreases as its thermal conductivity k_2 increases. As a result, the thick domain interaction with its surrounding is not affected by the presence of the thin layer as α_r increases and this implies that the predictions of both models become very close to each other. Also, low thermal

diffusivity α_1 implies that the thick domain has law thermal conductivity or large thermal capacity. If the thick domain has low thermal conductivity then its interaction with the thin domain is weak and as a result, the thick domain is not aware of the existence of the thin layer. On the other hand, if the thick domain thermal capacity is large, then the thermal effects of the thin layer can not cause significant thermal changes in the thick domain.

Figure (7.29) shows the effect of K_r on the validity of using the generalized thermal boundary condition. As a result the effect of K_r on the deviation between the predictions of both models is less significant than the effect of α_r. But relatively as K_r increases, then both models become in a better agreement. As the thin film thermal conductivity k_2 increases, then the thick domain can feel the external thermal effects of the surrounding perfectly as if the thin layer is in non-existence. Also, if the thick domain thermal conductivity decreases, then the existence of the thin layer does not affect the thermal interaction of the thick domain with the external boundary. As a result, the thick domain behaves as if the thin layer does not exist.

Figure (7.30) shows the effect of the thin layer thickness (R) on the accuracy of using the generalized thermal boundary condition. In which case the validity of using the generalized boundary condition is secured as R decreases. This is obvious since decreasing R decreases the total thermal capacity of the thin layer and this in turns decreases the thin layer ability to store energy. Also, as R decreases the thin layer thermal resistance decreases and this in turns justifies the replacing of the thin layer by its equivalence generalized thermal boundary condition. In the limit as (R-1) approaches 0.0, the interaction of the thick domain with its surrounding is not affected by the presence of the thin layer. As mentioned previously, the approximate model ignores the presence of the thin layer and replaces its effect by using the generalized thermal

boundary condition. This replacement becomes more accurate when the thin layer is of insignificant effect. This is satisfied when the thin layer has very small thickness, density and high thermal diffusivity.

Figure (7.31) shows the transient temperature variation as predicted by the parabolic diffusion and hyperbolic wave models at different values of $\tau_{q,1}$ and $\tau_{q,2}$. Hence, the deviation from the parabolic model increases as $\tau_{q,1}$ and $\tau_{q,2}$ increases.

Table (7.1) summarizes the ranges of α_r within which the generalized hyperbolic thermal boundary condition yields accurate predictions. It is clear that the ranges of α_r become narrower as R increases. As an example, when R=1.01, the generalized thermal boundary condition may be used over the entire ranges of α_r. On the other hand when R=1.5, the generalized boundary condition is secured when α_r is greater than 0.9.

7.3 Parabolic and hyperbolic heat conduction models for imperfect contact

Although neglected until now, it is important to recognize that, in composite systems, the temperature drops across the interface between materials may be appreciable. In the present work, the effect of imperfect contact and the temperature drop at the interface in the composite systems is studied for the hyperbolic model. Also, comparison between perfect and imperfect contact, and when the imperfect becomes perfect is obtained here.

Figures (7.32-7.35) show the effect of the interfacial *Biot* number on the spatial temperature distribution within the two domains. Figures (7.32 and 7.33) clearly demonstrate that the temperature distribution for the imperfect contact case approaches that for the perfect contact case as *Bi* increases. Also, the interfacial temperature jump decreases as *Bi* number increases. Using the perfect thermal contact assumption,

overestimates the temperature in the first domain, which is adjacent to the heat transfer boundary, i. e, the boundary at which the heating (or the cooling) effects are applied. On the other hand, the perfect thermal contact assumption underestimates the temperature within the second domain adjacent to the insulated boundary. Figures (7.34 and 7.35) show that interfacial *Biot* number larger than 50 yields predictions similar to that produced by the perfect contact models. Figure (7.36) shows the deviation between the predictions of both perfect and imperfect contact models at different interfacial *Biot* numbers. Therefore, the deviation decreases as *Bi* increases. The deviation in the domain adjacent to the heat transfer boundary is larger than that in the domain adjacent to the insulated boundary. Also, the deviation has its maximum value at the contact plane. As a result, it is concluded that the deviation between both the perfect and the imperfect contact models is significant near the contact plane and in locations having high heat transfer rates. Figure (7.23) shows the spatial temperature distribution using the perfect contact model at different thermal relaxation times $\tau_{q,1}$ and $\tau_{q,2}$. It is evident from this figure that for $\tau_{q,1}$ and $\tau_{q,2}$ less than 0.01; the thermal relaxation time has insignificant effect on the prediction of the diffusion parabolic model, which assumes that $\tau_{q1} = \tau_{q2} = 0.0$.

Figure (7.37) shows the effect of the interfacial *Biot* number on the transient temperature variation within the two domains at two different locations. It is confirmed from this figure that the transient temperature variation for the imperfect contact case approaches that for the perfect contact case as *Bi* increases. Also, this figure shows that interfacial *Biot* number larger than 50 yields predictions similar to that produced by the perfect contact model.

Figure (7.38) shows the effect of the second domain thickness (R-1) on the predictions of the perfect and imperfect contact models within the first domain. The

deviation between both models decreases as the second domain thickness decreases. As the thickness of the second domain decreases, its thermal capacity and thermal resistance decreases and as a result, the first domain is not affected by the presence of the second domain or by the type of the interfacial thermal conditions at the interface between both domains. For situations involving very thin second domain, perfect thermal contact assumption is justified. As an example, it is clear from Fig. (7.38) that the second domain has insignificant effect on the thermal behavior of the first domain when the dimensionless thickness of the second domain is less than 0.1.

Figure (7.39) shows the effect of the thermal conductivity ratio K_r on the predictions of both models within the two domains. As K_r increases, the deviation between the predictions of both models decreases in the second domain, which has the higher conductivity, and increases in the first domain, which has the lower conductivity. Domains that have high thermal conductivity are less sensitive to the type of the interfacial thermal conditions. Also, the temperature distribution in the second domain, which has higher conductivity, may be assumed to be spatially lumped.

Figure (7.40) shows the effect of the thermal diffusivity ratio α_r on the deviation between the predictions of both models within the two domains. It is illustrated that as α_r increases the deviation increases in the second domain and decreases in the first domain. Increasing α_r with a fixed value of K_r implies that the thermal capacity ratio $\rho_1 c_1 / \rho_2 c_2$ increases. The thermal capacity ratio $\rho_1 c_1 / \rho_2 c_2$ increases by increasing $\rho_1 c_1$ or decreasing $\rho_2 c_2$. As the thermal capacity of the first domain increases, then the type of interfacial thermal boundary condition does not cause a significant change in the temperature distribution of the first domain. On the other hand, as $\rho_2 c_2$ decreases, then the type of the interfacial thermal boundary condition

78

causes a significant change in the temperature distribution of the second domain. Temperature distribution within low thermal capacity domains is very sensitive to any change in the interfacial thermal boundary conditions.

7.4 Dual phase model for perfect and imperfect contact

Figures (7.41 and 7.42) obtain the lagging behavior of the dual phase model. If $\tau_T < \tau_q$, then temperature gradient is the cause and the heat flux vector is the effect as shown in Fig. (7.41). On the other hand, if $\tau_T > \tau_q$ as shown in Fig. (7.42) then the heat flux vector is the cause and the temperature gradient is the effect. Figures (7.43 and 7.44) show the exact temperature distributions in both domains under the effect of the hyperbolic and the dual phase heat conduction models. From these figures it is obvious, that both models give almost the same predictions since the values of $\tau_{T,1}$ and $\tau_{T,2}$ are relatively small. This implies that the phase-lag concept has insignificant effect on the predictions of the dual phase heat conduction model when $\tau_{T,1}$ and $\tau_{T,2}$ are less than 0.001. This indicates that as $\tau_{T,1}$ or $\tau_{T,2}$ increases, the deviation between both models increases.

Figures (7.45 and 7.46) show the effect of the interfacial *Biot* number on the spatial temperature distribution within the two domains. From these figures, it is shown that the temperature distribution for the imperfect contact case approaches that for the perfect contact case as *Bi* increases. Also, the interfacial temperature jump decreases as *Bi* number increases. Figures (7.47-7.48) show that interfacial *Biot* number larger than 100 yields predictions similar to that of the perfect contact models.

7.5 Perturbation technique

The present work was done for the case of convection heat transfer model as in the case study in chapter 6 and some dimensionless parameters at which the exact and the perturbed solution become identical are obtained here.

Figures (7.49-7.53) show comparisons between the predictions of the exact and perturbation models under the effect of different dimensionless parameters H_1, H_3 and H_4, which are described previously. It is shown that the validity of using the perturbation technique is secured for large values of H_3 and small values of H_1 and H_4. It is obvious that the validity of the perturbation technique is secured for large values of H_3 since the perturbation parameter ε is defined as $\varepsilon = 1/H_3$. As H_3 increases, ε decreases and the using of the perturbation technique is justified. Physically, H_3 is proportional to the convection heat transfer coefficient between the fluid and the solid wall. As the convection heat transfer coefficient increases, then the solid temperature approaches the fluid temperature and the normalized difference between them may be considered as a small-perturbed quantity. Also, it is obvious that using the perturbation technique is justified for small values of H_1 and H_4. Small values of H_1 imply that the role of the enthalpy flow $V\rho_f c_f$ is more significant than the role of the convected heat between the fluid and the solid domains. Increasing the enthalpy flow into the channel implies that more energy is carried to each axial location and as a result, solid wall has enough energy to evaluate its temperature in order to become very near the fluid temperature. Also, from the definition of H_4, H_4 represents the ratio between the convective losses from the solid wall to the ambient and the energy stored within the solid domain. If the convective losses from the solid wall to the ambient decreases, then the temperature of the solid wall remains very near the flowing fluid temperature. As these losses increase, the fluid has to provide the solid wall with enough energy to maintain approximately the same small difference between their temperatures.
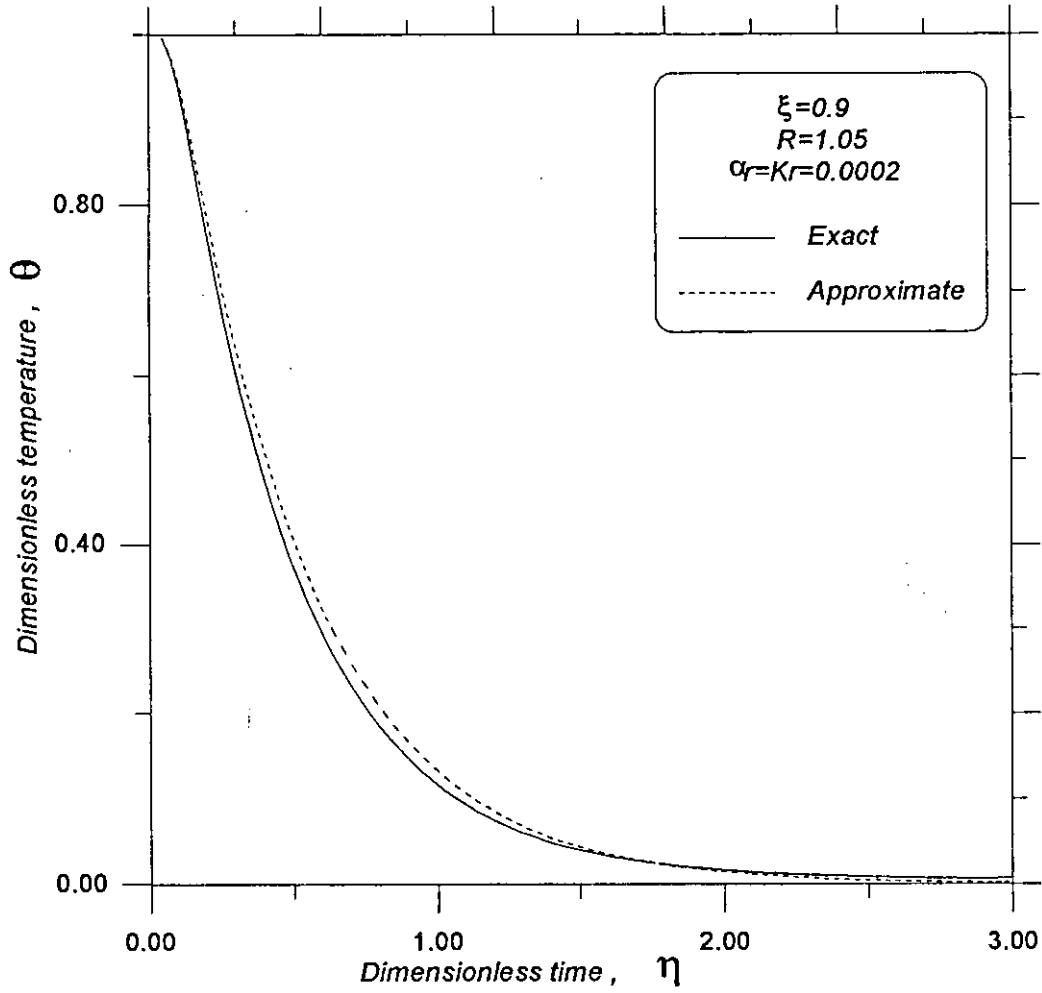
Fig. 7.1 : Exact and approximate transient temperature variation in the thick domain.
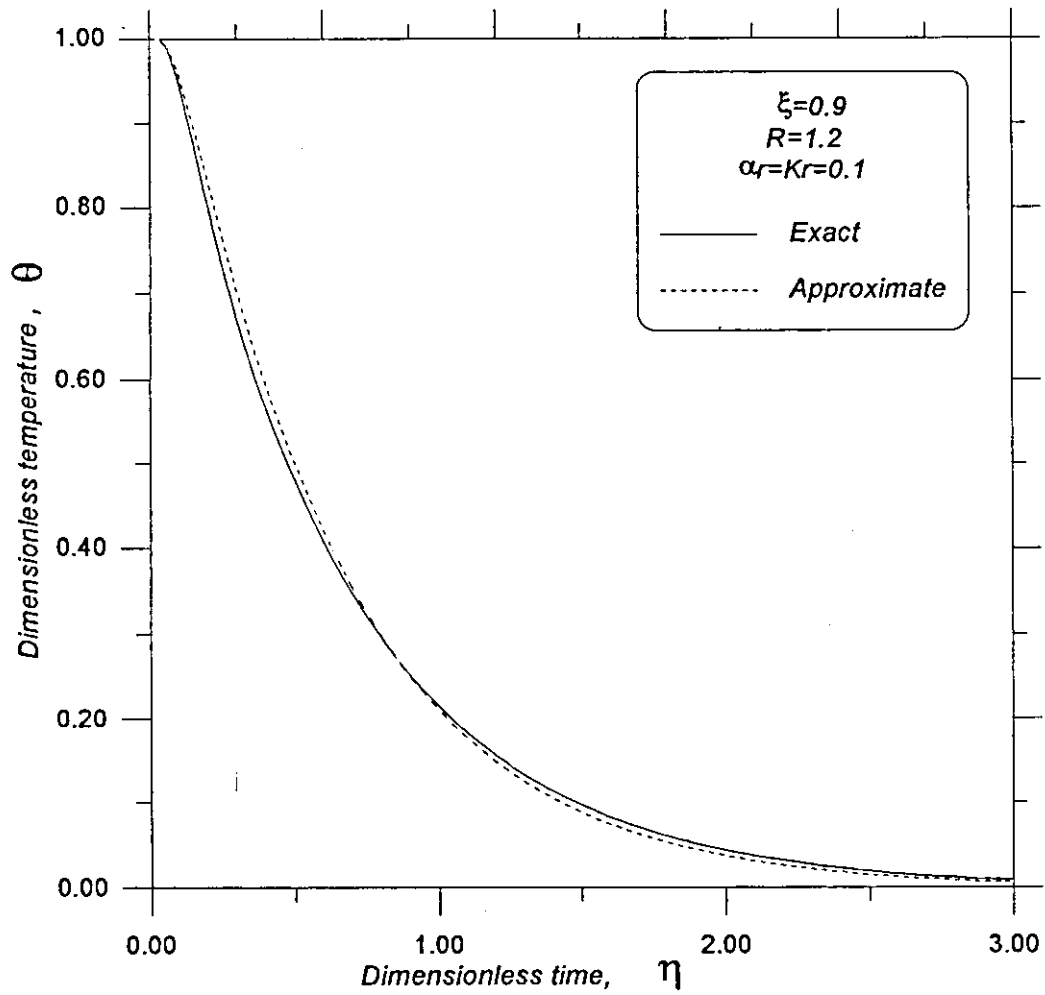
Fig. 7.2 : Exact and approximate transient temperature variation in the thick domain.
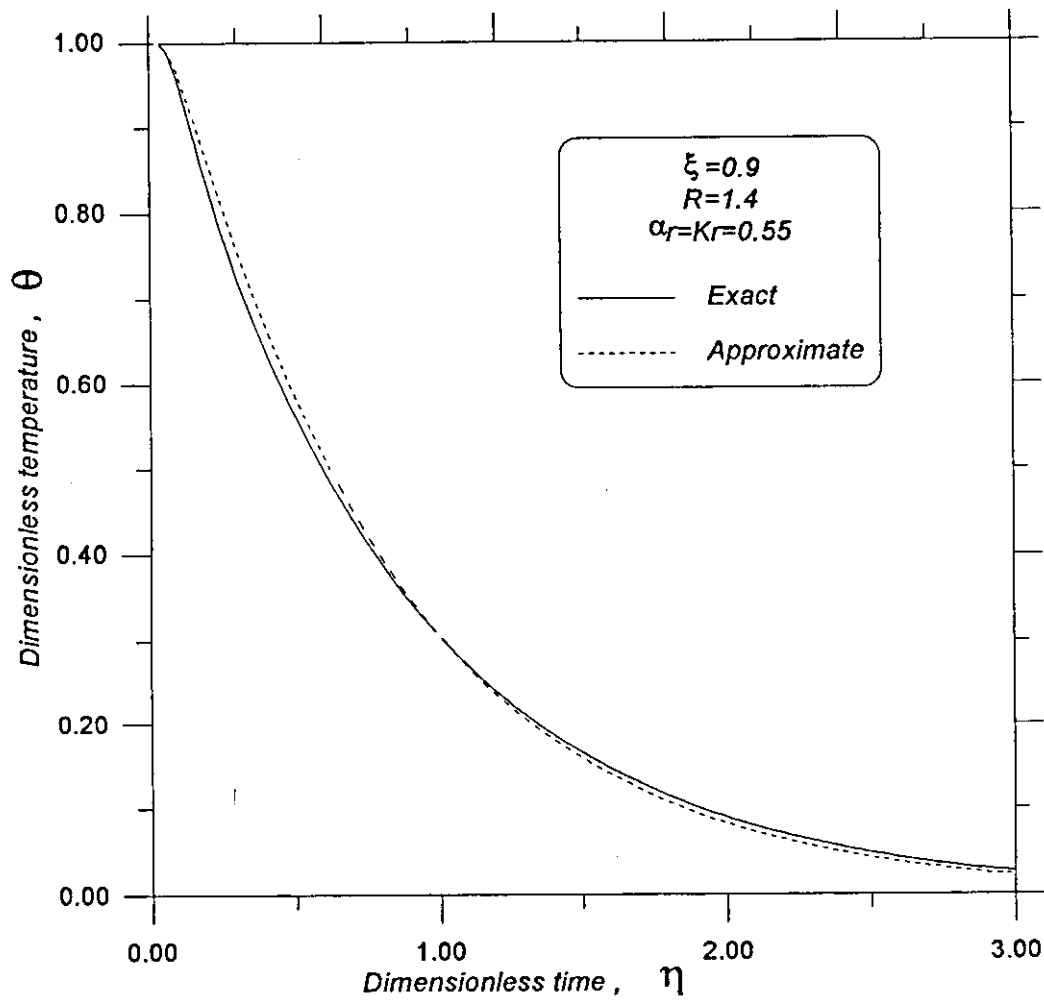
Fig. 7.3 : Exact and approximate transient temperature variation in the thick domain.
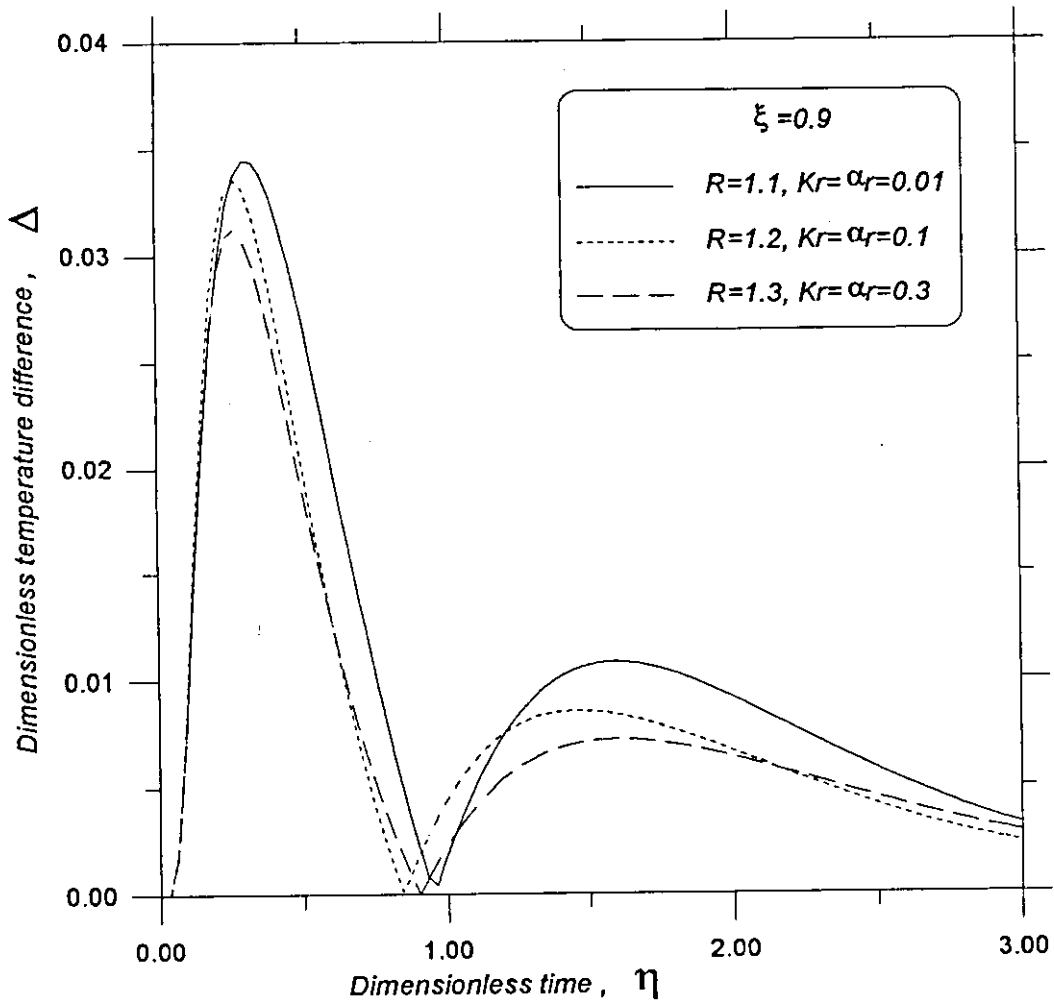
Fig. 7.5: Effect of α_r and Kr on the transient temperature difference at different R.
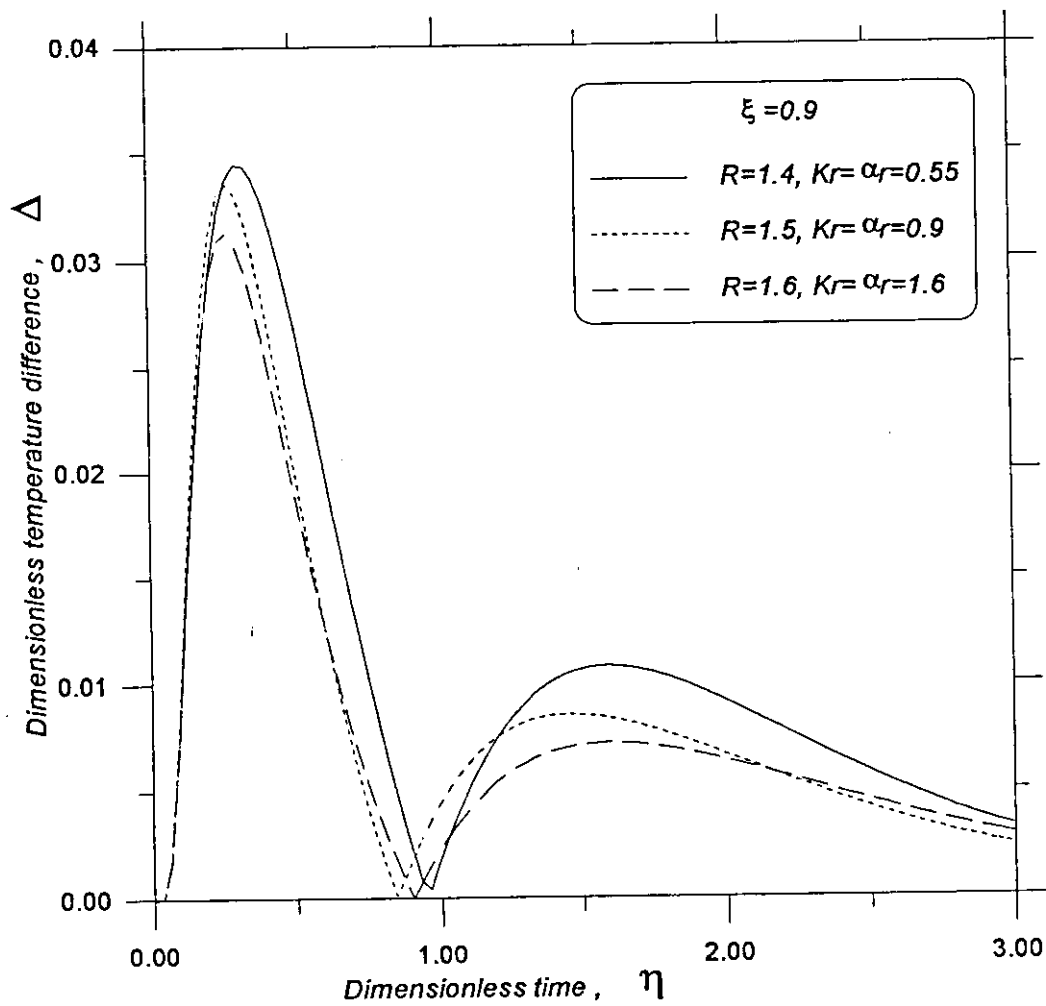
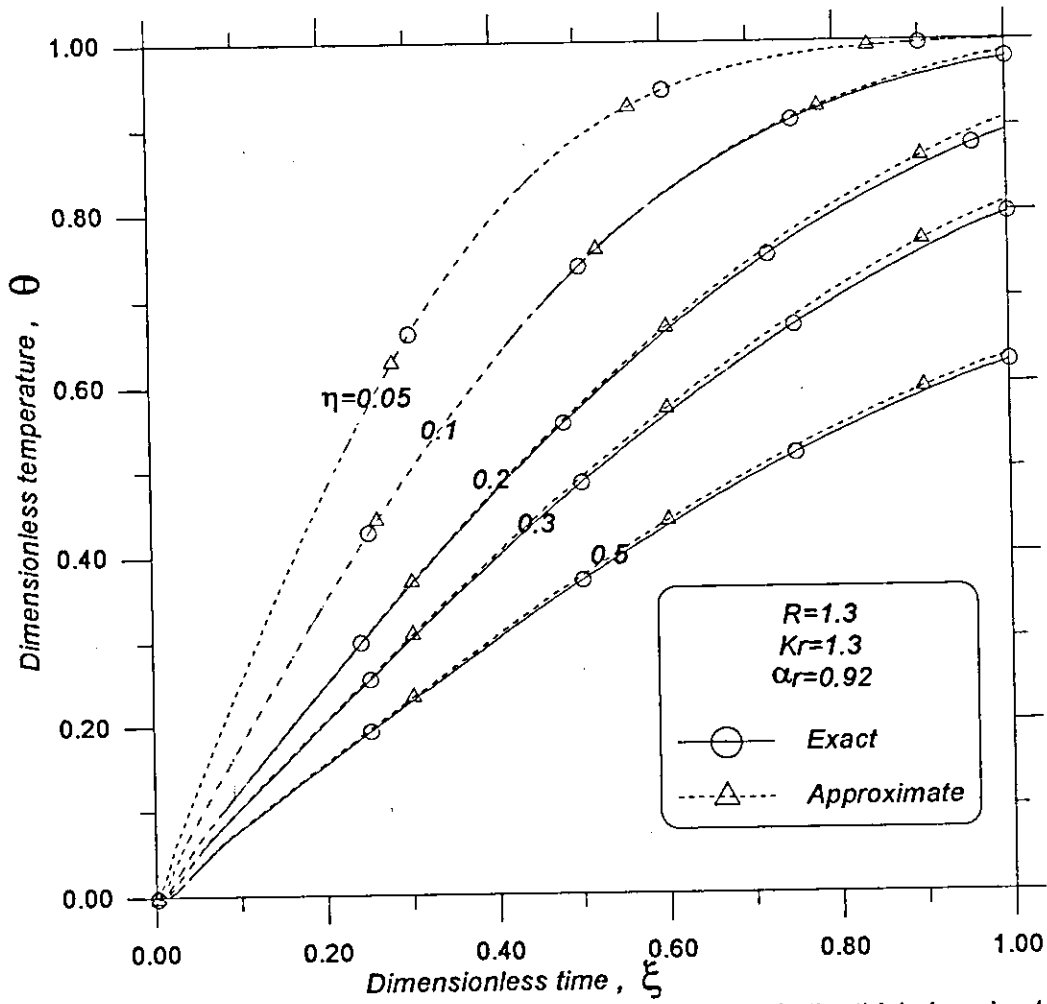Fig. 7.6: Effect of α_r and Kr on the transient temperature difference at different R.
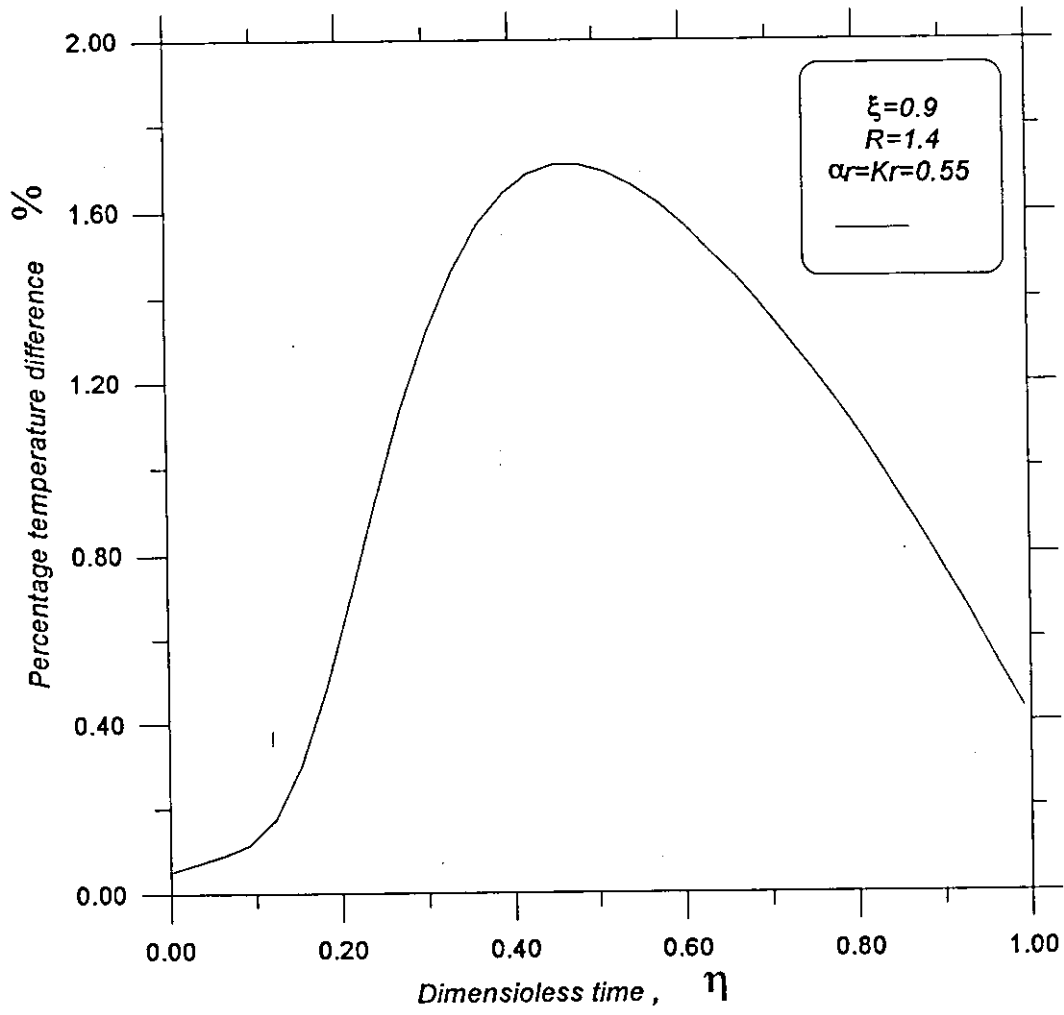
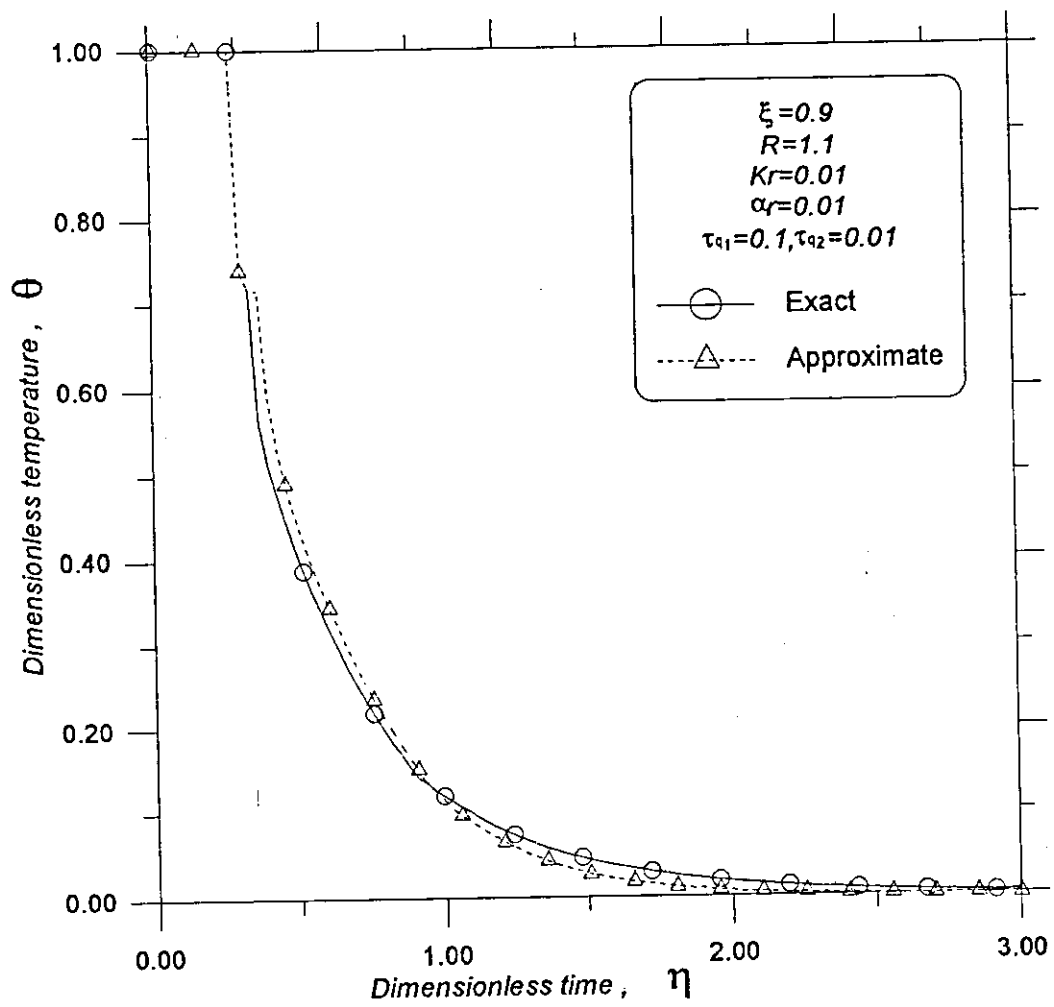Fig.7.7: Effect of αr and Kr on the percentage transient temperature difference
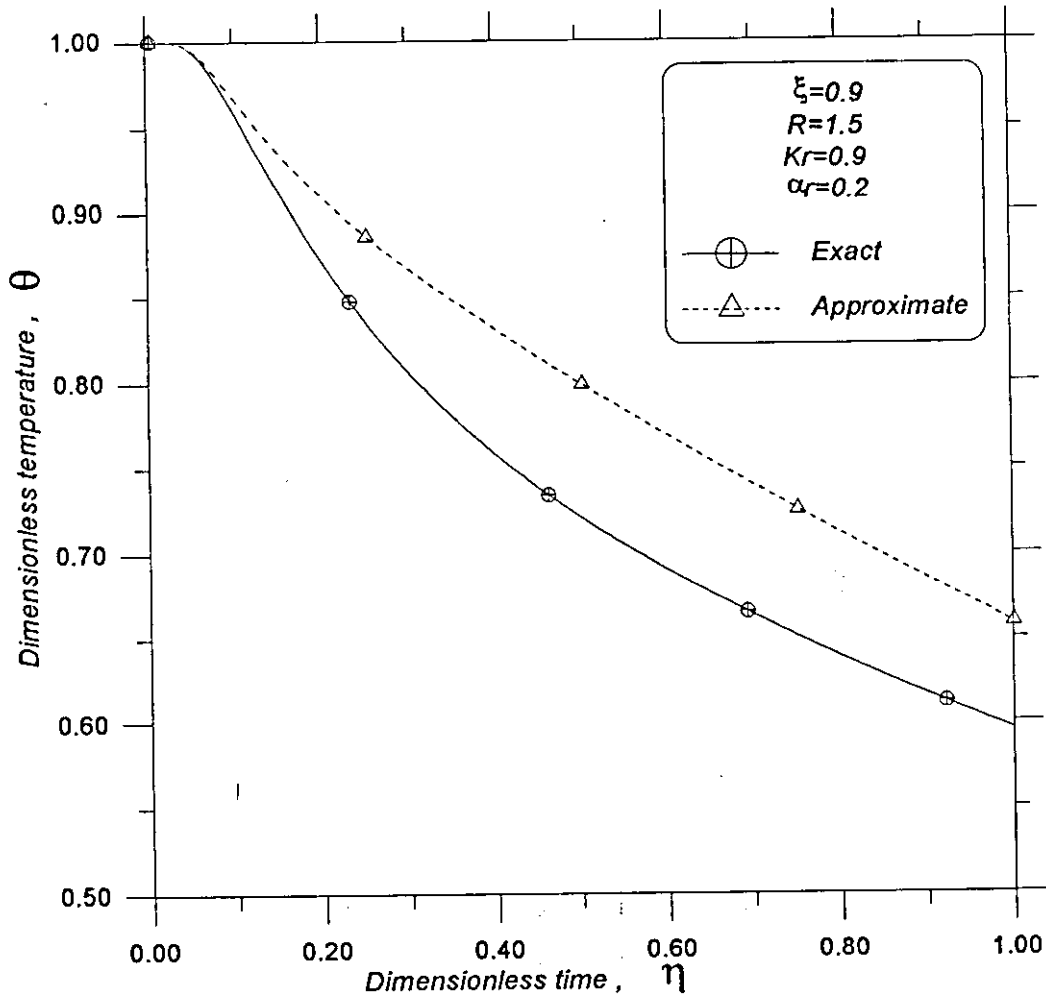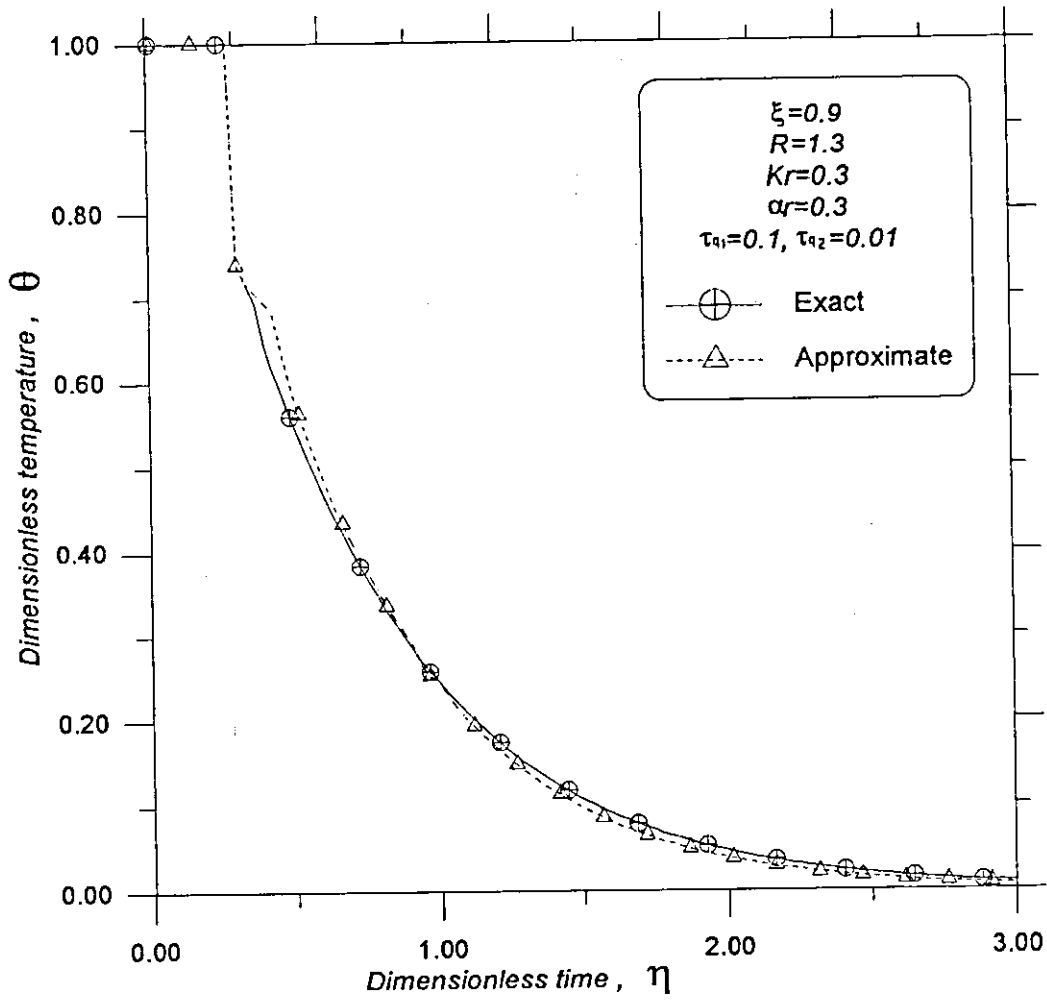
Fig. 7.8 : Exact and approximate transient temperature variation within the thick domain.
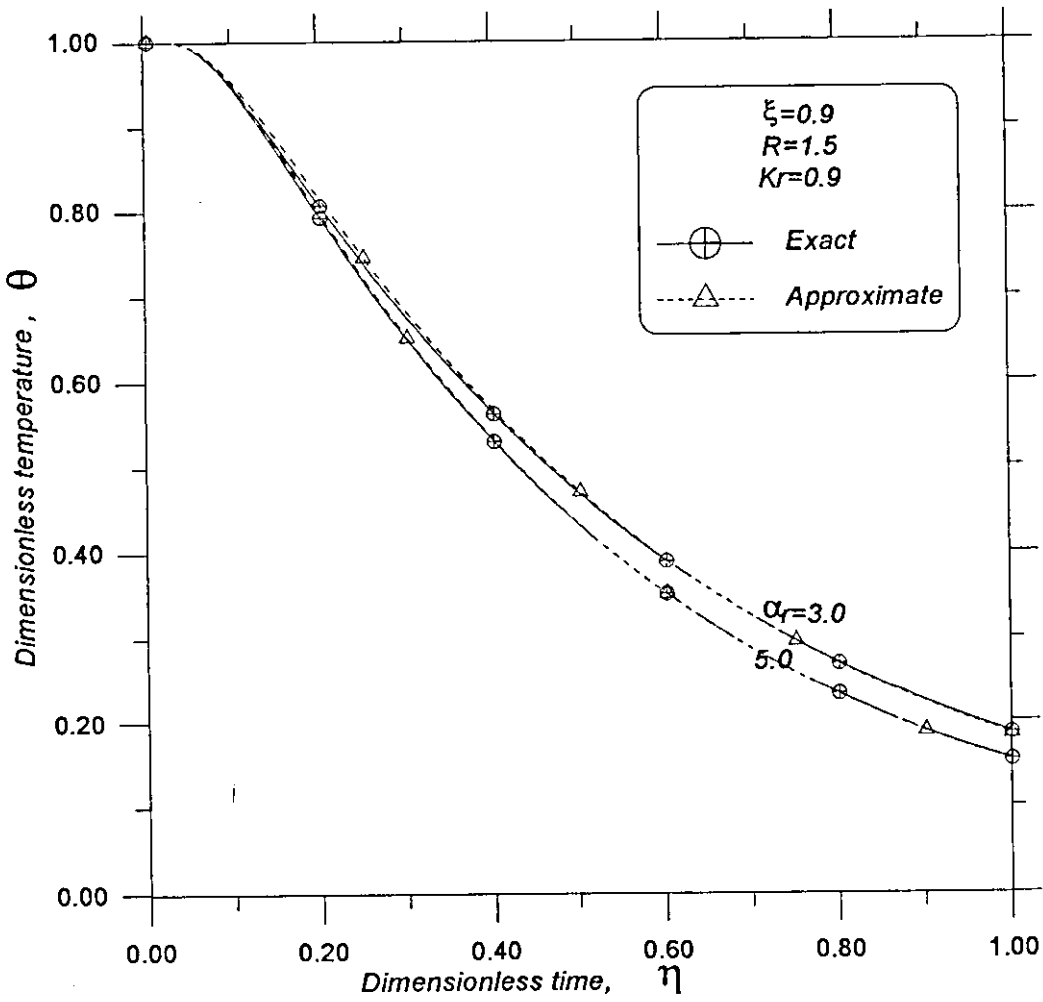
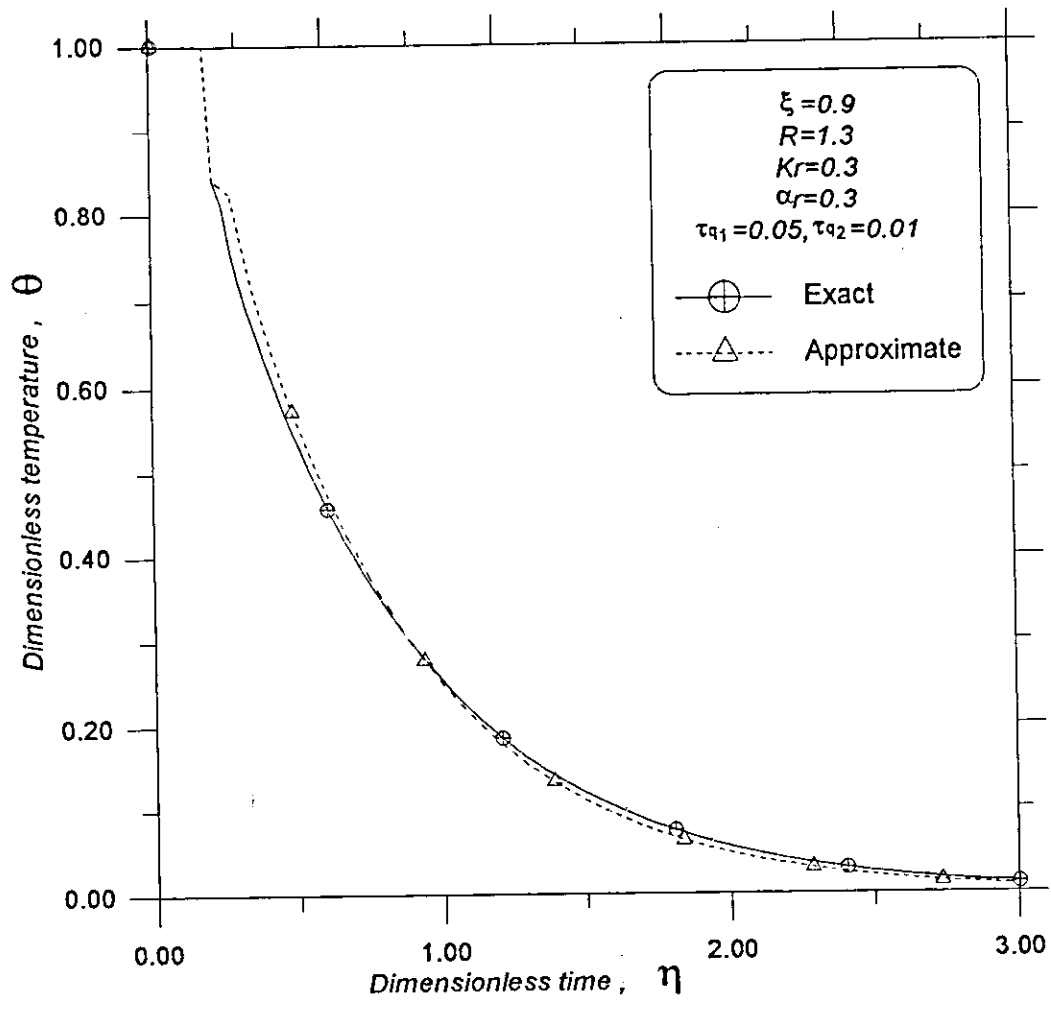Fig. 7.9 : Exact and approximate transient temperature variation within the thick domain at different αr.
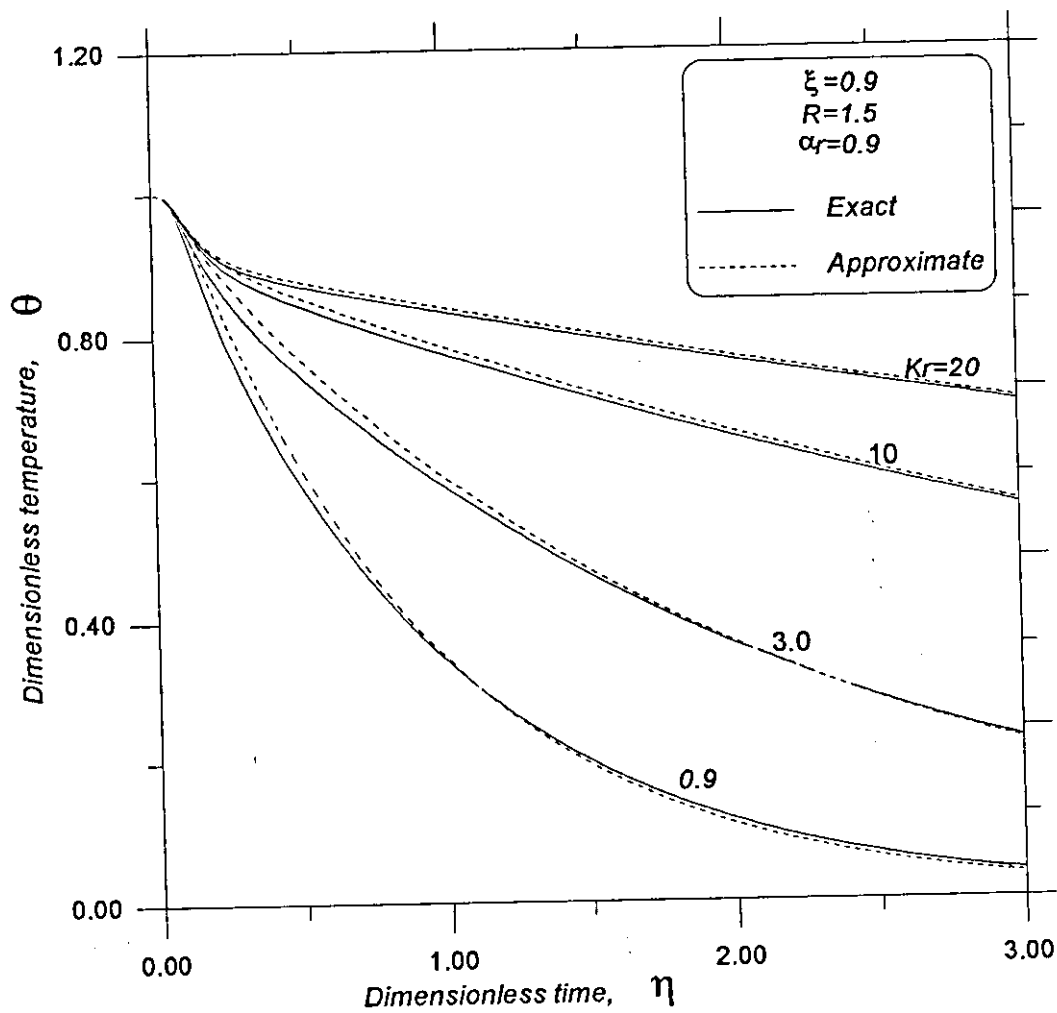
Fig. 7.10 : Transient variation in the dimensionless temperature at different thermal conductivity ratios.
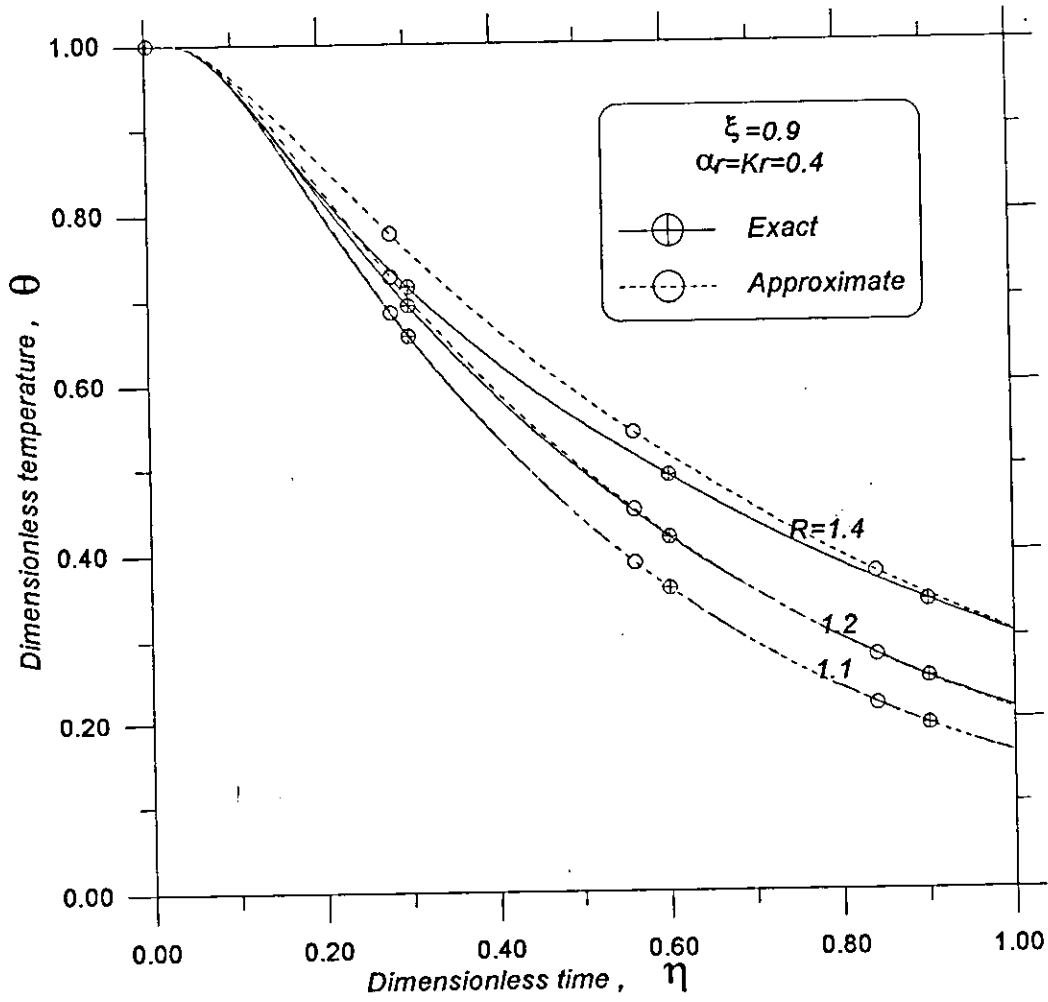
Fig. 7.11 : Exact and approximate transient temperature variation within the thick domain at different R.
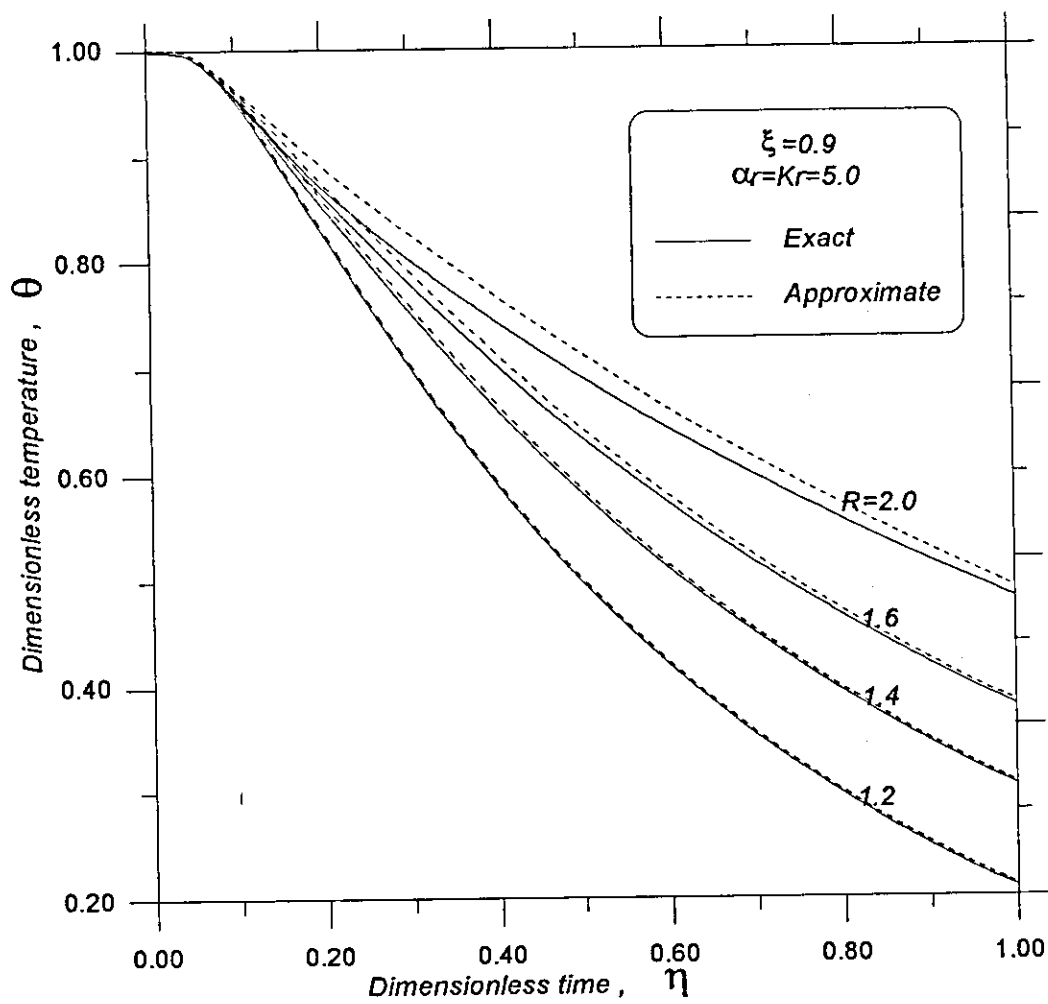
Fig. 7.12 : Exact and approximate transient temperature variation within the thick domain at different R.
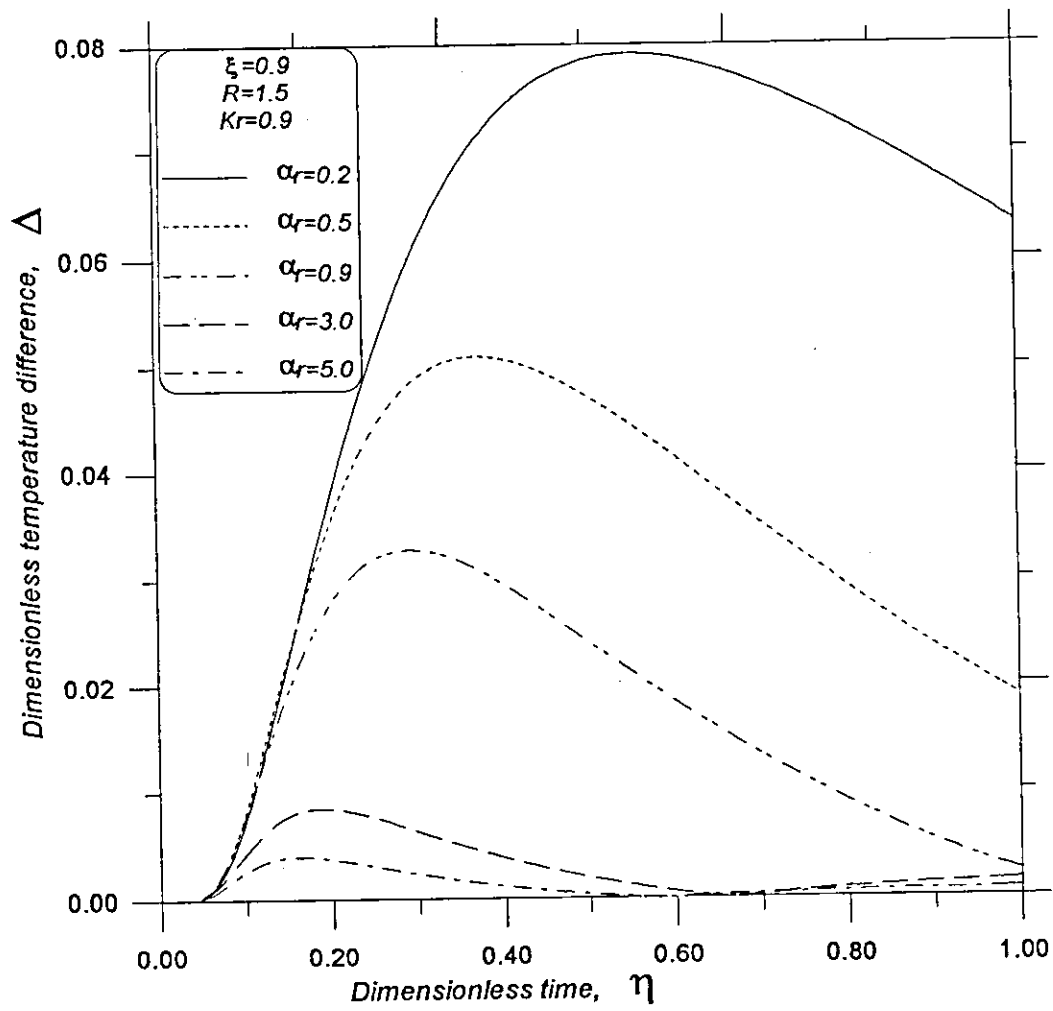
Fig. 7.13 : Effect of thermal diffusivity ratio on the transient temperature difference
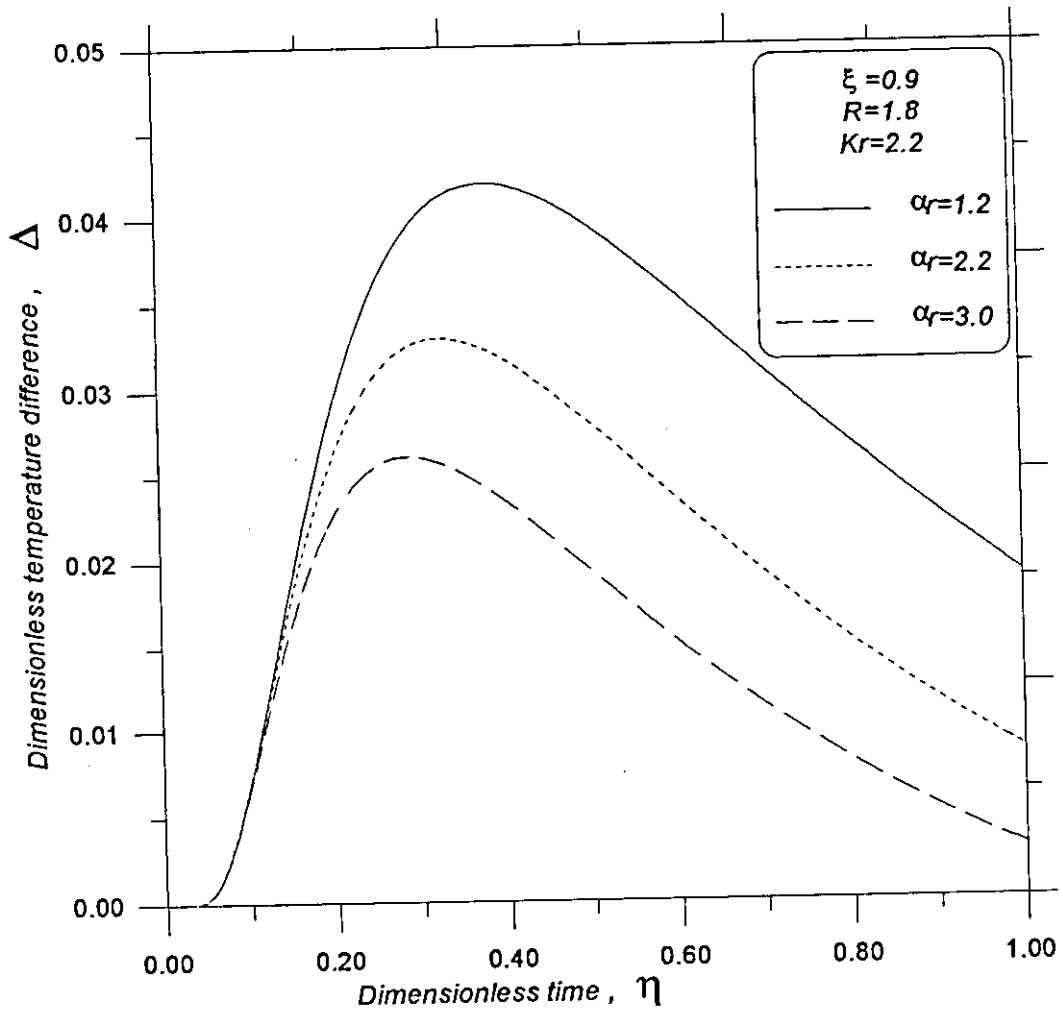
Fig. 7.14 : Effect of thermal diffusivity ratio on the transient temperature difference.
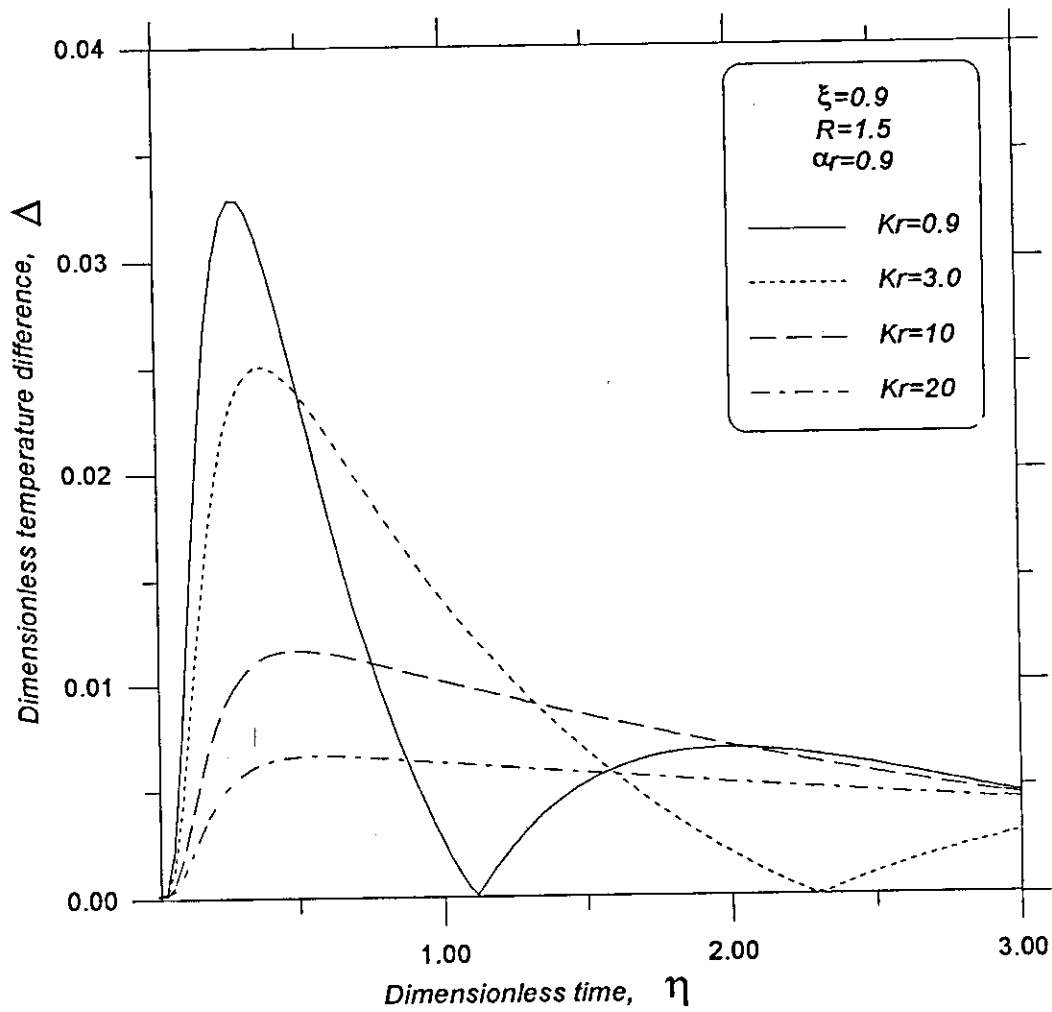
Fig. 7.15 : Effect of thermal conductivity ratio on the transient temperature difference
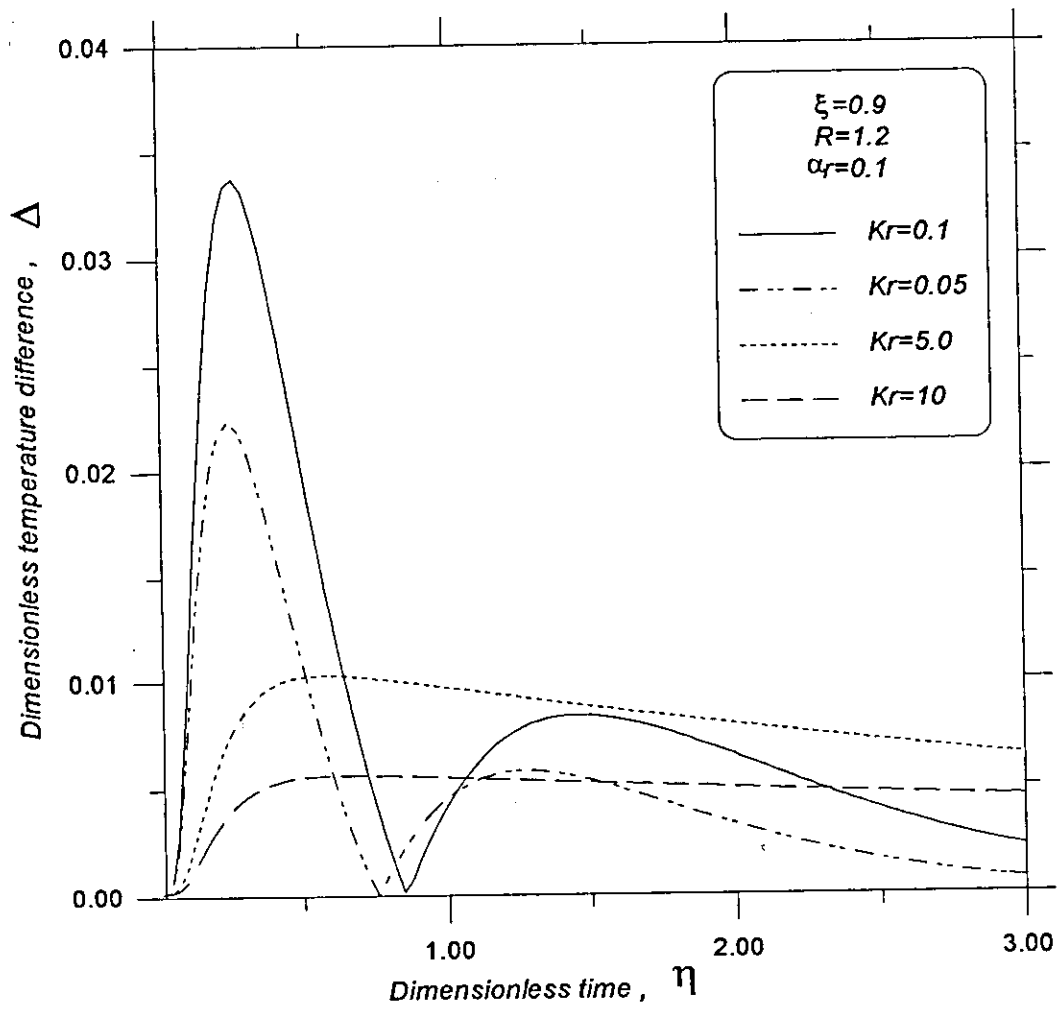
Fig. 7.16 : Effect of thermal conductivity ratio on the transient temperature difference
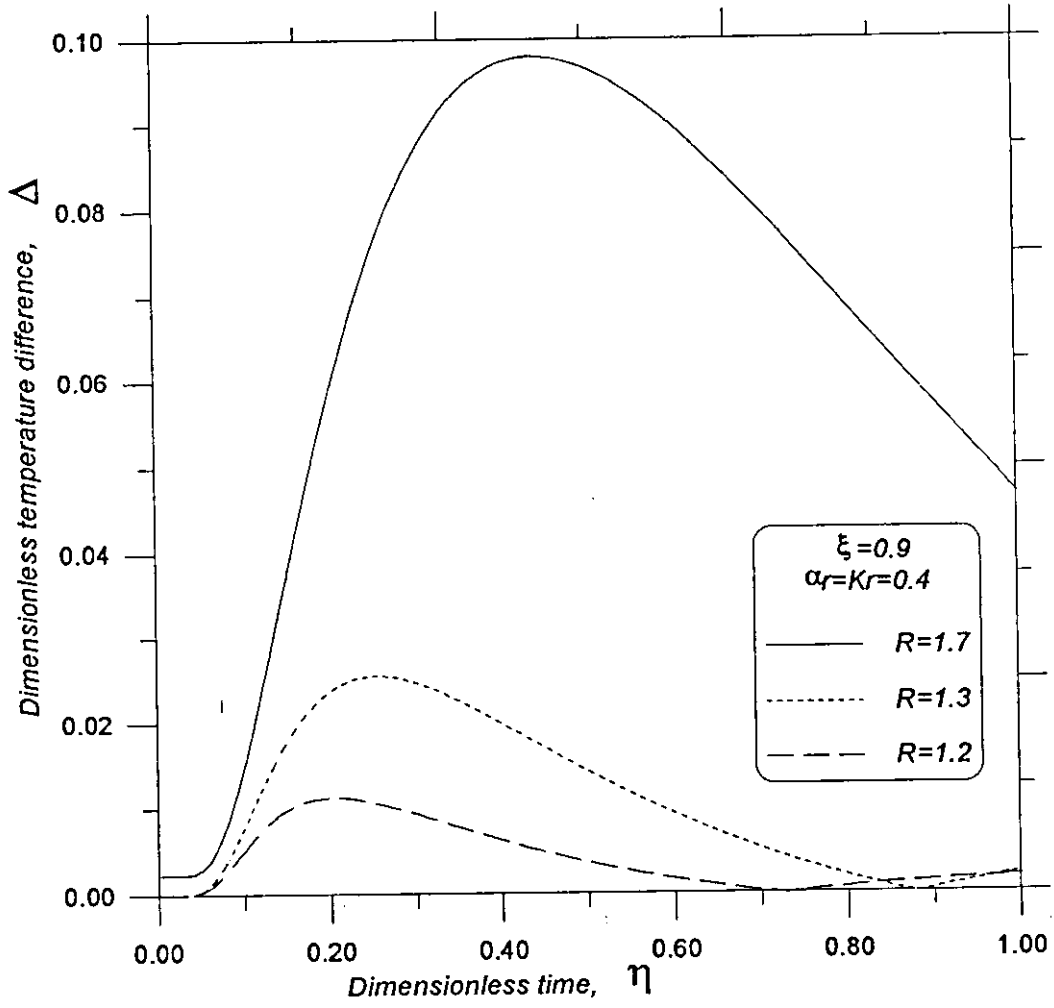
Fig. 7.17 : Effect of thickness ratio on the transient temperature difference
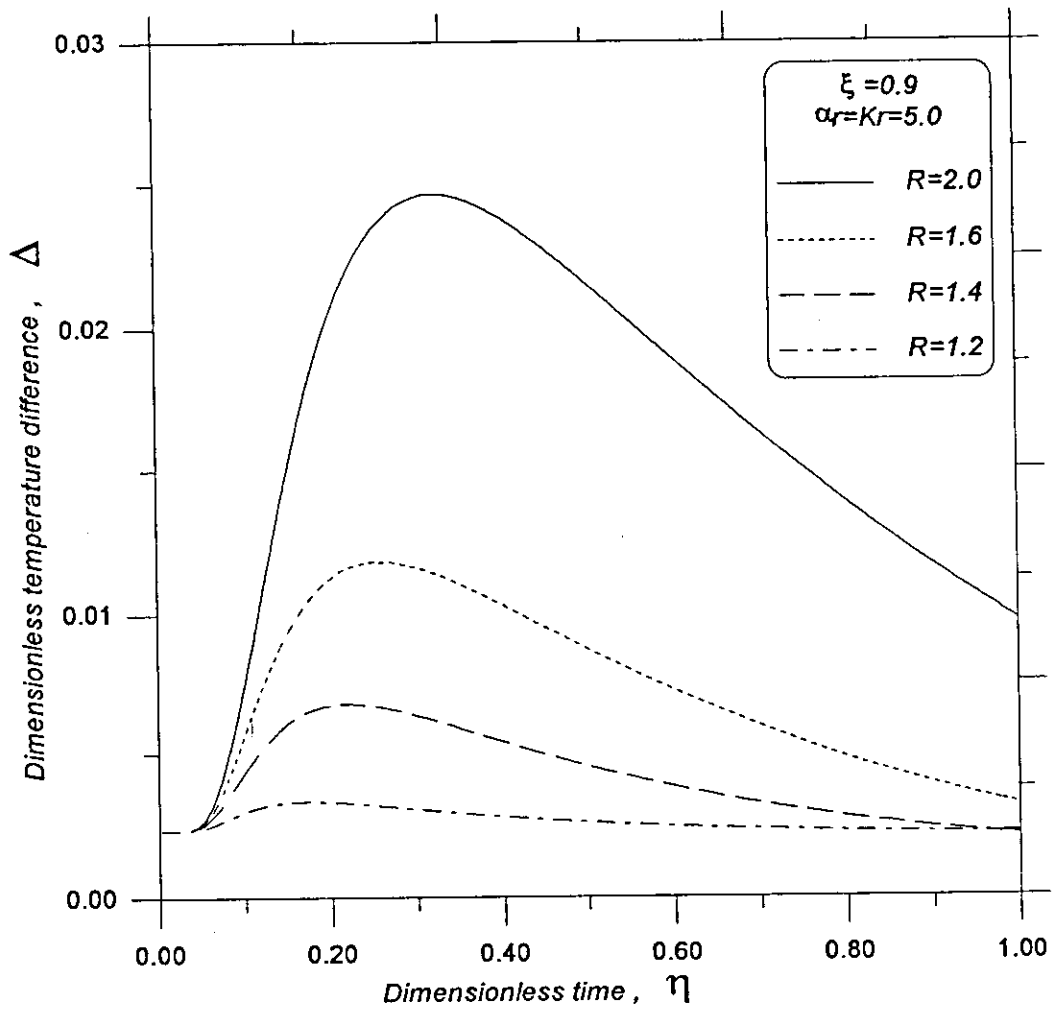
Fig. 7.18 : Effect of thickness ratio on the transient temperature difference.
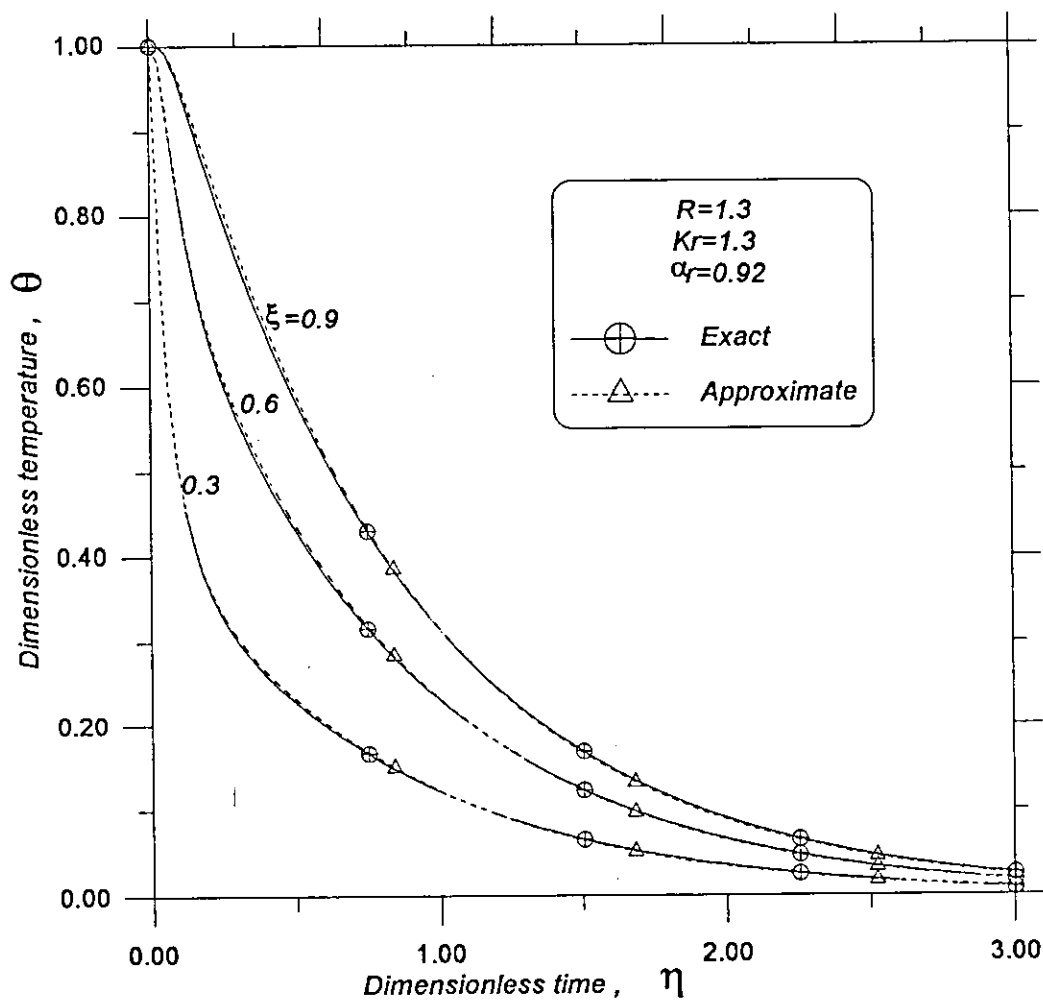
Fig. 7.19 : Exact and approximate transient temperature variation in the thick domain at different ξ .
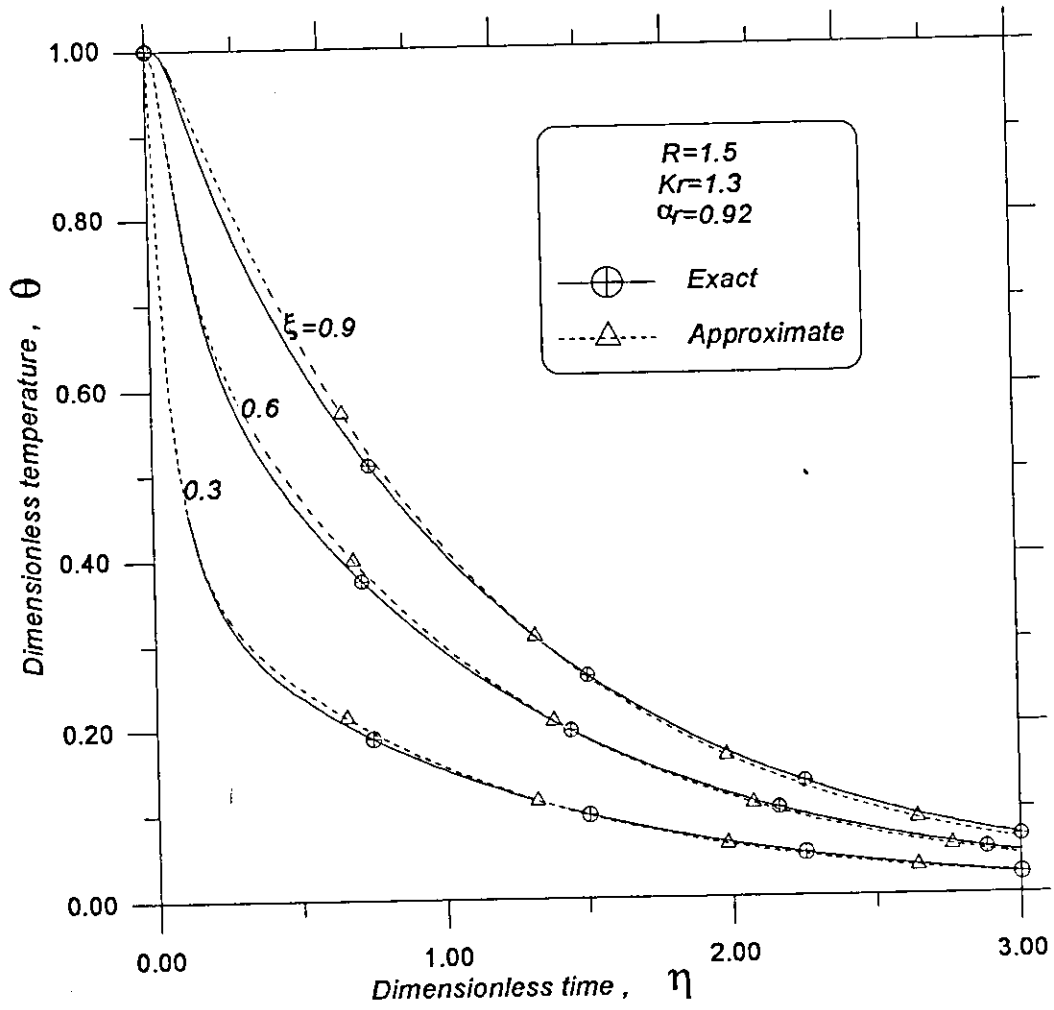
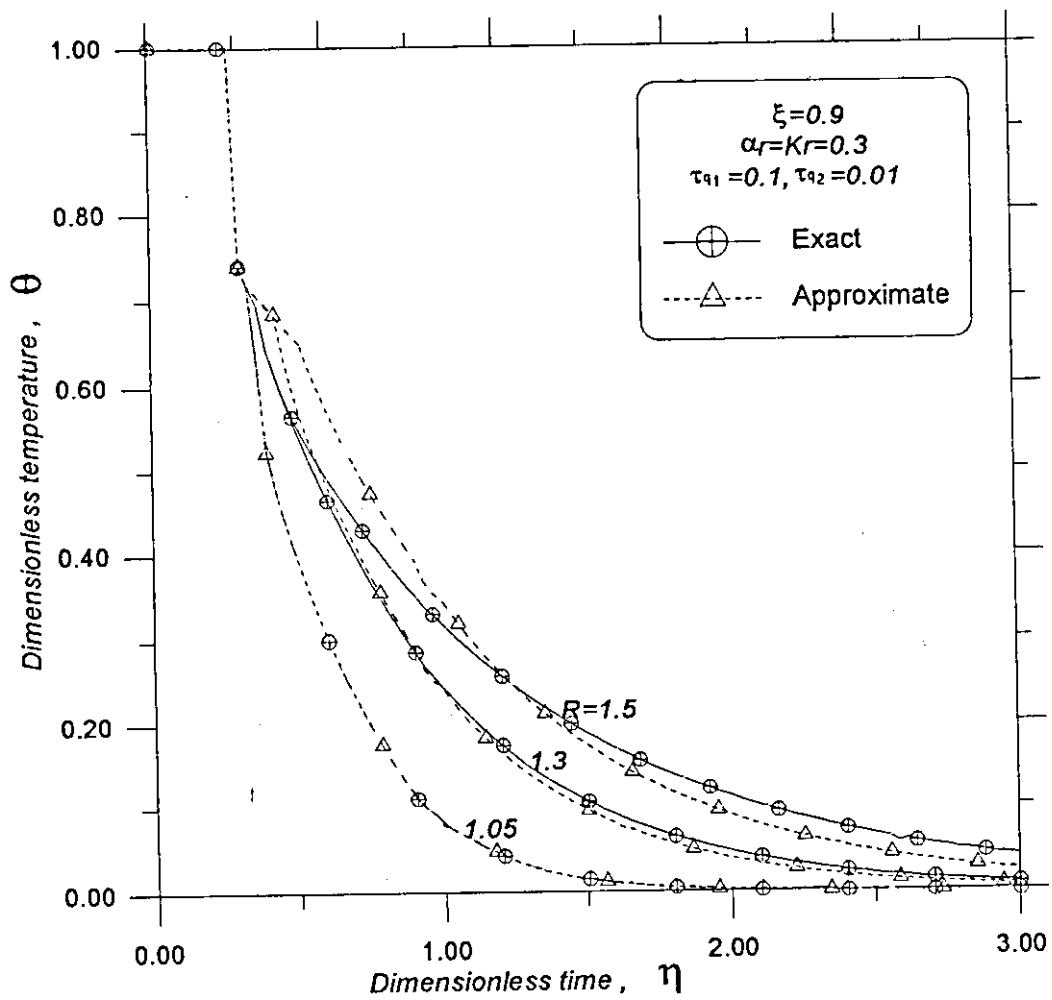Fig. 7.20 : Exact and approximate transient temperature variation in the thick domain at different ξ .

Fig. 7.21 : Exact and approximate temperature distribution in the thick domain at different η.

Generalized boundary is valid
for all Kr

α_r

Generalized boundary is invalid

R
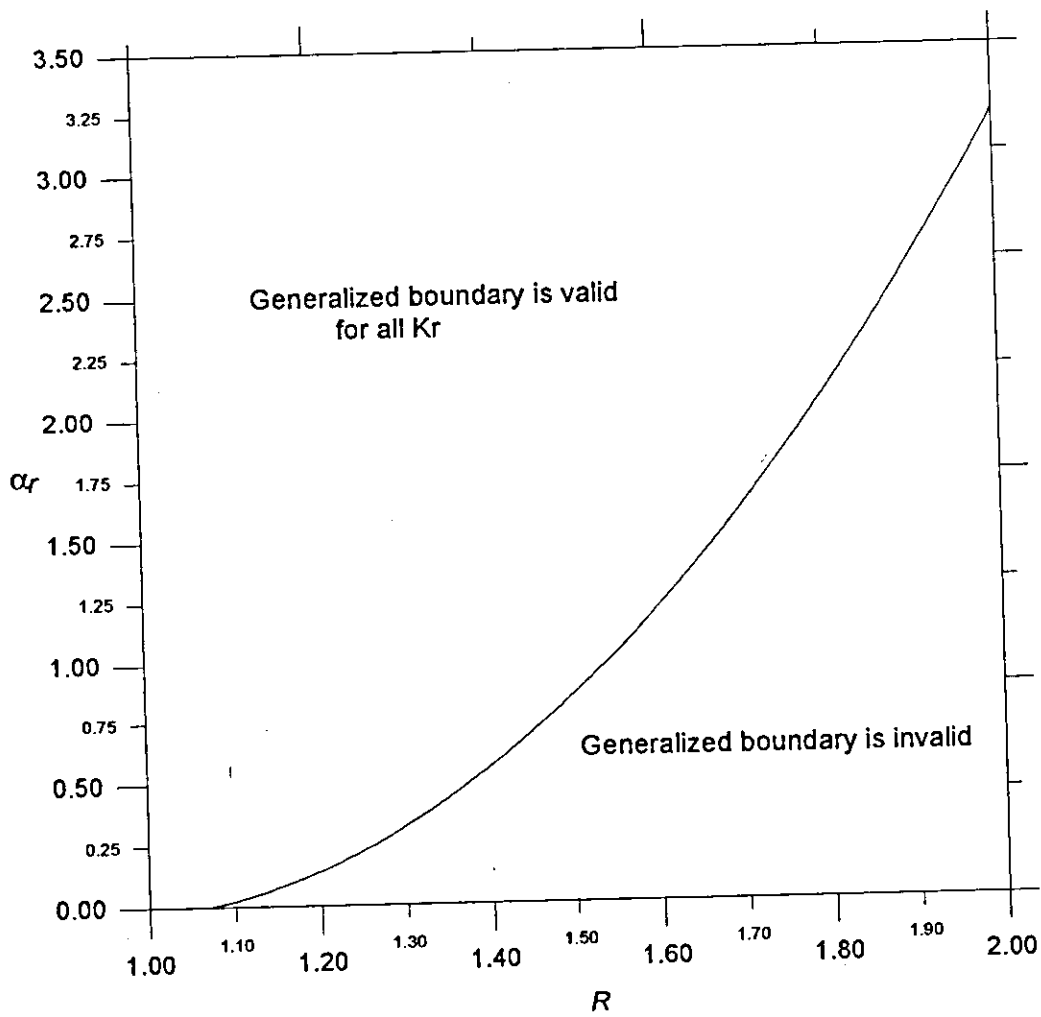
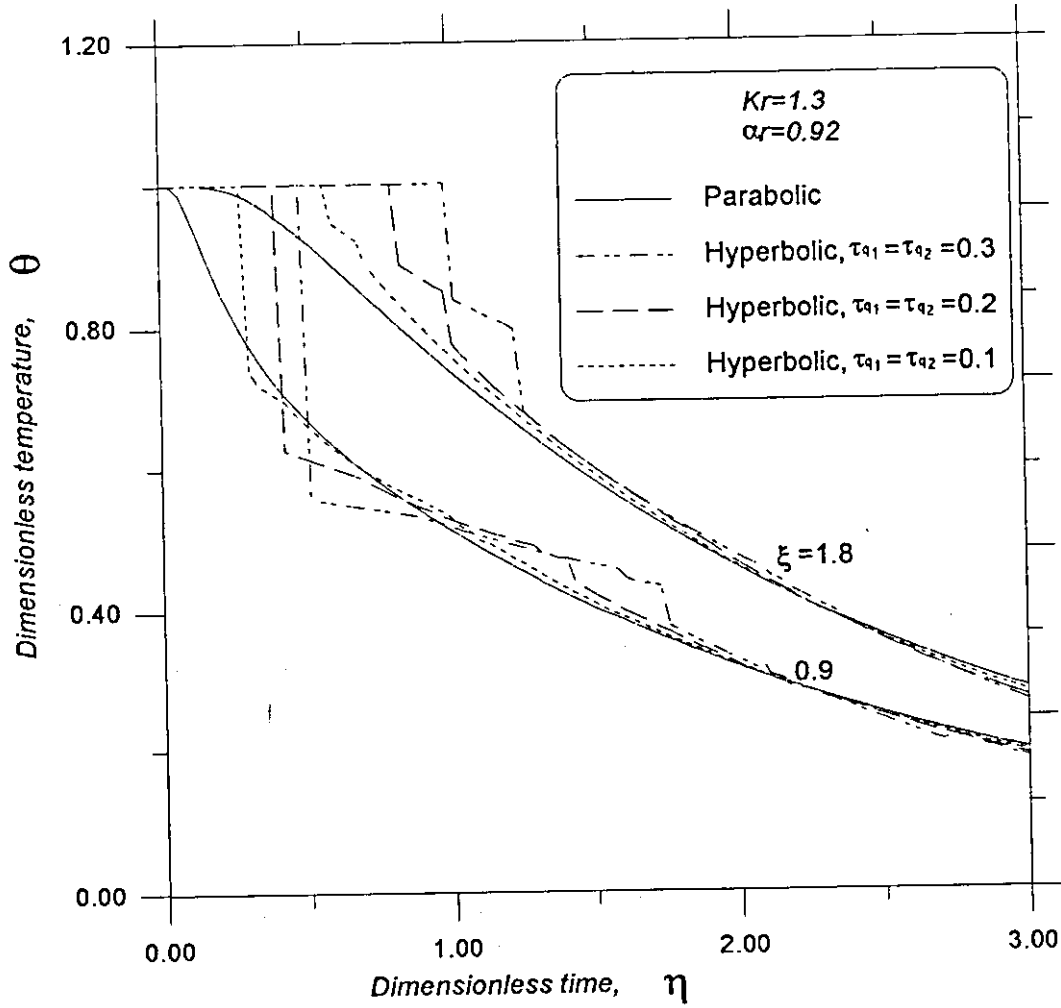Fig. 7.22 : The validity region of the generalized thermal boundary condition.
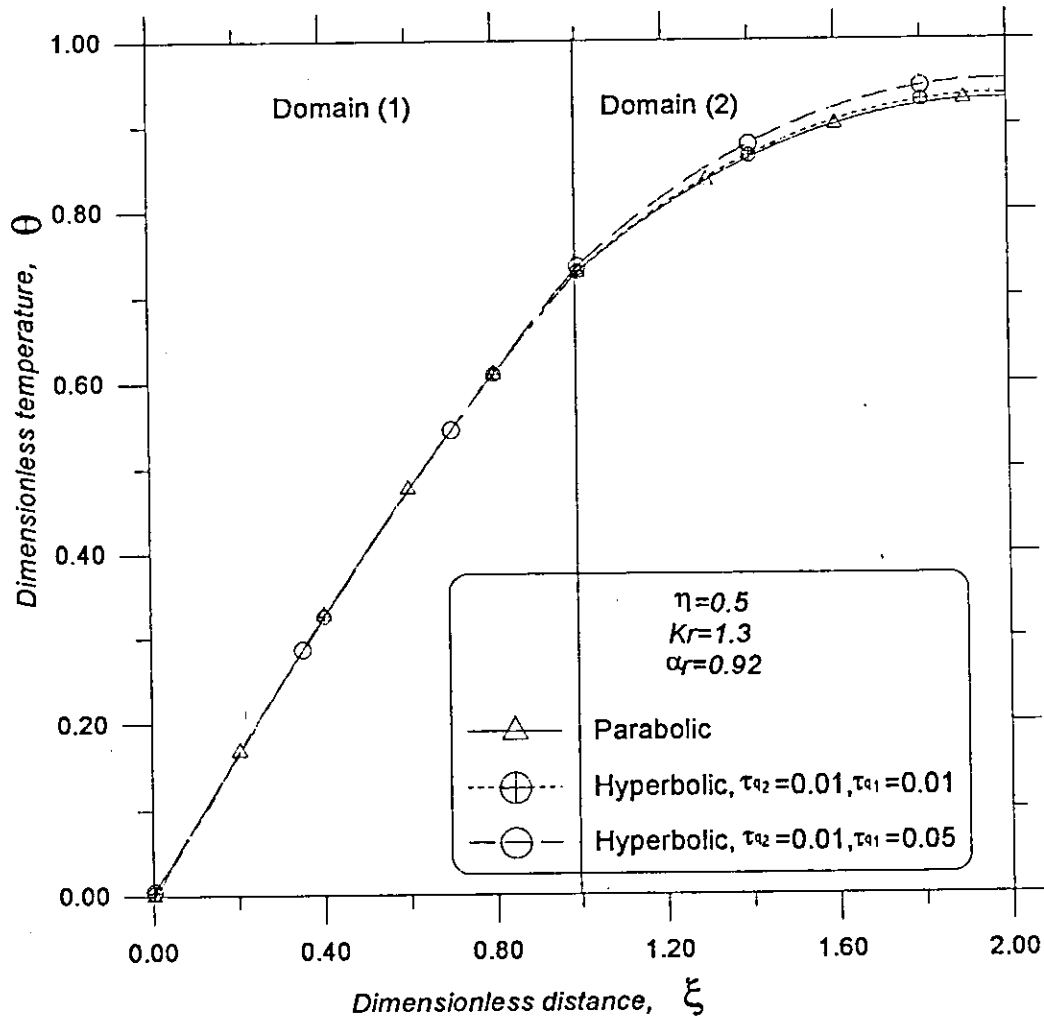
Fig. 7.23 : Spatial temperature distribution within the two domains using the parabolic and the hyperbolic heat conduction models.
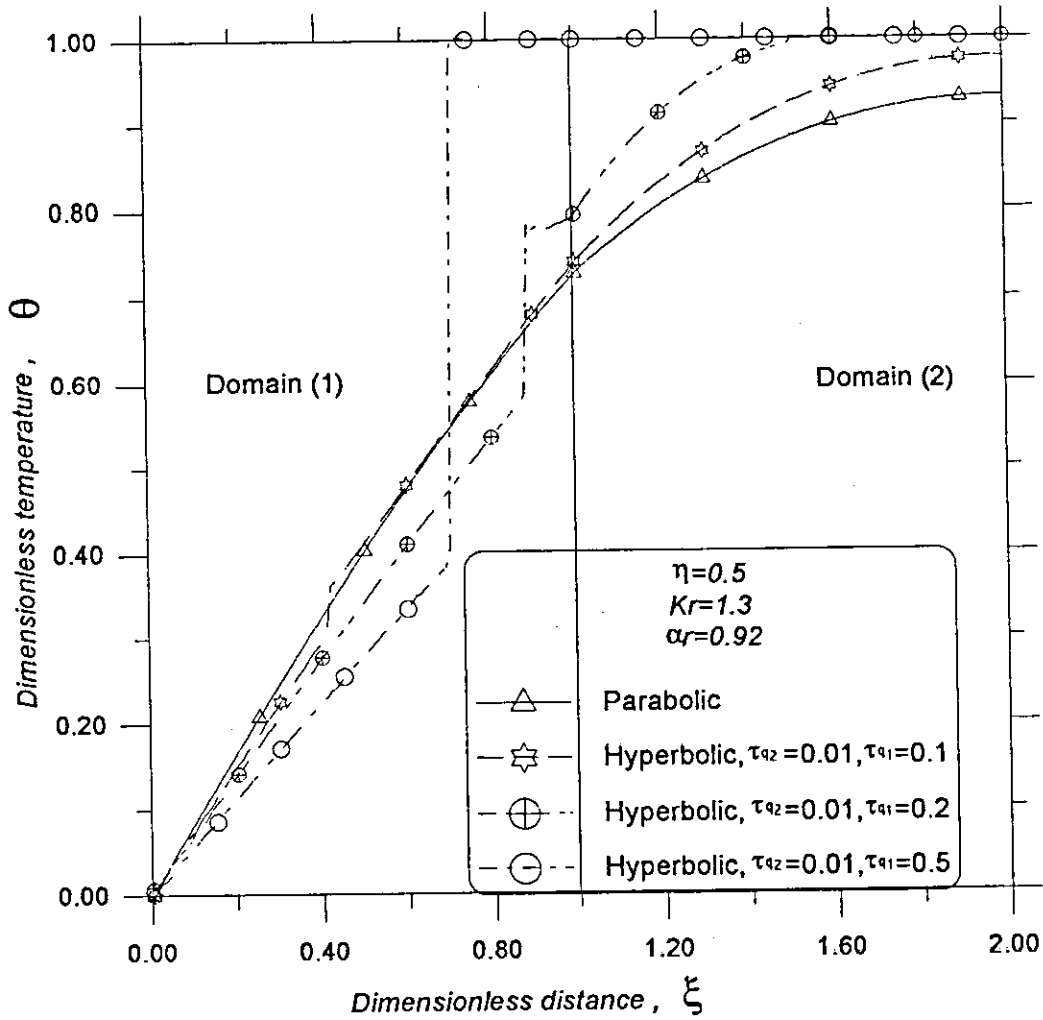
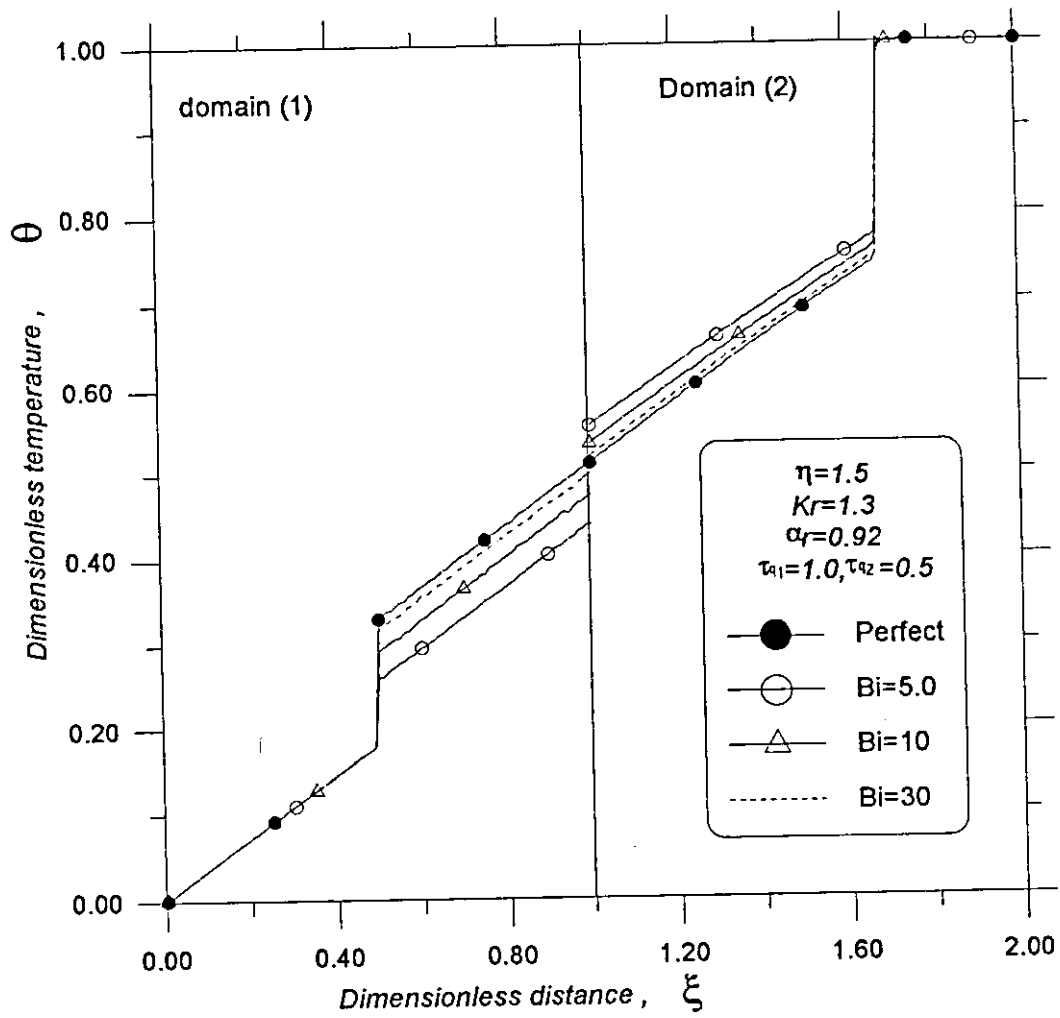Fig. 7.24 : Spatial temperature distribution within the two domains using the parabolic and the hyperbolic heat conduction models.

Fig. 7.25 : Exact and approximate transient temperature variation in the thick domain.

Fig. 7.26 : Exact and approximate transient temperature variation in the thick domain.

Fig. 7.27 : Exact and approximate transient temperature variation in the thick domain.
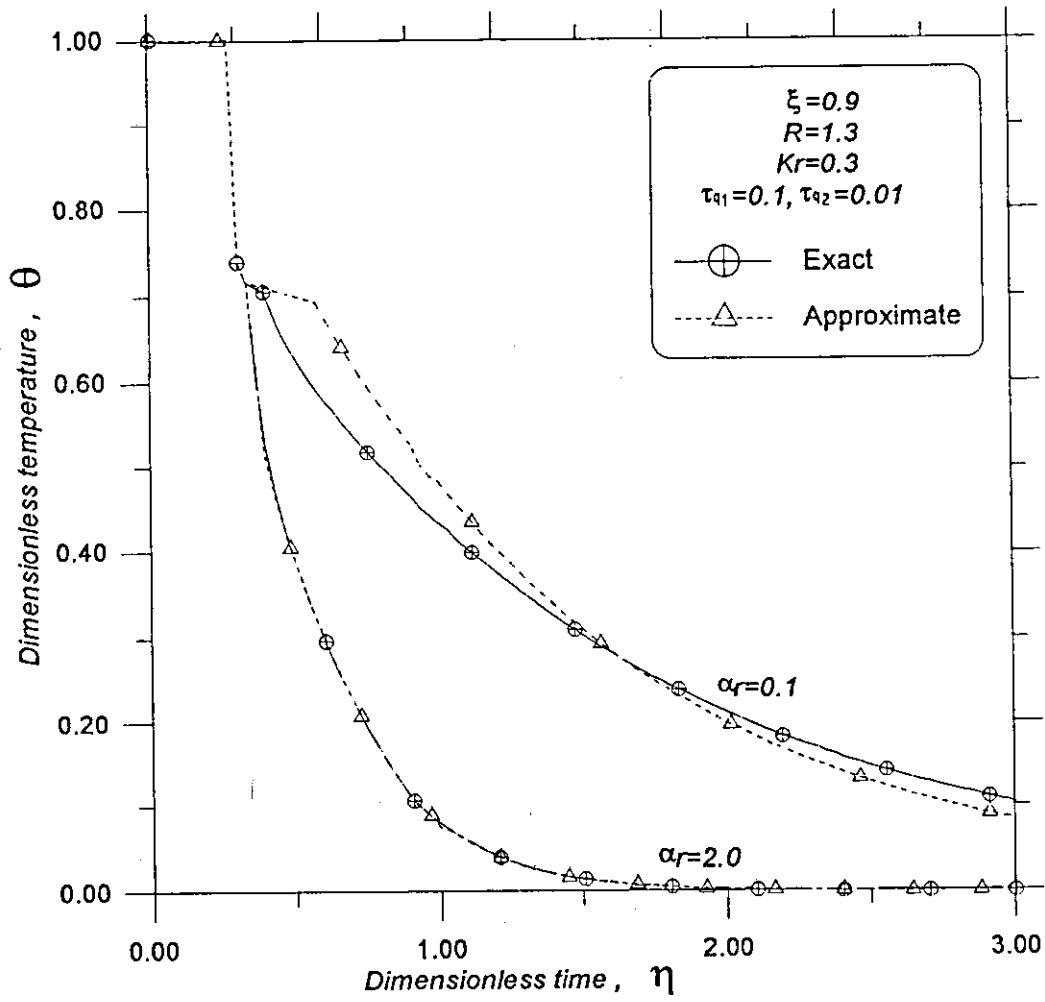
Fig. 7.28 : Exact and approximate temperature variation within the thick domain at different α_r
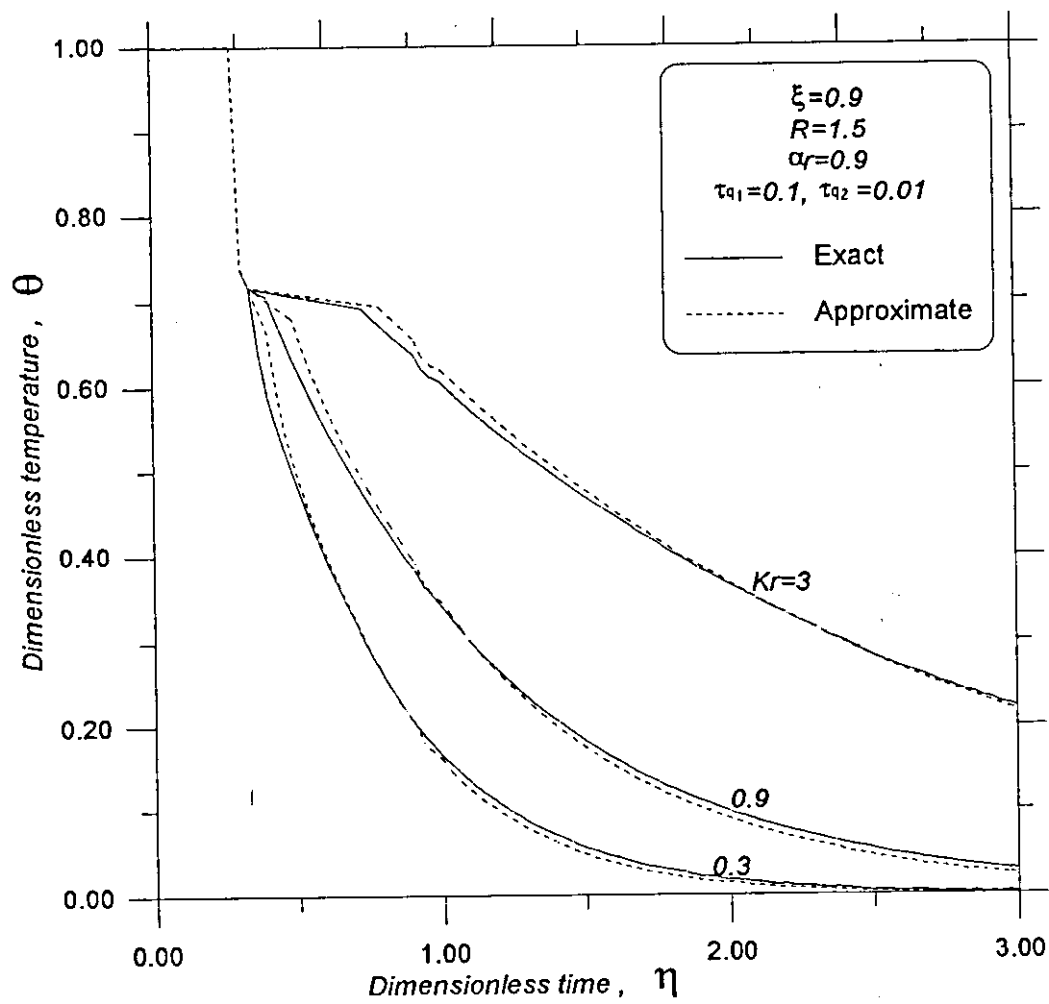
Fig. 7.29 : Exact and approximate temperature variation within the thick domain at different Kr .

109

Fig. 7.30 : Exact and approximate temperature variation within the thick domain at different R .

Fig. 7.31: Transient temperature variation within the two domains using the parabolic and the hyperbolic heat conduction models.
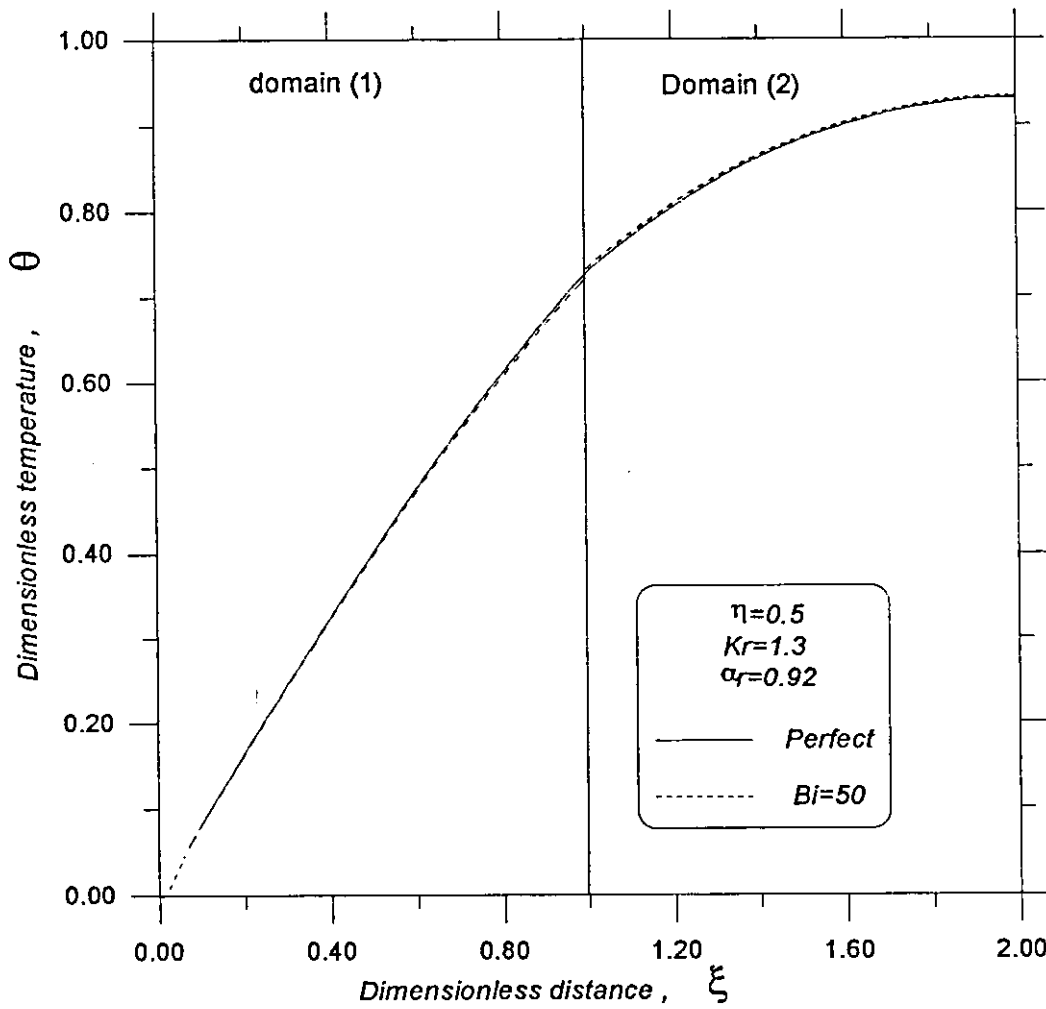
Fig. 7.32 : Spatial temperature distribution within the two domains for perfect and imperfect contact using the hyperbolic heat conduction model.
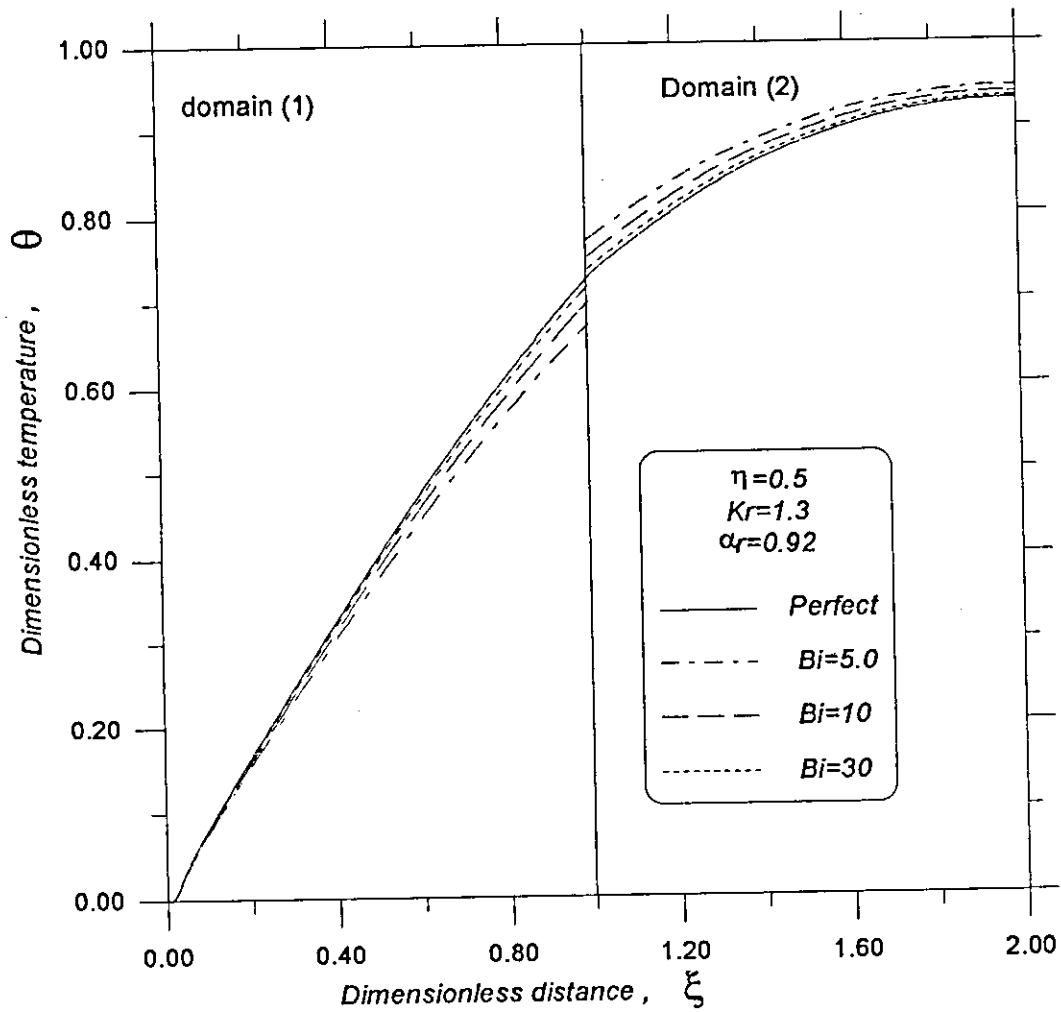
Fig. 7.33 : Spatial temperature distribution within the two domains for perfect and imperfect contact using the parabolic heat conduction model.

Fig. 7.35 : Spatial temperature distribution within the two domains for perfect and imperfect contact using the parabolic heat conduction model.
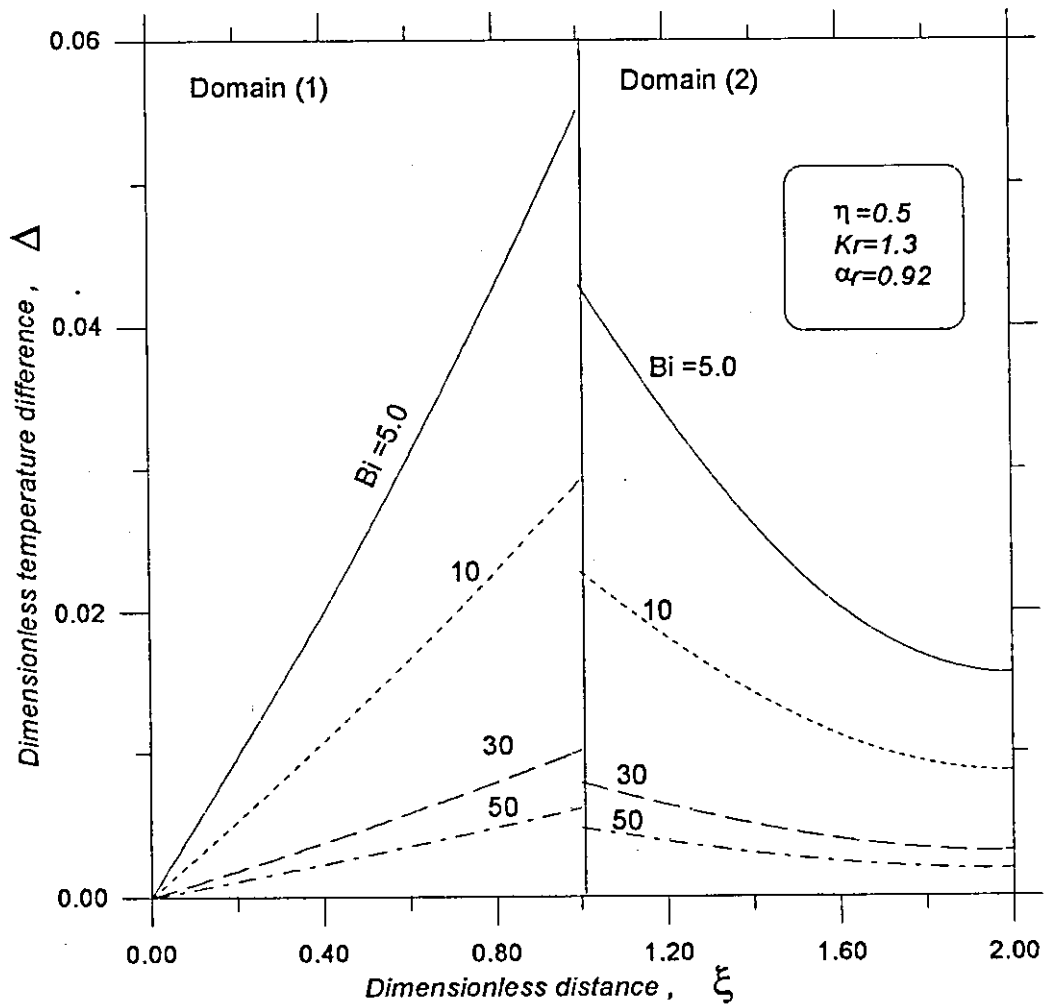
Fig. 7.36 : Effect of Biot number on the temperature distribution difference within the two domains for perfect and imperfect contact using the parabolic heat conduction model.
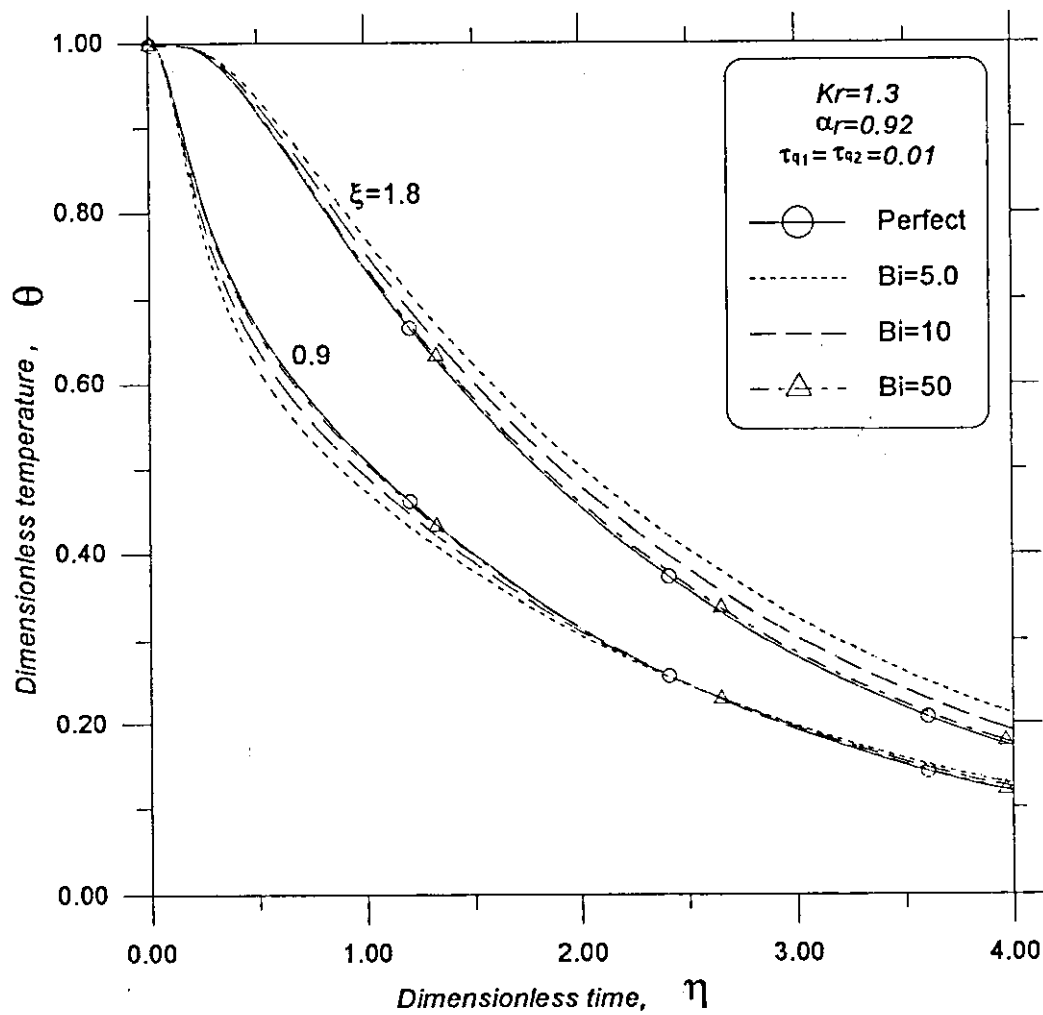
Fig. 7.37 : Transient temperature variation within the two domains for perfect and imperfect contact using the hyperbolic heat conduction model.
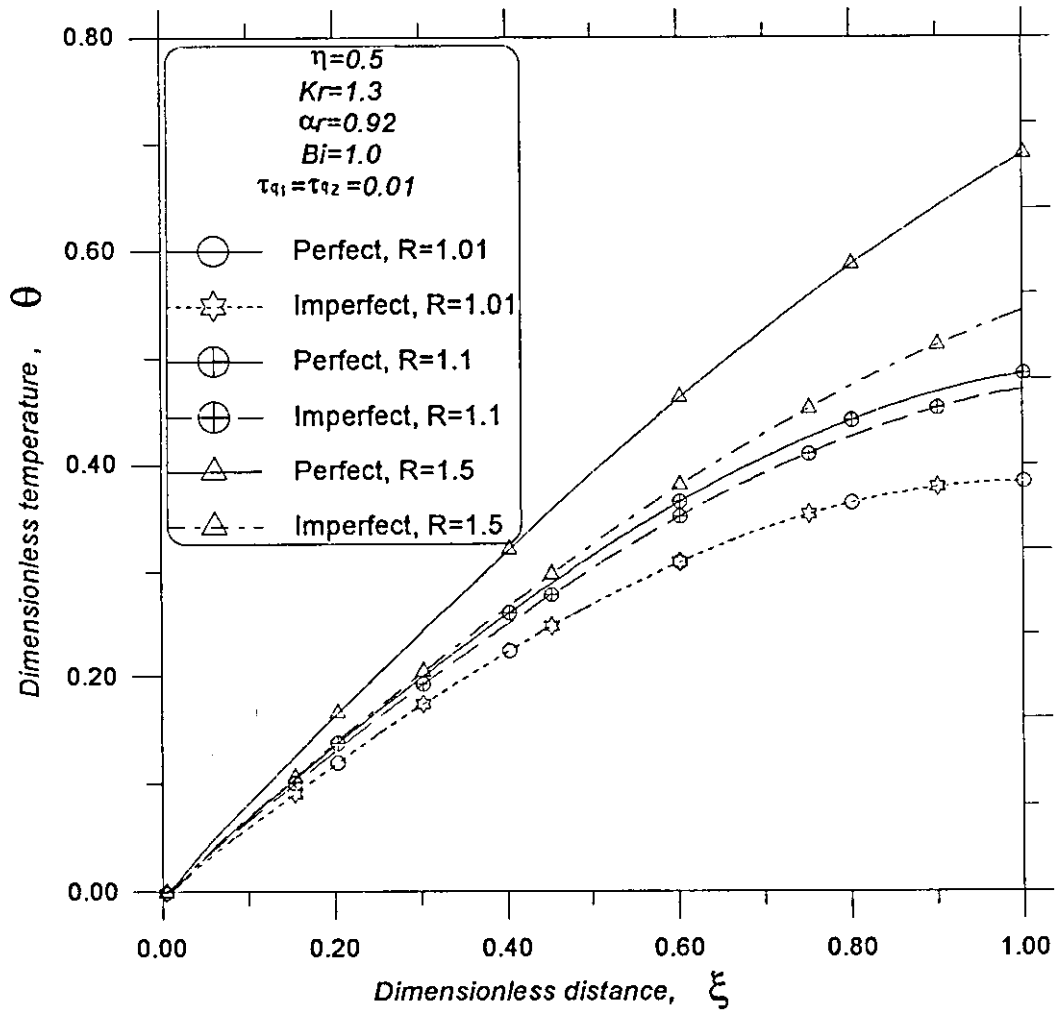
Fig. 7.38: Spatial temperature distribution within the first domain for perfect and imperfect contact using the hyperbolic heat conduction model at different R.
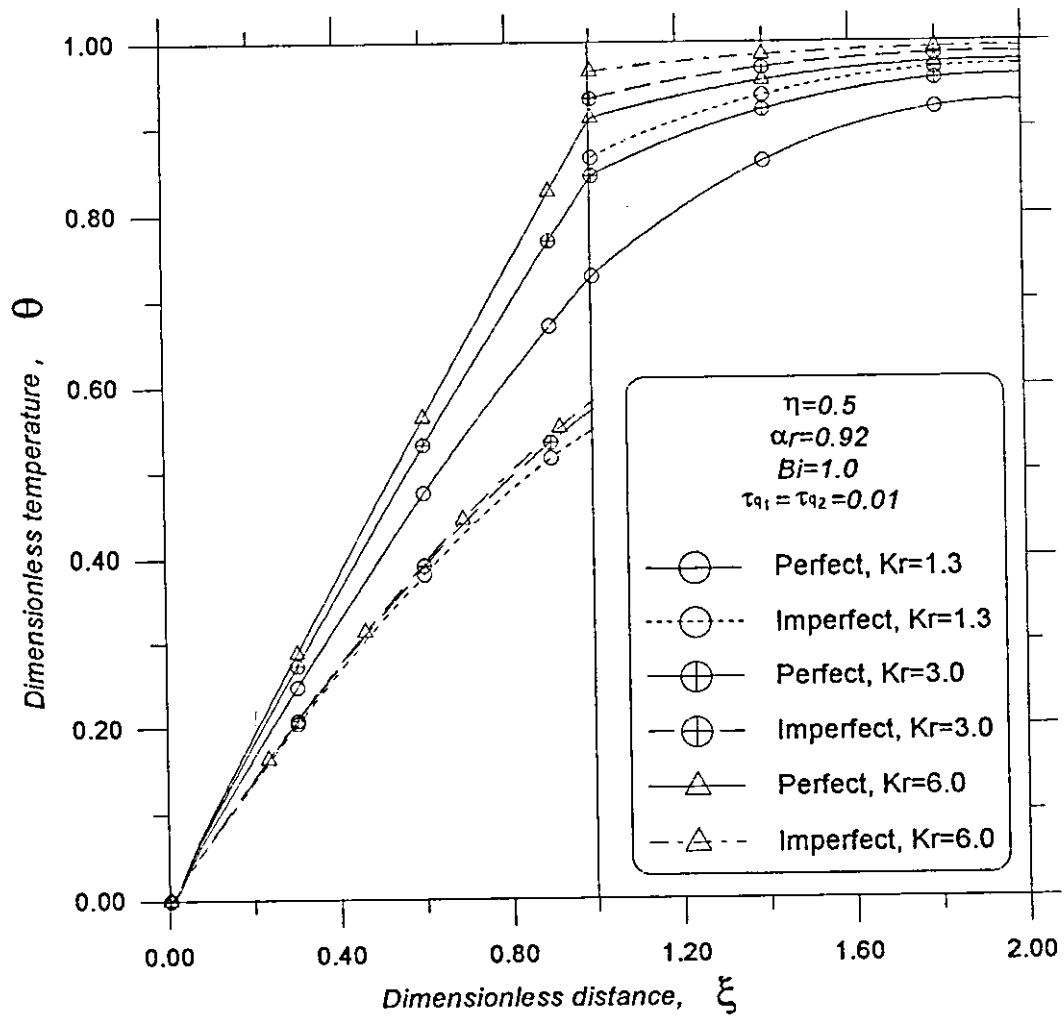
Fig. 7.39 : Spatial temperature distribution within the two domains for perfect and imperfect contact using the hyperbolic heat conduction model at different Kr.
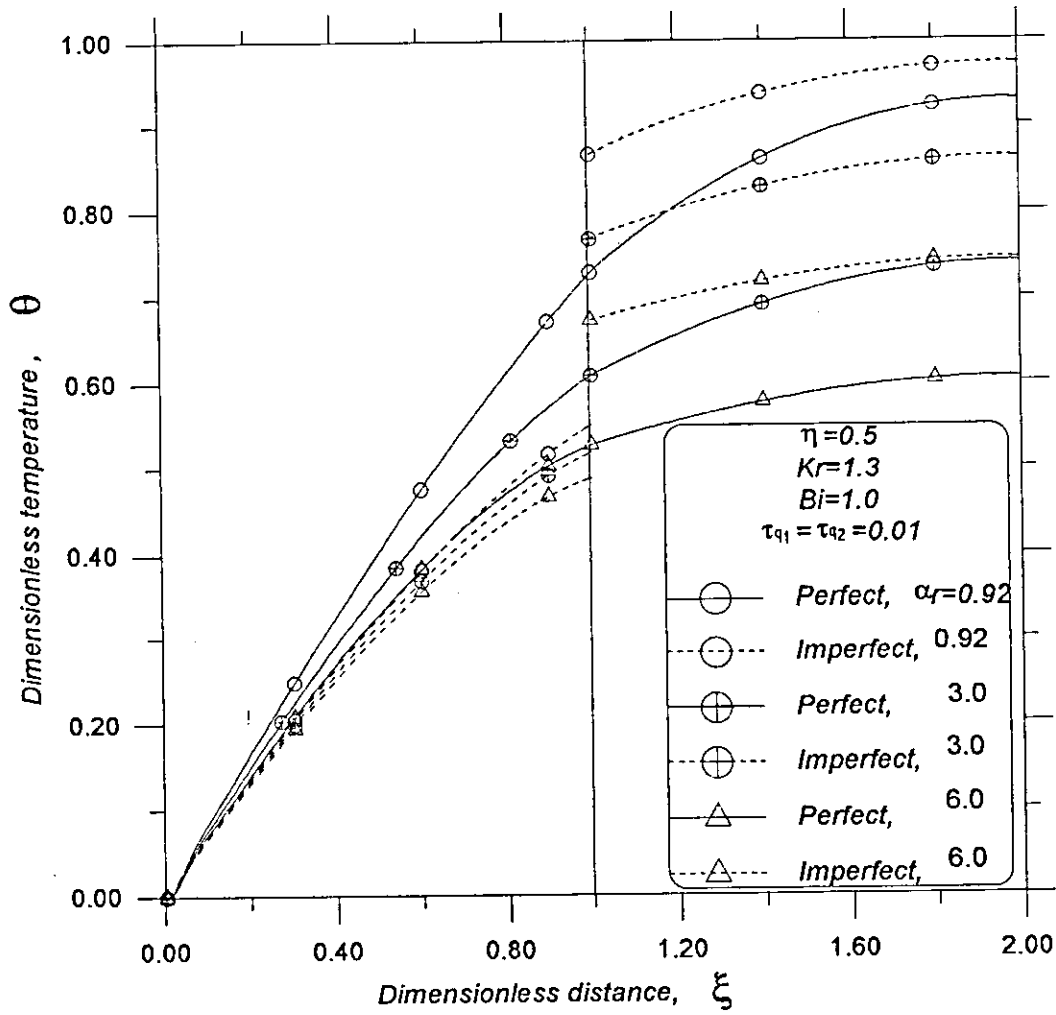
Fig. 7.40 : Spatial temperature distribution within the two domains for perfect and imperfect contact using the hyperbolic heat conduction model at different α_r.
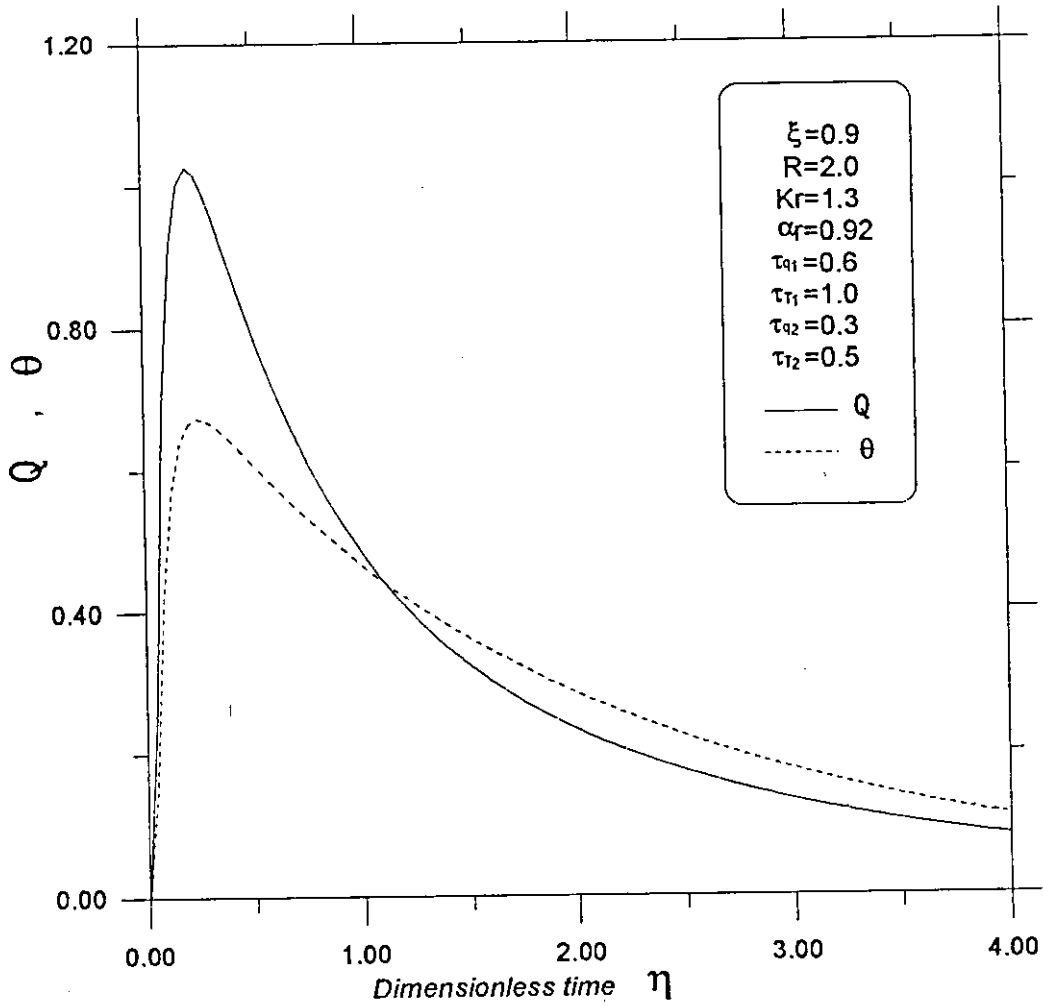
120

Fig. 7.41 : Change of dimensionless heat flux (cause) and dimensionless temperature gradient (effect) with dimensionless time.

Legend inside the figure:
$\xi = 0.9$
$R = 2.0$
$Kr = 1.3$
$\alpha_r = 0.92$
$\tau_{q_1} = 0.6$
$\tau_{T_1} = 1.0$
$\tau_{q_2} = 0.3$
$\tau_{T_2} = 0.5$
——— Q
------- θ

Axis labels: Q , θ (vertical); Dimensionless time η (horizontal)
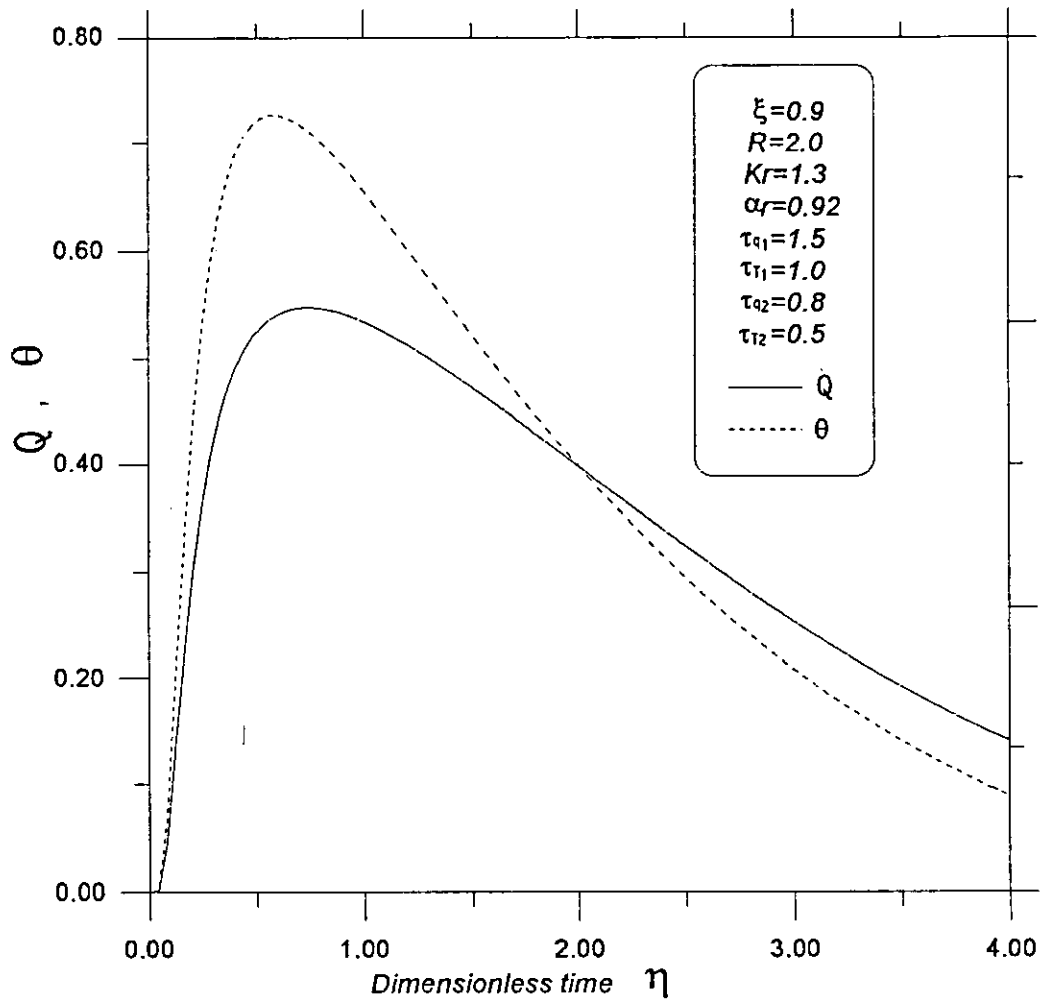
Fig. 7.42 : Change of dimensionless heat flux (effect) and dimensionless temperature gradient (cause) with dimensionless time
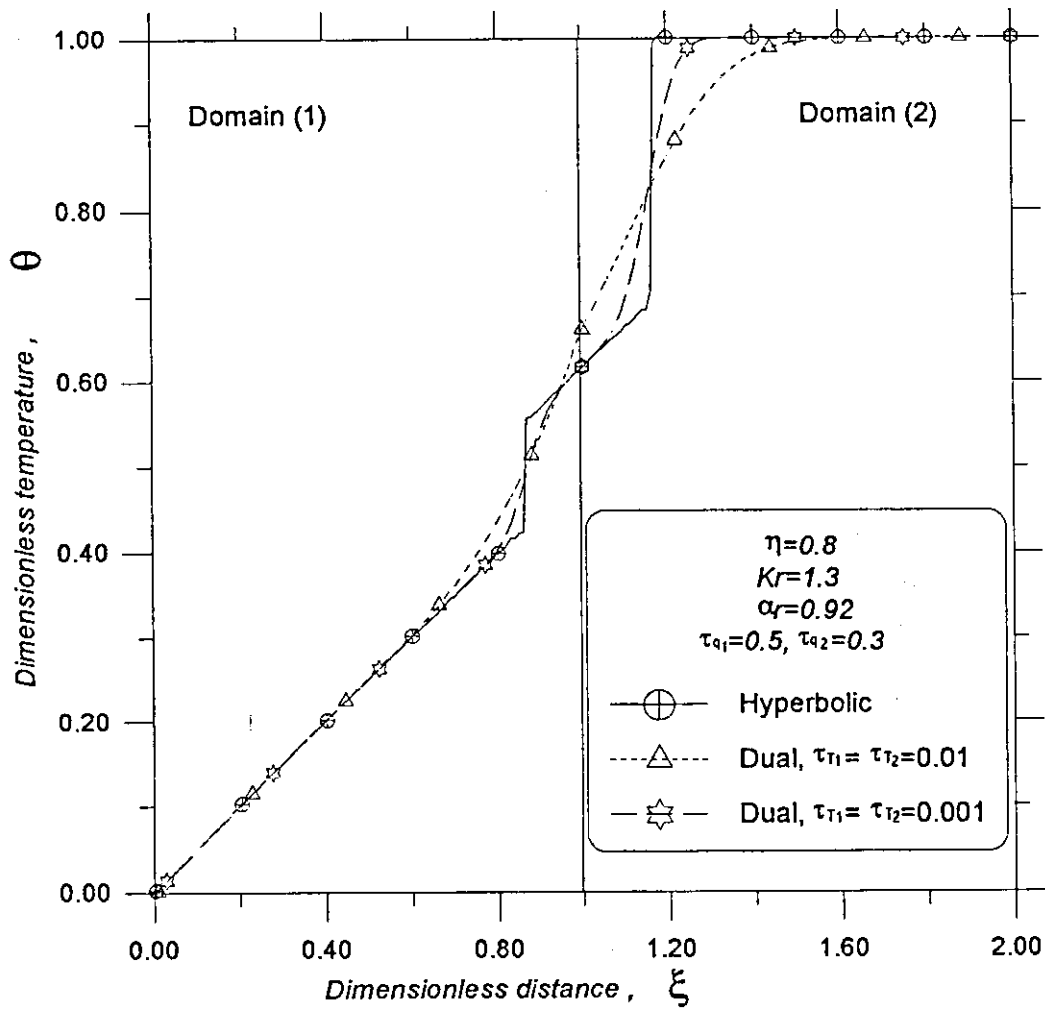
Fig. 7.43 : Spatial temperature distribution within the two domains using the hyperbolic and the dual phase heat conduction models.
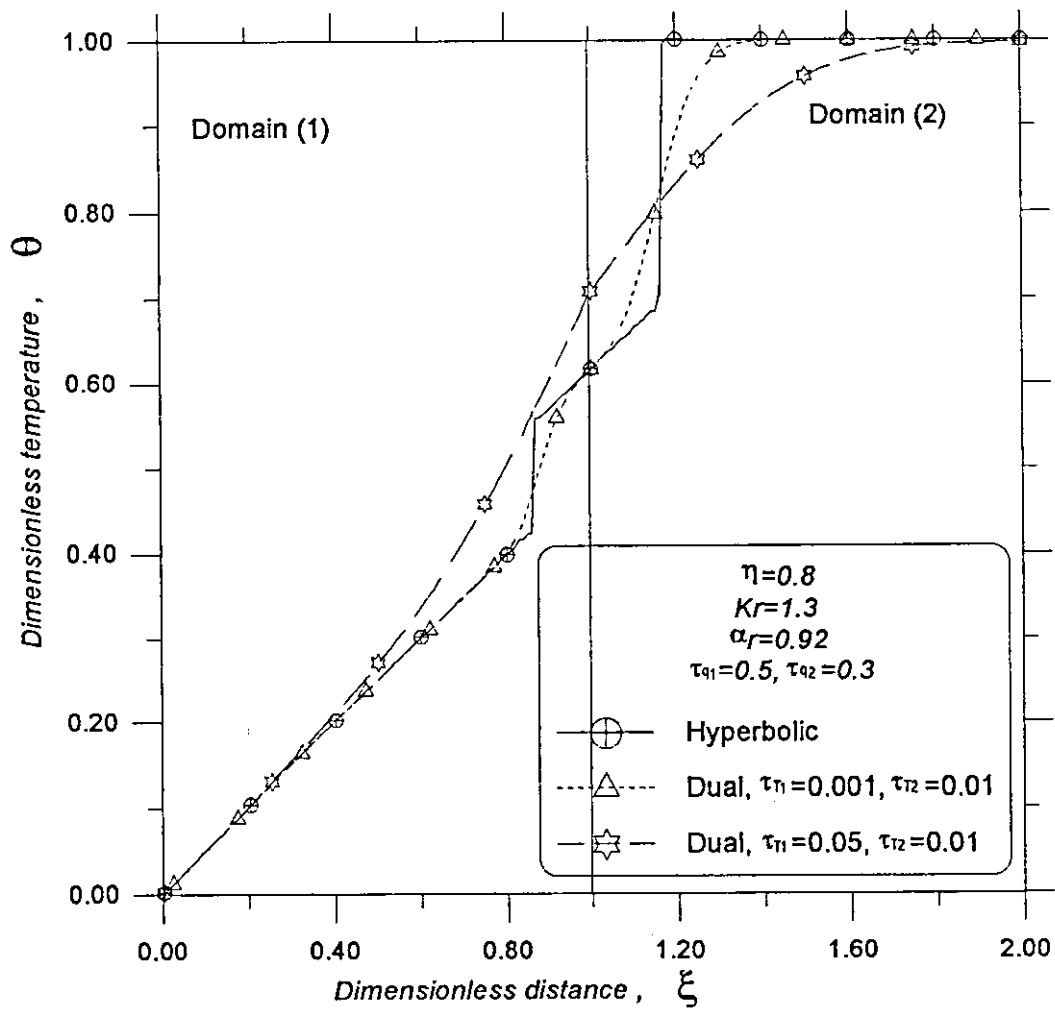
Fig. 7.44: Spatial temperature distribution within the two domains using the hyperbolic and the dual phase heat conduction models.

Fig. 7.45 : Spatial temperature distribution for perfect and imperfect contact within the two domains using the dual phase heat conduction model at different Biot number.

Fig. 7.46 : Spatial temperature distribution for perfect and imperfect conatct within the two domains using the dual phase heat conduction model.
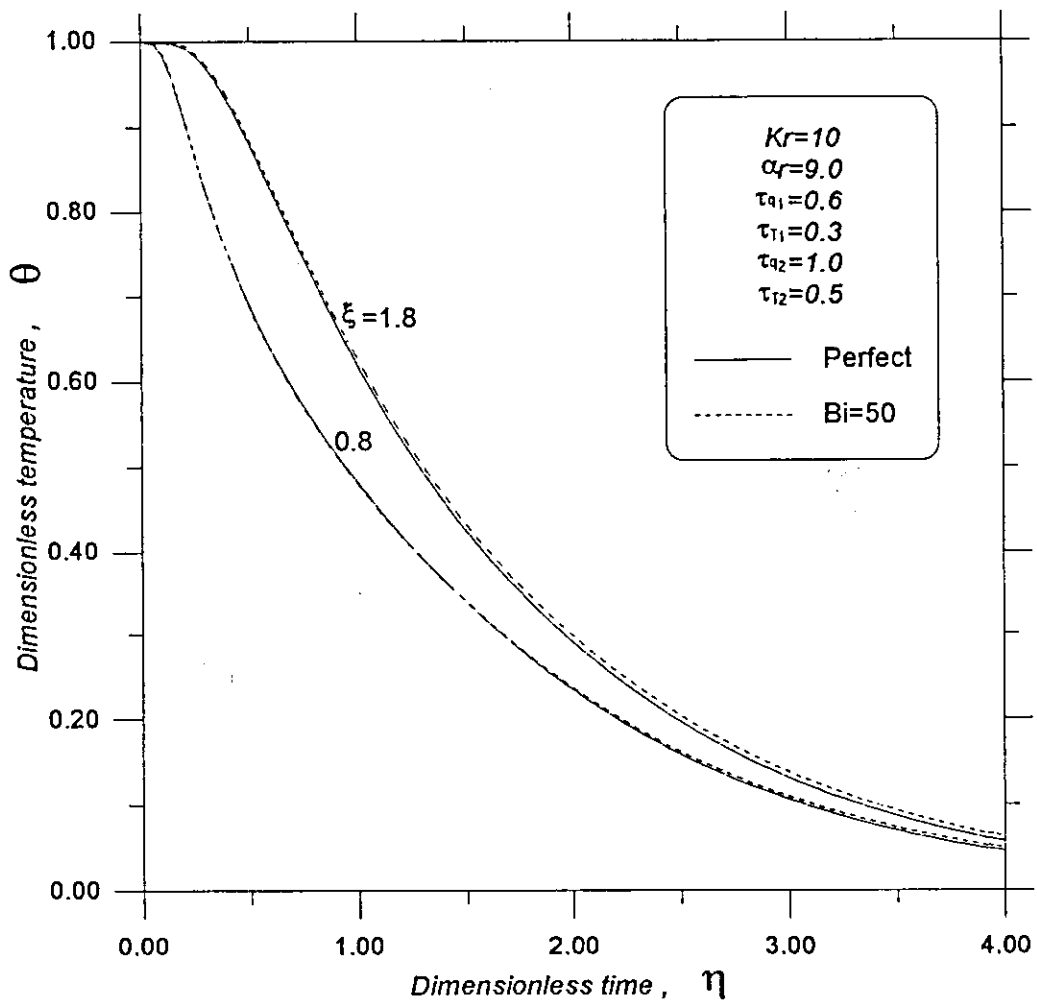
Fig. 7.47: Transient temperature variation within the two domains for perfect and imperfect contact using the dual phase heat condution model.
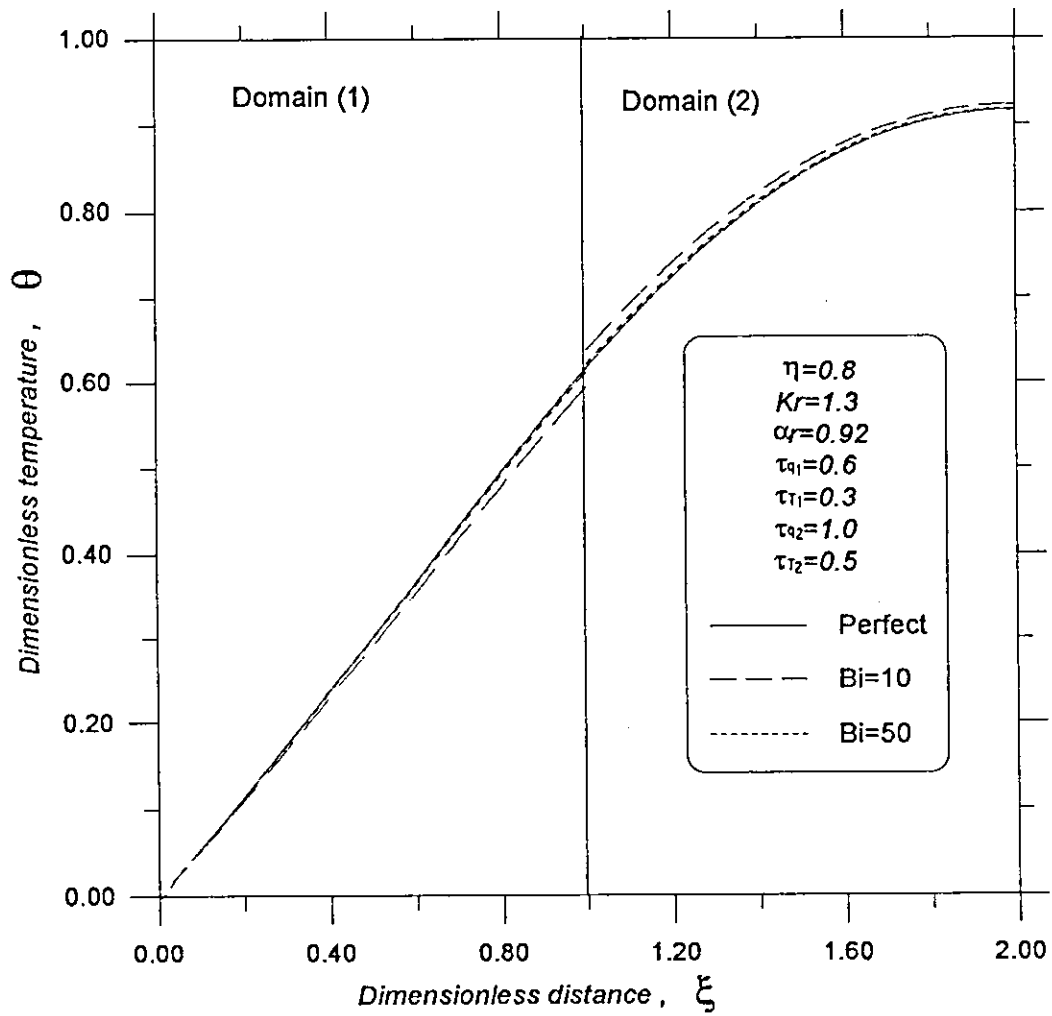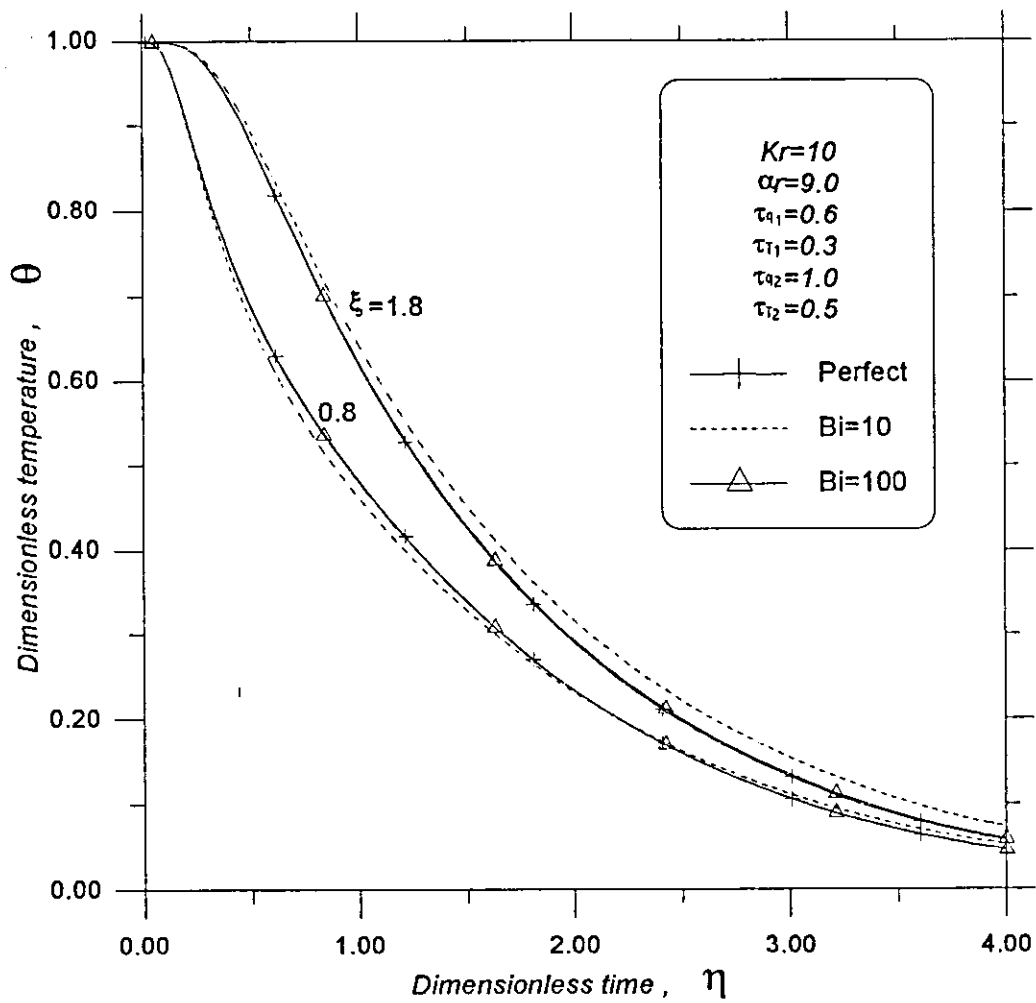
Fig. 7.48 : Transient temperature variation for perfect and imperfect contact within the two domains using the dual phase heat conduction model at different Biot number.
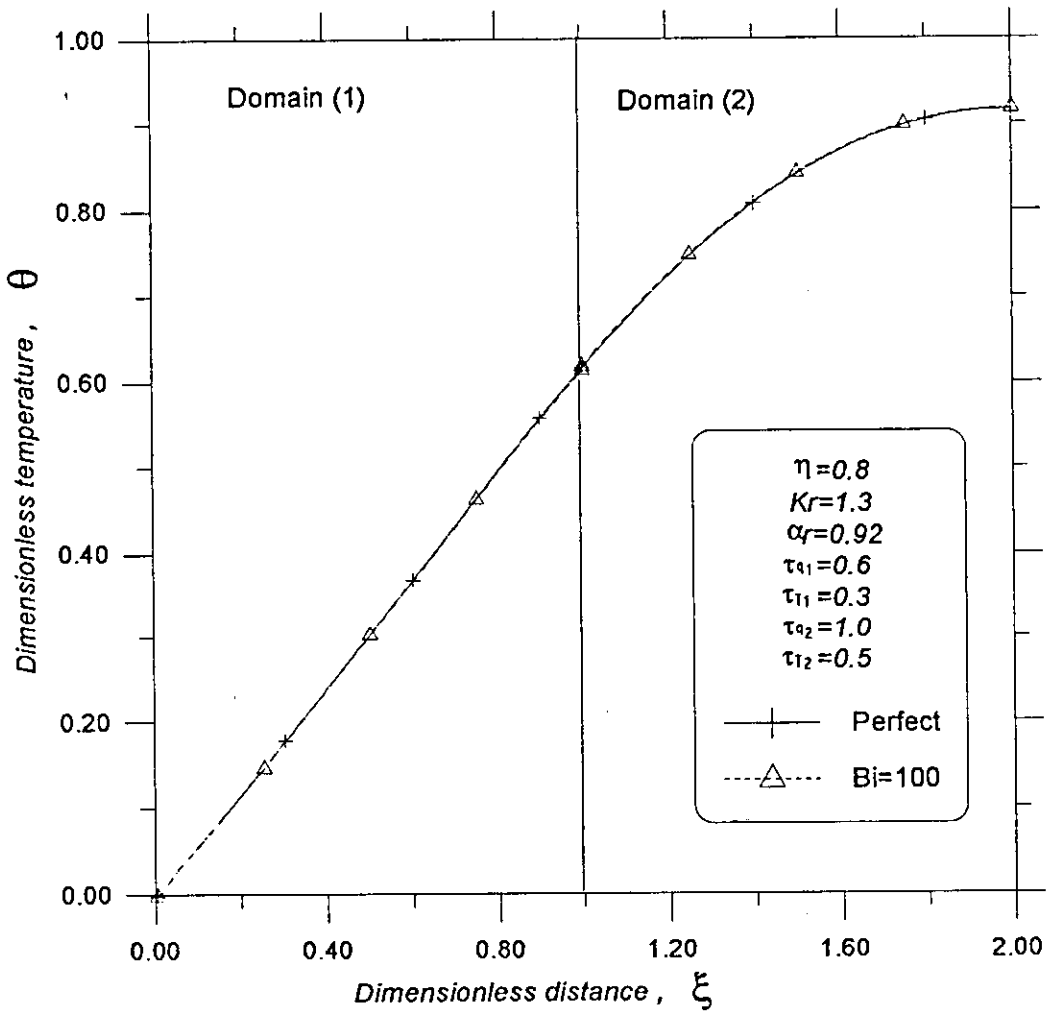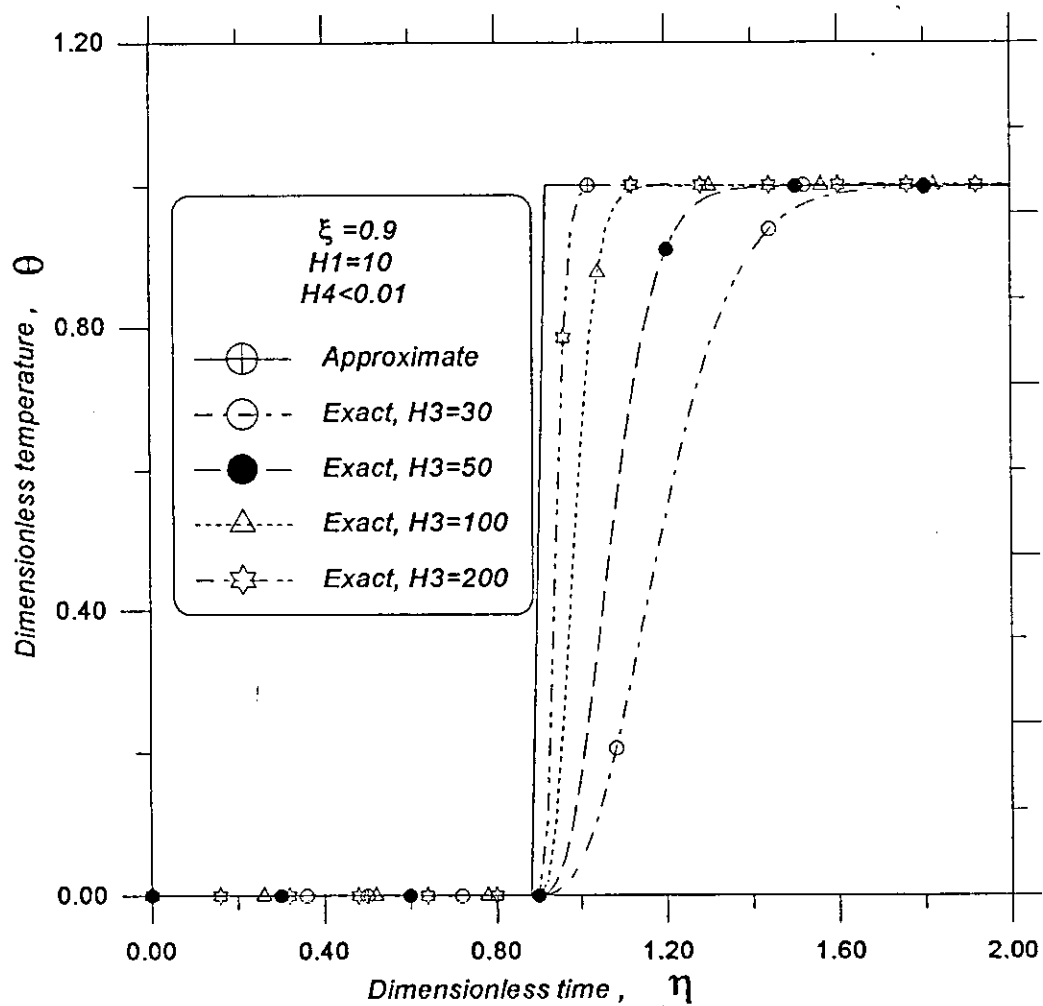
Fig. 7.49 : Exact and approximate transient temperature vatriation in the fluid domain
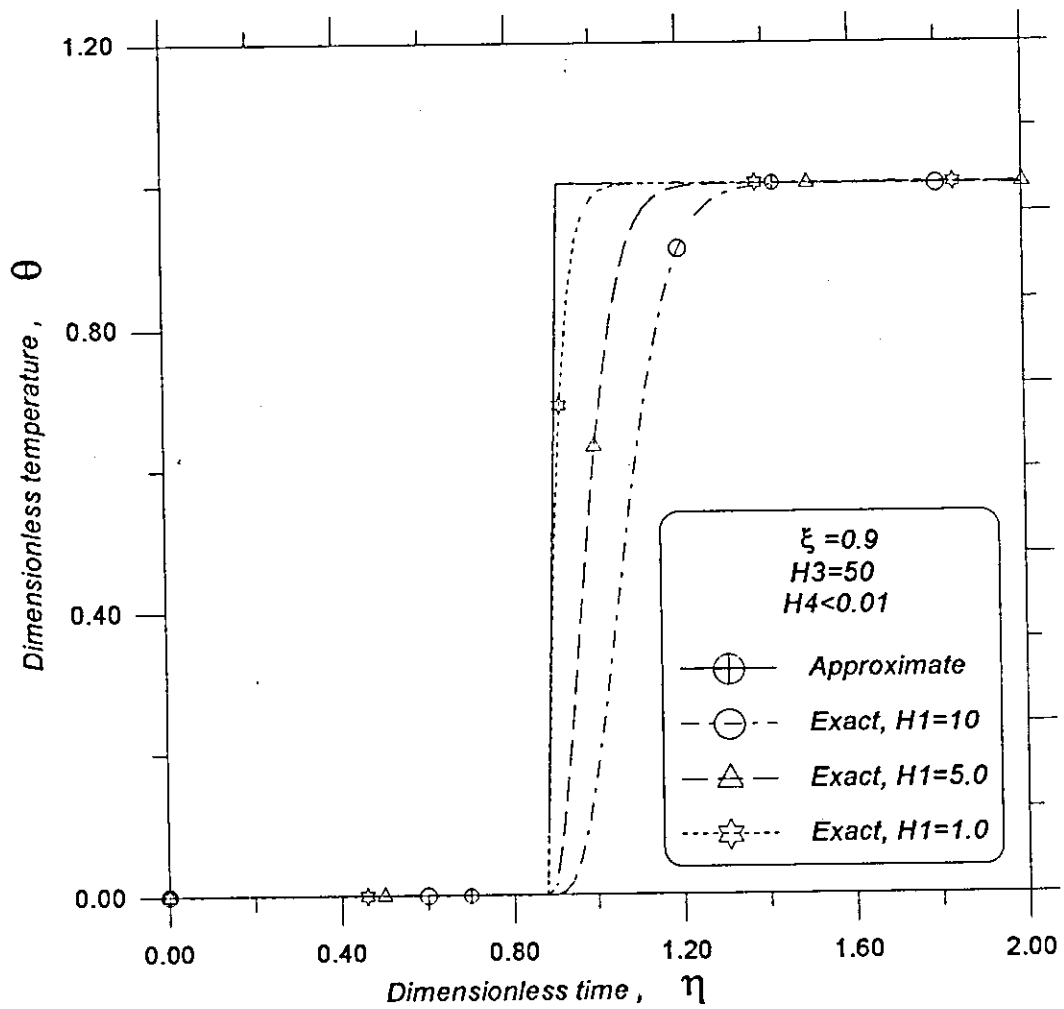
Fig. 7.50 : Exact and approximate transient temperature variation in the fluid domain.

Legend (inside plot):

$\xi = 0.9$
$H3 = 50$
$H4 < 0.01$

Approximate
Exact, $H1 = 10$
Exact, $H1 = 5.0$
Exact, $H1 = 1.0$

Axis labels:
Dimensionless temperature, θ
Dimensionless time, η

Fig. 7.51 : Exact and approximate transient temperature variation in the fluid domain.

Fig. 7.52 : Excat and approximate temperature distribution in the fluid domain at different η .

Fig. 7.53 : Exact and approximate temperature distribution in the fluid domain.

8-CONCLUSIONS

A generalized thermal boundary condition, which takes into account all thermal effects of a thin layer in thermal contact with an adjacent domain, is derived for parabolic and hyperbolic models. These effects are the thermal capacity, enthalpy flow, thermal di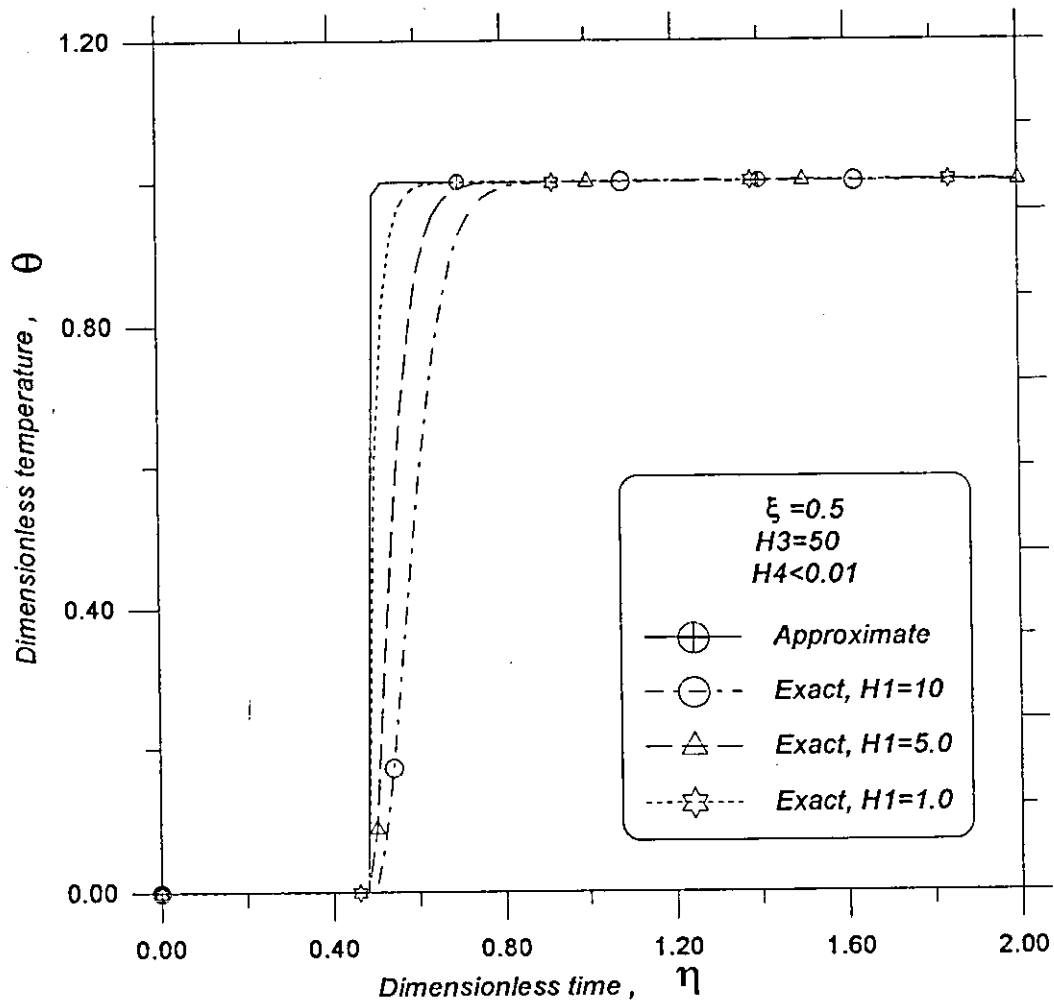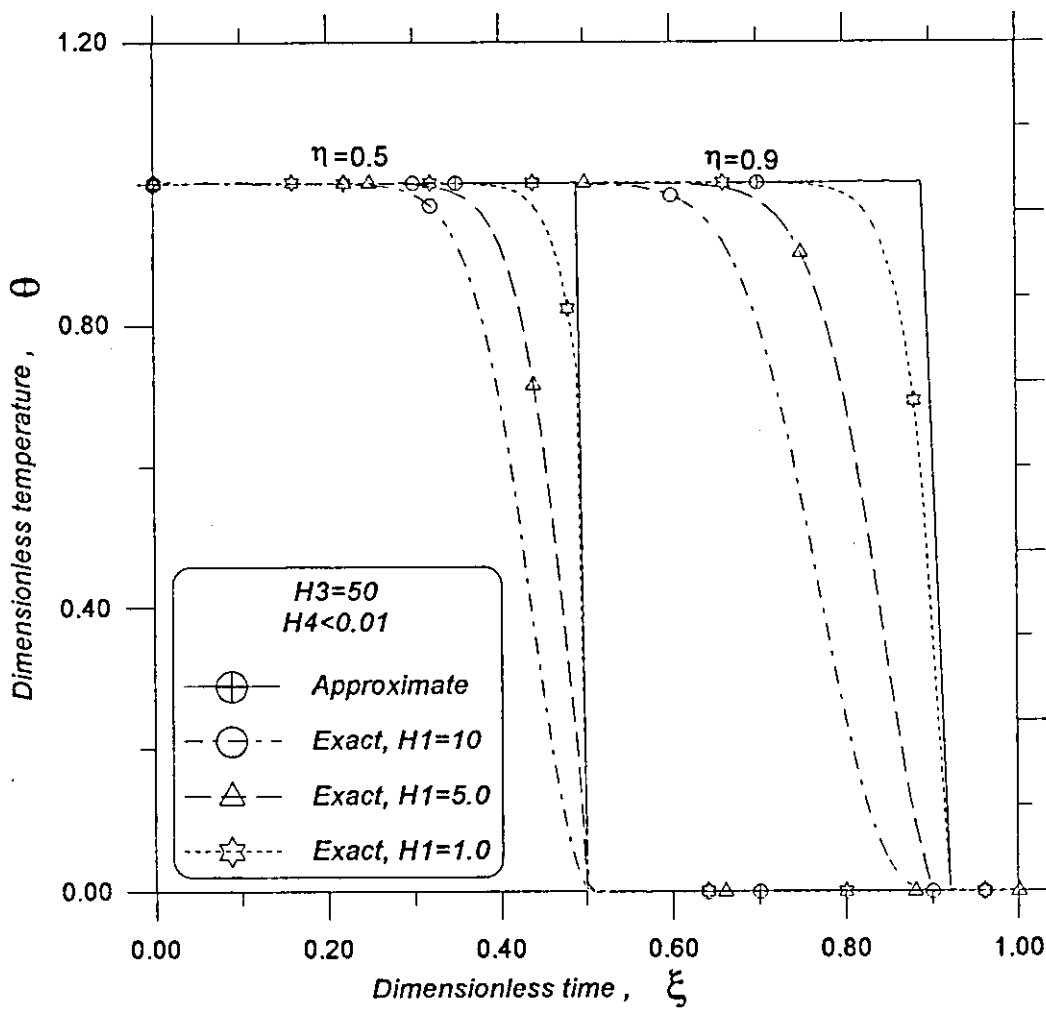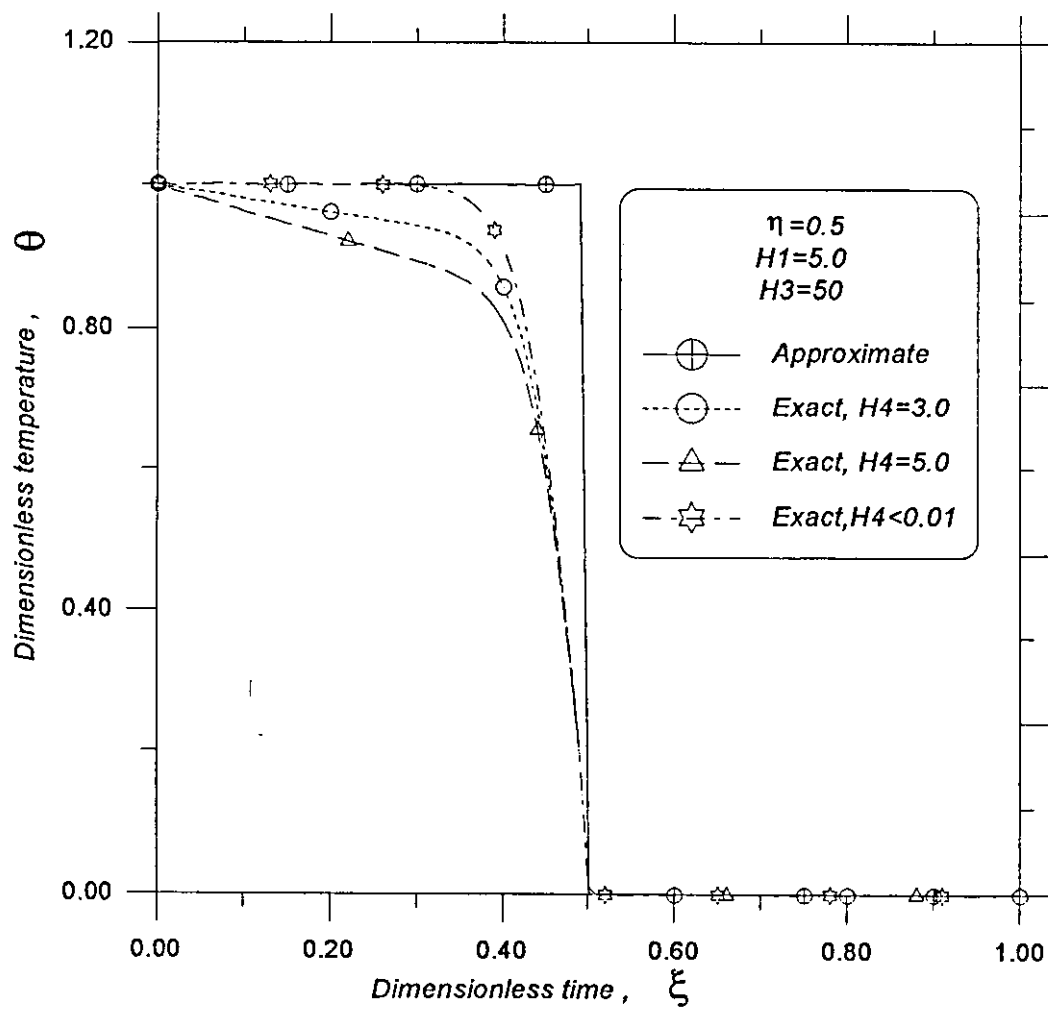ffusion, viscous dissipation and other aspects of thermal interaction between the thin layer and both its surroundings and adjacent domain. An example is given to demonstrate the importance of the introduced generalized thermal boundary condition.

It is found that the validity of the generalized thermal boundary condition is secured in layers having large thermal conductivity and diffusivity ratios and in layers having small thicknesses. However, the effect of the thermal conductivity ratio on the validity of the generalized boundary is less significant as compared to the effect of the thin layer thickness or thermal diffusivity. As an example, the generalized boundary condition is secured in layers having thickness less than 0.01 whatever the values of α_r and K_r are. The ranges of α_r within which the generalized boundary condition is valid become narrower as the film thickness increases.

For $\tau_{q,1}$ and $\tau_{q,2}$ less than 0.01; the thermal relaxation time has insignificant effect on the predictions of the diffusion parabolic model, which assumes that $\tau_{q1} = \tau_{q2} = 0.0$. Also, the phase-lag concept has insignificant effect on the predictions of the dual phase heat conduction model when $\tau_{T,1}$ and $\tau_{T,2}$ are less than 0.001. As $\tau_{T,1}$ or $\tau_{T,2}$ increases, the deviation between both models increases.

The transient temperature variation for the imperfect contact case approaches that for the perfect contact case as *Biot* number *(Bi)* increases. Also, the interfacial *Biot*

135

number larger than 50 yields predictions similar to that of the perfect contact model. Also, for situations involving very thin second domain, perfect thermal contact assumption is justified. On other hand, it is concluded that the deviation between both the perfect and the imperfect contact models is significant close to the contact plane and in locations having high heat transfer rates.

The coupling between the two energy equations, which describes the thermal behavior of the transient conjugated heat transfer problem in circular ducts, is eliminated using a simple perturbation technique. Elimination of this coupling is possible in applications involving high convective heat transfer coefficient between the flowing fluid and the solid wall. As a result of this elimination, solving the produced decoupled governing equations becomes an easy matter. A case study is presented to investigate the validity of the proposed perturbation technique. The predictions of both the exact and the approximate models are found to be in a very good agreement especially at large values of the dimensionless group

$$H_3 = \frac{2 h_i r_1^2}{V \rho_s c_s \left(r_2^2 - r_1^2 \right)}$$ and at small values of both $H_1 = \frac{2 h_i}{V \rho_f c_f}$ and

$$H_4 = \frac{2 h_o r_2 r_1}{V \rho_s c_s \left(r_2^2 - r_1^2 \right)}.$$

9-REFERENCES

Al-Nimr, M. A. and Al-Huniti, Naser S., 2000, "Thermal stresses under the effect of the dual-phase-lag heat conduction model," Accepted for publication in *J. Thermal stresses*.

Al-Nimr, M. A., and Alkam, M., 1997, "A generalized thermal boundary condition," *Heat and Mass Transfer*, 33, 157-161.

Al-Nimr, M. A. and El-Shaarawi, M. A., 1992, "Analytical Solutions For Transient Conjugated Heat Transfer In Parallel Plate and Circular Ducts", *Int. Comm. Heat Mass Transfer*, 19, 869-878.

Al-Nimr, M. A. and Hader, M. A., 1994, "Transient Conjugated Heat Transfer In Developing Laminar Pipe Flow", *J. Heat Transfer*, 116, 234-236.

Al-Nimr, M. A., Haddad, O. M. and Arpaci, V., 1999, "Thermal behaviour of metal films-A hyperbolic two-step model," *Heat and Mass Transfer*, 35(6), 459-464.

Al-Nimr, M.A., and Kiwan, S., 2000, "Effect of thermal losses on the microscopic two-step heat conduction model," Accepted for publication in *Int. J. Heat Mass Transfer*.

Al-Nimr, M. A. and Naji, M., 1999, "Heat transfer in an anisotropic material under the effect of the hyperbolic heat conduction model," *Heat and Mass Transfer*, 35(6), 493-497.

Al-Nimr, M. A., 1998, "A Simple Approach To Solve Conjugated Heat Transfer Problems In Circular and Parallel Plate Ducts", *Int. J. Energy Res.*, 22, 161-168.

Al-Nimr, M. A., 1993, "Temperature Distribution Inside A Solar Collector Storage Tank Of Finite Wall Thickness", *Journal of Solar Energy Engineering*, 115, 112.

Barozzi, G. S. and Pagliarini G., 1985, "A Method To Solve Conjugate Heat Transfer Problems: The Case of Fully Developed Laminar Flow In A Pipe", *ASME J. Heat Transfer*, 107, 77-83.

Beck, J. V., Cole, K. D., Hali-Sheikh, A., and Litkouhi, B., 1992, *"Heat Conduction Using Green's Function"*, Hemisphere, London, 23-37.

Carslaw, H. S., and Jaeger, J. C., 1980, *"Conduction of Heat In Solids"*, 2nd ed., Oxford University Press, 1-49.

Catteneo, C., 1958, "A Form of Heat Conduction Equation Which Eliminates The Paradox of Instantaneous Propagation", *Compte Rendus*, 247,431-433.

Chen, Han-Taw, and Lin, Jae-Yuh., 1994, "Analysis of Two-Dimensional Hyperbolic Heat Conduction Problems", *Int. J. Heat and Mass Transfer*, 37(1), 153-164.

Chen, S. C., Anand, N.K. and Tree, D. R., 1983, "Analysis of Transient Convective Heat Transfer Inside A Circular Duct", *J. Heat Transfer*, 105, 922-924.

Chung, B. T. F., and Kassami, S. A., 1980, "Conjugated Heat Transfer For Laminar Flow Over Flat Plate With A Non-Steady Temperature At The Lower Surface", *J. Heat Transfer*, 102, 177.

Cotta, R. M., Mikhailov, M. D., and Ozisik, M. N., 1987, "Transient Conjugated Forced Convection In Ducts With Periodically Varying Inlet Temperature", *Int. J. Heat Transfer*, 30, 2073.

Cotta, R. M., Ozisik, M. N. and McRae, D.S. 1986, "Transient Heat Transfer In Channel Flow With Step Change In Inlet Temperature", *Numer. Heat Transfer*, 9, 619-630.

El-Shaarawi, A. L., Al-Nimr, M. A., and Hader, M. A., 1995, "Transient Conjugated Heat Transfer In Concentric Annuli", *Int. J. Num. Meth. Heat Fluid*, 5, 459-473.

Gembarrovic, J. and Majernik, V., 1988, "Non-Fourier Propagation of Heat Pulses In Finite Medium", *Int. J. Heat Mass Transfer*, 31, 1073-1080.

Issa, M., and Al-Nimr, M. A., 1989, "Temperature Distribution Inside Hot Water Storage Tanks Collector", *ASME Journal of Solar Energy Engineering*, 111, 311.

Kakac, S., Li. W. and Cotta, R. M., 1990, " Unsteady Laminar Forced Convection In Ducts With Periodic Variation of Inlet Temperature", *Trans. ASME Journal of Heat Transfer*, 112, 913.

Kim,W. S., Hector, L. G, and Ozisk, M. N., 1990, " Hyperbolic Heat Conduction Due to Axisymmetric Continuous or Pulsed Surface Heat Sources", *J. Applied Phys.*, 68, 5478-5485.

Krishan, B., 1982, "On Conjugated Heat Transfer In Fully Developed Flow", *Int. J. Heat Mass Transfer*, 25, 288.

Kumar, K. Tamma., and Raju, R. Namburu., 1991, "Hyperbolic Heat Conduction problems: Numerical Simulations via Explicit Lax-Wendroff-Based Finite Element Formulations", *J. Thermophysics*, 5, 232-239.

Lin, T. F., and Kuo, J. C., 1988, "Transient Conjugated Heat Transfer In Fully Developed Laminar Pipe Flows", *Int. Heat and Mass Transfer*, 31, 1093.

Maurer, M. J., and Thompson, H. A, " Non-Fourier Effects At High Heat Flux", *J. Heat Transfer*, 95, 284-286.

Maxwell, J. C., 1867, "On The Dynamic Theory of Gases", *Philos, Trans. Soc. London*, 157, 49-88.

Olek, S., Elias, E., Wachold'er, E., and Kaiserman, S., 1991, "Unsteady Conjugated Heat Transfer In Laminar Pipe Flow", *Int. J., Heat Mass Transfer*, 34, 1443.

Ozisik, M. and Tzou, D., 1994, "On The Wave Theory In Heat Conduction", *ASME J. Heat Transfer*, 116, 526-535.

Ozisik, M., 1993, *"Heat Conduction"*, 2nd ed., John Wiley and Sons, 214-256.

Perlmutter, M., and Siegel, R., 1961,"Two-Dimensional Unsteady Incompressible Laminar Duct Flow With A Step Change In Wall Temperature", *Int. J. Heat Mass Transfer*, 3, 94.

Peshkov, V., 1944, "Second Sound In Helium II", *J. Physics*, USSR, VIII, 381-387.

Qui, T. Q., And Tien, C. L., 1992, " Short-Pulse Laser Heating on Metal", *Int. J. Heat and Mass Transfer*, 53(3), 719-726.

Sakakibara, M., Mori, S. and Tanimoto, A., 1987, "Conjugate heat transfer with laminar flow in an annulus", *Canadian J. Chem. Engng*, 65, 541- 549.

Shah, R. K. and London, A. L., 1978, *"Laminar Flow Forced Convection in Ducts "*, Academic Press, New York.

Siegel R., 1959, "Transient Heat Transfer For Laminar Slug Flow In Ducts", *J.Appl. Mech.*, 81, 140.

Sparrow, E. M., and de Faries, F. N., 1986, "Unsteady Heat Transfer In Ducts With Time Varying Inlet Temperature and Participating Walls", *Int. J. Heat Mass Transfer*, 11, 837.

Sucec, J. and Swant, A., 1984, "Unsteady Conjugated Forced Convection Heat Transfer In Parallel Plate Duct", *Int. J. Heat Mass Transfer*, 27, 95.

Sucec, J., 1981, "An Improved Quasi Steady Approach For Transient Conjugated Forced Convection Problems", *Int. J. Heat Mass Transfer*, 24, 1711.

Travelho, T. S. and Santos, W. F. N., 1991, "Solution For Transient Conjugated Forced Convection In The Entrance Region Of A Duct With Periodically Varying Inlet Temperature", *J. Heat Transfer*, 113, 558.

Tzou, D. Y., 1997, *"Macro To Microscale Heat Transfer, The Lagging Behavior"*, Taylor and Francis, 1-64.

Tzou D.Y., M. N., Ozisik and R.J, Chiffele, 1994, "The Lattice Temperature In Microscopic Two-Step Models", *J. Heat and Mass Transfer*, 116, 1034-1038.

Tzou, D. Y., 1995a, "A Unified Field Approach For Heat Conduction From Micro-to Macro-scale", *ASME Journal of Heat Transfer*, 117, 8-16.

Tzou, D. Y., 1995b, " The Generalized Lagging Response In Small-Scale and High-Rate Heating", *International Journal of Heat and Mass Transfer*, 38, 3231-3240.

Tzou, D. Y., 1995c, "Experimental Support For the Lagging Response In Heat Propagation", *AIAA Journal of Thermophysics and Heat Transfer*, 9, 686-693.

Vernotte, P., 1961, "Some Possible Complications In The Phenomena of Thermal Conduction", *Compte Rendus*, 252, 2190-2191.

Vick, B. and Ozisik, M., 1983, "Growth and Decay of A Thermal Pulse Predicted by The hyperbolic heat Conduction Equation", *ASME J. Heat Transfer*, 105, 902-907.

Yan, W. M., Tasy, Y. L., and Lin, T. F., 1989, "Transient Conjugated Heat Transfer In Laminar Pipe Flows", *Int. J. Heat Mass Transfer*, 32, 775.

APPENDEX A

FORTRAN 77 CODE FOR THE NUMERICAL INVERSION OF THE LAPLACE TRANSFORM

The FORTRAN 77 code that performs the Laplace inversion in terms of the Riemann-sum approximation, Eq. (2.22), is enclosed here. The sample program performs inversion of the transformed temperature, resulting from the solution of Eqs. (2.16) and (2.17) subject to the case study,

$$W_1(\xi, P) = C_1 e^{z\sqrt{P}} + C_2 e^{-z\sqrt{P}} + \frac{1}{P} \tag{A.1}$$

where z is the space variable (equivalent to ξ used throughout the thesis), P is the Laplace transform variable to be inverted to the real time η (equivalent to S used in the program). The temperature distribution is calculated at a fixed instant of time, S=0.05,0.1......,0.5 for parabolic (the real time), in the physical domain from Z=0.0 to 1.0. The "Do-loop" is thus placed on (z) at a constant value of S. Should a time distribution of temperature be intended, the Do-loop should be placed on (S) instead. In all cases, the program will automatically adjust the optimal value of γ according to Eq. (1.18). Line numbers are generated at the beginning of every statement for later illustrations.

This program only shows a working example, with emphasis on illustrating the essence of the Laplace inversion technique via the Riemann-sum approximation.

```
1       PROGRAM LAG

2       IMPLICIT DOUBLE PRECISION (A-H,O-Z)
```

142

***double precision is used due to possible intensive iterations (especially

***recommended for the use of personal computers(PC))

3   EXTERNAL FUNC

***FUNC defines the Laplace transformed solution

4   COMMON/DA/ z, Kr, Ar, R

5   OPEN (5,FILE='A:\H.DAT',STATUS='UNKNOWN')

6   S=0.5

***S is the real time. Its value can be the physical time with a dimension (t)

or*** the dimensionless time without a dimension (η).

***This sample program computes the temperature distribution in space (z)

from 0 (z0) to 1.0 (zf) at S=0.5

7   NTERMS=40000.

***Maximum number of terms used in the Riemann-sum approximation,

***Eqs. (2.16) and (2.17). Default value is set to 20000.

8   GMMA=0.0

*** GMMA is the value for the product of $\gamma\eta$ in Eqs. (2.16) and (2.17). A value of 0.0

intrigues the default value of $\gamma\eta = 4.7$

9   Kr=1.3

10   Ar=0.92

11   R=1.1

12   z0=0.

13   zf=1.0

***Define the initial (z0) and the final (zf) positions for the temperature distribution

14   DO 10 I=1,101

15   Z=Z0+(Zf-Z0)*(I-1)/100.

143

*** Z is the space variable. This sample program discretizes the physical domain
***from 0 to 1.0 into 100 intervals

16   CALL LAPINV (FUNC,GMMA,S,RESULT,NTERMS)

***LAPINV is the subroutine for the Riemann-sum approximation of the Laplace
***inversion. RESULT= temperature at (z,s)

17   WRITE (5,*)Z,RESULT

18   10 CONTINUE

19   CLOSE (5)

20   END

*** The function subroutine FUNC (P) defines the solutions of temperature in the
***Laplace transform domain. This block needs to be modified for different problems
***with different solutions.

21   FUNCTION FUNC (S)

22   IMPLICIT DOUBLE PRECISION (A-H, O-Z)

23   COMMON /DA/Z, Kr, Ar, R

24   COMPLEX P, FACZ

*** The Laplace transform variable P must be complex. Any other functions of P
***used in defining the transformed solution of temperature (C1 and C2 in this program
***for example) must be declared to be complex accordingly.

25   C2=-1/P/(1+(EXP (-2*SQRT (P))*((1+AK)+(1-AK)*EXP ((2*R-2)*
      $ SQRT (P/AL)))/((1-AK)+(1+AK)*EXP ((2*R-2)*SQRT (P/AL)))))
      C1=-1/P/(1+(EXP (-2*SQRT (P))*((1+AK)+(1-AK)*EXP ((2*R-2)*
      $SQRT (P/AL)))/
      $((1-AK)+(1+AK)*EXP((2*R-2)*SQRT(P/AL)))))*EXP(-2*SQRT(P))*
      $((1+AK)+(1-AK)*EXP((2*R-2)*SQRT(P/AL)))/((1-AK)+(1+AK)*

144

```fortran
     $EXP ((2*R-2)*SQRT(P/AL)))

26   FUNC=C1*EXP (SQRT(P)*Z)+C2*EXP(-SQRT(P)*Z)+1/P

27   RETURN

28   END
```

***Subroutine LAPINV performs the Riemann-sum to approximate the Laplace

***inversion of the function specified in FUNC (P)

```fortran
29   SUBROUTINE LAPINV (FUNC, GMMA, S, RESULT, NTERMS)

30   IMPLICIT DOUBLE PRECISION (A-H, O-Z)

31   EXTERNAL FUNC

32   COMMON Z, TRASH1, TRASH2, TRASH3

33   COMPLEX GAM, B, CPR, PARTB, CHKCON

34   EPS=1.0D-10
```

***EPS defines the convergence threshold for the ratio test of partial sums,

***EPS=(Temperature (N+1)-Temperature (n))/Temperature(N)),

***with N denoting the partial sum of the first N terms in Eq. (2.16) and (2.17)

```fortran
35   GAM=(0.0,0.0)
```

***Avoid the use of initial condition at S=0.0 in this program.

***If needed, select a very small value of S, such as 0.001, to evaluate the initial

***temperature for validating purposes.

```fortran
36   IF (S.EQ.0.0) THEN

37   WRITE (*,*)'LAPLACE VARIABLE CANNOT BE ZERO!'

38   RETURN

39   ENDIF
```

***The default value of GMM*S=4.7

```fortran
40   IF (GMMA.EQ.0.0) GMMA=4.7/S
```

145

```fortran
41      GAM=GMMA
```

***Default number of terms used in the Riemann-sum is 20000 terms

```fortran
42      IF (NTERMS.EQ.0.0) NTERMS=20000

43      PI=ACOS (-1.)

44      B=(0.0,1.0)

45      FIRST=(1./S)*EXP(GAM*S)

46      PARTA=0.5*FUNC (GAM)

47      PARTB=(0., 0.)

48      I=0.
```

***Check convergence for the first NTERMS in the Riemann-sum

***Raise warning flags if EPS is larger than the specified value

```fortran
49  5   IF (I.EQ.NTERMS) THEN

50      WRITE (*,*)'NO CONVERGENCE FOR S=',S

51      GO TO 15

52      ENDIF

53      I=I+1

54      CPR=GAM+B*(I*PI/S)

55      CHKODD=MOD(I,2)

56      CHKCON=PARTB

57      IF (CHKODD.EQ.0) THEN

58      PARTB=PARTB+FUNC(CPR)

59      ELSE

60      PARTB=PARTB+FUNC(CPR)*(-1)**I

61      ENDIF

62      RESULT2=FIRST*(PARTA+REAL(PARTB))
```

```
63      RESULT1=FIRST*(PARTA+REAL(CHKCON))
```

***If summation is zero, apply different convergence check

```
64      IF (RESULT1.EQ.0.0)THEN

65      IF(ABS(RESULT2).LT.EPS)GO TO 15

66      GO TO 5

67      ENDIF
```

***The convergence check is then abs (abs(f(n)-f(n-1))/f(n)).

***First avoid divide by zero error

```
68      IF (RESULT2.EQ.0.0) THEN

69      IF(ABS(RESULT1).LT.EPS)GO TO 15

70      GO TO 5

71      ENDIF

72      CCON=ABS(ABS((RESULT2-RESULT1))/RESULT2)

73      IF(CCON.LE.EPS)GO TO 15

74      GO TO 5
```

***If the Laplace variable is changed in successive calculations, such as the multible-

***time calculations, make sure to reset gamma to zero for the next case

```
75  15  GMMA=0.0

76      RESULT=RESULT1

77      RETURN

78      END
```

الملخص

طرق مبسطة لحل مسائل انتقال الحرارة المزدوج تحت تأثير نماذج التوصيل الحراري الإنتشاري والموجي

إعداد

عبدالمطلب فضل علي خضراوي

المشرف

الاستاذ الدكتور محمود حماد

المشرف المشارك

الدكتور محمد النمر

يركز هذا العمل على إيجاد طرق مبسطة لحل مسائل انتقال الحرارة المزدوج تحت تأثير نماذج التوصيل الحراري الإنتشاري , الموجي والثنائي الطور (Parabolic, hyperbolic and dual phase models). حيث تم تقديم حل رياضي تقريبي لحل معادلات التوصيل الحراري الإنتشاري والموجي لطبقة رقيقة ملاصقة لطبقة أخرى وذلك باستخدام الظرف المحيطي العام (Generalized boundary condition) بالاشتراك مع تحويل لابلاس (Laplace transform). حيث تم تطبيق الظرف المحيطي العام على حدود الطبقة الأولى بدلا" من الطبقة الرقيقة أثناء الاتصال التام بينهما وذلك لتجنب حل معادلتين بينهما ازدواج (Coupling) وحل معادلة توصيل حراري واحدة مع الظرف المحيطي العام. وكذلك تم عمل مقارنة بين الاتصال التام (Perfect contact)والاتصال غير التام (Imperfect contact) لطبقتين من المعدن تحت تأثير نماذج التوصيل الحراري الانتشاري ,الموجي والثنائي الطور. حيث تبين أن الاتصال غير التام يعطي نفس نتائج الاتصال التام لجميع النماذج عندما يكون سمك الطبقة الثانية صغير

148

جدا" مقارنة مع الطبقة الأولى وكذلك عندما يكون معامل انتقال الحرارة للمائع بين الطبقتين (Interfacial heat transfer coefficient) عالي جدا" (أي أن المقاومة الحرارية بين الطبقتين صغيرة).

كذلك تم استخدام طريقة القلقلة (Perturbation technique) لحل معادلات التوصيل الحراري لمائع يجري في أنبوب دائري (Circular tube) له سمك محدد وذلك عندما يكون فرق درجات الحرارة المطبع (Normalized temperature difference) بين المائع والجدار الصلب صغير جدا" ولا يزيد عن 0.2 .

لتوضيح مدى دقة وفعالية الحلول التقريبية. تم تطبيق الحلول التقريبية(Approximate solutions) على معادلات خاصة بالتوصيل الحراري الانتشاري ,الموجي والثنائي الطور في بعد واحد. حيث تم حل المعادلات حلا" تقريبيا" وحلا"صحيحا". وجدنا أن استخدام الحلول التقريبية يعطي نفس نتائج الحلول الصحيحة عند متغيرات محددة.

وباستخدام الحلول التقريبية ينتج بمجموعة معادلات تفاضلية عادية يمكن حلها بواسطة طرق الرياضيات المعروفة بدلا" من المعادلات التفاضلية الجزئية المعقدة. واخيرا" ننقل الحلول التقريبية إلى المجال الزمني بأخذ معكوس لابلاس.